ORNL-3306
UC-34 – Physics
TID-4500 (17th ed., Rev.)

# THE ANGULAR DISTRIBUTION OF FISSION FRAGMENTS FROM THE FAST NEUTRON-INDUCED FISSION OF U-234

R. W. Lamphere

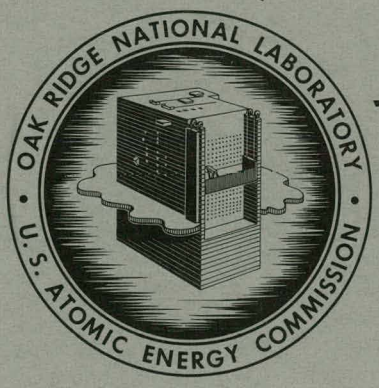


**OAK RIDGE NATIONAL LABORATORY**
operated by
**UNION CARBIDE CORPORATION**
for the
**U.S. ATOMIC ENERGY COMMISSION**

## DISCLAIMER

ORNL-3306

Contract No. W-7405-eng-26

PHYSICS DIVISION

# THE ANGULAR DISTRIBUTION OF FISSION FRAGMENTS FROM THE FAST NEUTRON-INDUCED FISSION OF U-234

R. W. Lamphere

This report was prepared as a thesis and submitted to the Graduate Council of The University of Tennessee in partial fulfillment of the requirements for the degree of Doctor of Philosophy

DATE ISSUED

AUG 27 1962

OAK RIDGE NATIONAL LABORATORY
Oak Ridge, Tennessee
operated by
UNION CARBIDE CORPORATION
for the
U.S. ATOMIC ENERGY COMMISSION

THIS PAGE

WAS INTENTIONALLY

LEFT BLANK

# PREFACE

One aspect of nuclear fission in particular is treated herein, namely the angular distribution of the two fragments relative to a beam of fast monoenergetic neutrons impinging upon a suitable thin target of U-234 or U-235. From this measured distribution it is possible to make reasonable estimates of the channels contributing to fission, although for neutron energies considerably in excess of the threshold, only statistical methods can apply since levels become closely spaced, and the neutron beam has of necessity an appreciable energy spread. The way in which this aspect of fission fits into the overall picture is discussed in Chapter II.

The experimental work, taking as it did some three years to complete, involved the cooperative efforts of many people to whom the author is indebted. Members of the High Voltage Laboratory were amazingly tolerant with the author's persistent requests for more and more Van de Graaff accelerator time! Their frequent help in "setting up" and "lining up" the beam was much appreciated. To the machinists who were called upon to make all sorts of odd things, often on short notice, my thanks. In particular is the author indebted to A. W. Lynch who spent many painstaking weeks making, among other things, the two collimators shown in the illustrations later on. These served to collimate fission fragments emitted from foils containing thin deposits of uranium, and so constitute the very core of the experimental equipment. Members of the ORNL library staff were often very helpful with the reference material. It is a pleasure to acknowledge with gratitude, helpful discussions of

various theoretical topics with L. C. Biedenharn, J. L. Fowler, F. K. McGowan, R. D. Present, P. H. Stelson, J. A. Wheeler, H. B. Willard, and in particular G. R. Satchler, whose unfailing patience with a rather untheoretical experimenter was greatly appreciated. Much of the data were taken by A. J. Wyrick, who frequently took over the operation of the accelerator and the experiment during the evenings. This contributed materially toward shortening the duration of the experimental work.

# ABSTRACT

The fast neutron-induced fission cross section of U-234 has been measured from threshold to 4-Mev neutron energy. A maximum of 1.26 barns was found at 850 kev followed by a minimum of 1.10 barns at 1050 kev. The angular anisotropy of the fragment distribution was measured for neutron energies from 400 kev to 4 Mev. Extrema in the ratio $\sigma_f(0°)/\sigma_f(90°)$ were found at 500, 850, and 1050 kev; the distribution at 500 kev showing a maximum in the direction normal to the beam (sidewise peaking) while that at 850 kev showed a maximum along the beam direction. The distribution at 1050 kev showed forward peaking but to a lesser extent than for energies immediately higher or lower.

The behavior has been analyzed according to the theories of Bohr and Wheeler. The dip in cross section between 850 and 1050 kev is consistent with the suggestion of Wheeler that neutron competition in the decay of the compound nucleus enters with increased strength in this area. Vibration-rotational levels in U-234 beginning at 790 kev are known to exist and inelastic neutron scattering to these levels serves to depress the fission cross section.

The changes in fragment angular distribution are shown to be explainable in terms of the theory of Bohr which states that fission occurs through distinct channels composed of a K-band structure analogous to that observed at low excitations in heavy deformed nuclei. More detailed angular distribution measurements were carried out at 850 and 1050 kev. The overall picture is consistent with a K-band structure in U-235* near the saddle point deformation of K equals

1/2+ ,3/2-, 1/2- in that order, the bands being separated from each other by a few hundred kilovolts.

TABLE OF CONTENTS

# LIST OF TABLES

# LIST OF FIGURES

# CHAPTER I

## HISTORY

The mechanism of the fission process was first explained by N. Bohr and J. A. Wheeler (Bo39) in a classic paper wherein they based their considerations on hydrodynamical concepts which they embodied in their "liquid-drop" model of heavy nuclei. This model was quite successful in accounting for the broader aspects of fission, and particularly valuable in directing ensuing experiments along profitable lines. Although detailed agreement with experiment is lacking, many of the basic ideas are still in use. An excellent review paper by Louis Turner (Tu40) summarized much of the work published prior to the voluntary censorship imposed as a result of World War II.

An extensive analysis of fission was made by Hill and Wheeler (Hi53) in 1953 from the point of view of a "collective Model," which included both individual particle and liquid-drop aspects of nuclear behavior. This permitted at least a qualitative understanding of a few phenomena which were at variance with a strict liquid drop picture. It lead, for example, to a better understanding of charge division, and also to angular anisotropy of fragment distribution for which the liquid-drop model predicted only isotropy.

A symposium was held at Chalk River in May of 1956, the results of which were summarized in an unpublished report (Ha56) which is well worth reading by those interested in a general survey. Practically all aspects of the matter were covered, including some interesting observa-

tions on fission induced by high energy (over 50 Mev) particles. These seem to indicate that high energy fission does not differ appreciably from low energy fission, the extra energy being largely dissipated prior to fission by the evaporation of single nucleons. More angular momentum is brought in, which has the effect of raising the barrier to neutron emission from the excited compound nucleus more than it does for fission (Ha59a); and also alters fragment angular distributions (Bo55, Wh56). Much experimentally-determined information was presented on the finer details of mass-yield curves, and the way they are affected by the species of target nucleus and the nature and energy of the exciting projectile. It is clear that a large number of channels are open to fission at high energy, so that comparisons between theory and experiment can only be made on a statistical basis (due to instrumental limitations on resolutions, etc.).

An excellent review article was published by Halpern in 1959 (Ha59a). It deals with the current status of fission knowledge and theory and also contains a very good bibliography of important articles published prior to January, 1959. It is important to note that there is in existence even now no really adequate theory for fission. Useful as the liquid-drop model is in many ways, it does predict symmetrical division as the most probable mode, in contrast to a roughly 3-2 ratio observed experimentally for heavy-light fragment masses. However, if calculations were to be carried out in sufficient detail it is just possible that this might not be the case. A program of much more detailed calculations including deformation parameters to high order is

now being carried out by Swiatecki (Sw60), but as of June, 1960, these calculations (incomplete at that time) did not explain the preference for asymmetric division. The collective model probably comes closest to accounting for all the observed results, yet neither can it predict the proper shapes for mass-yield curves, nor does it give detailed agreement with experiment in other respects. If angular momentum is brought in by the incident particles, the theory of A. Bohr (Bo55) states that in general the fragments will exhibit angular asymmetry with respect to the beam of incoming particles or photons. This theory accounts in a quantitative way for this asymmetry without conflicting with liquid-drop concepts.

Angular asymmetry in the emission of fragments from induced fission was first detected in the photofission of thorium (Wi52) in 1952. The liquid-drop theory which was in general use at the time predicted only isotropy, so the asymmetry was quite unexpected. However, a distribution of the form, $A + B \sin^2 \theta$, was confirmed over an energy range from 8 to 16 Mev with ratios of B/A of 1.2, 0.5, and 0.3 at energies of 8, 12, and 16 Mev, respectively. This was followed by a more detailed investigation by one of the authors and reported by him in a Ph. D. thesis in 1953 (Wi53). He found also that a similar anisotropy existed for U-238, and that U-235 showed no anisotropy. The ratio, B/A, a measure of anisotropy, increased roughly linearly with fragment mass ratio. Angular anisotropy was quickly thereafter found for fast neutron induced fission of isotopes of uranium and for neptunium to be of the form, $1 + A \cos^2 \theta$, but with no real evidence for dependence on fragment mass ratio (Di53, Br54). Fission induced

by fast charged particles was also found to be characterized by fragment angular anisotropy, and to be of the form, $1 + A \cos^2\theta$, where A increases for greater mass ratios of heavy to light fragment (Co54). More recently experiments with nuclei of U-233 and U-235 aligned at low temperature and excited by thermal neutrons have been carried out at Oak Ridge National Laboratory (Da60). The results are at variance with what might be expected from the Bohr picture. Work is continuing, and the results should be most interesting from the point of view of the collective model of heavy nuclei generally, and for fissioning nuclei in particular.

Many other experiments on angular distributions have been carried out in the past eight years. The next chapter summarizes the information obtained from them.

# CHAPTER II

## ANGULAR CORRELATIONS

Fission characteristics can logically be broken down into two major classifications:

1. Probability of fission taking place, i.e., fission cross section, as a function of all possible variables.

2. Relative widths of available exit channels for fission as functions of all possible parameters. Under this classification come the mass and charge distributions, kinetic energy, excitation, spin, and angular distribution of the fragments as functions of such parameters as type of target nucleus and the nature and energy of the projectile.

Clearly the number of fission channels, if a channel be defined in the usual sense of complete individuality regarding all aspects of the reaction products (fragments), is truly large even close to threshold. Consequently it is necessary to define in the case of fission at least, what the author means by channel. Fragment angular distribution measurements contain information concerning the state of the compound nucleus near saddle point, that state of deformation from which the nucleus may equally well fission as return towards symmetry. The measurements do not ordinarily differentiate between different states of the fragments. Consequently the word fission channel as used herein will refer to a state of the compound nucleus defined by $(IK\pi)$, where I is the total angular momentum, K is its projection along the

major axis, z', of symmetry of the deformed nucleus, and $\pi$ is parity. The anisotropic nature of the fragment angular distribution discovered by Winhold and others led to Bohr's classic paper (Bo55) which offers an explanation in terms of the probability distribution of the parameters (KIM) where M is the projection of I on an axis, the z axis, fixed in space, ordinarily taken along the direction of the projectile beam.

## I. BOHR'S THEORY AND THE COLLECTIVE MODES OF MOTION OF HEAVY NUCLEI

The introduction from Bo55 outlines the fundamental concepts of the theory:

> When a heavy nucleus captures a neutron or absorbs a high energy photon, a compound nucleus is formed in which the excitation energy is distributed among a large number of degrees of freedom of the nucleus. The complex state of motion thereby initiated may be described in terms of collective nuclear vibrations and rotations coupled to the motion of individual nucleons.
>
> The compound nucleus lives for a relatively very long period, usually of the order of a million times longer than the fundamental nuclear periods, after which it decays by emission of radiation or of neutrons, or by fission. The latter process occurs if a sufficient amount of energy becomes concentrated on potential energy of deformation to enable the nucleus to pass over the saddle point shape, at which the repulsive Coulomb forces balance the cohesive nuclear interactions.
>
> For excitation energies not too far above the fission threshold, the nucleus, in passing over the saddle point, is "cold," since the major part of its energy content is bound in potential energy of deformation. The quantum states available to the nucleus at the saddle point are then widely separated and represent relatively simple types of motion of the nucleus. These states are expected to form a similar spectrum as the observed low-energy excitations of the nuclear ground state.
>
> This ordered character of the motion of the nucleus at saddle point gives rise to a number of regularities in the fission process.

> Thus, the nuclear angular momentum may be concentrated, at least to a major part, on a collective rotational motion of the nucleus with a resulting characteristic angular distribution of the fission fragments. Moreover, the wide spacing of the levels implies that the fission threshold may depend significantly on the spin and parity of the compound nucleus, and thus gives rise to peculiar selection rules in the fission process. Experimental data on these aspects of the fission phenomenon may thus provide valuable information on the structure of the fissioning nuclei at a crucial stage of the process.

The collective aspects of the unified model have been developed in considerable detail in the writings of A. Bohr and of Mottelson. An excellent review paper by Moszkowski (Mo57) appears in the Encyclopedia of Physics, and another by Kerman (Ke59) in a book edited by Endt and Demeur. The intrinsic (individual particle) states of heavy nuclei have been considered by Mottelson and Nilsson (Mo59, Ni55) but as yet not enough is known about conditions at saddle point to make quantitative applications to fission channel analyses. From these works have been chosen for discussion here only those aspects of collective motion which have a direct bearing on fission fragment angular distributions in the spirit of Bohr's theory.

The fissionable nuclei have many nucleons outside the closed shells, the eccentricities of the orbits of these nucleons producing a shape distortion which leads to the large quadrupole moments characteristic of nuclei in this region of mass number. The ground state equilibrium shapes have been found to be axially symmetric, either prolate or oblate spheroids but most commonly prolate. Such nuclei possess rotational and vibrational degrees of freedom much like diatomic molecules. The rotational motion takes place about an axis normal to the major symmetry axis. The moment of inertia is largest about such an

axis and hence the energy for unit angular momentum is a minimum. The rotational motion is wave-like in character with associated moment of inertia intermediate between the rigid body moment and the purely irrotational (surface wave) moment. The vibrations most often observed are of three kinds. The beta vibration is a quadrupole symmetric motion parallel to the symmetry axis, an oscillation about the equilibrium shape. It carries no angular momentum (K = 0). The octupole vibration is an asymmetric (pear-shaped) oscillation otherwise similar to the beta. The so-called gamma vibration is a shape vibration involving oscillations along all three principal axes (x'y'z') of the spheroid and with time-space phase such that two units of angular momenta are produced along the symmetry axis (z'), so K = 2.

These vibrations are found to lie of the order of an Mev above the ground state, so are not of direct concern to the fission process, since none of them are believed to be excited near the saddle point. Therefore, discussion of the collective motion will be limited to the rotational states. These are separated by energies of the order of tens of kilovolts from the ground state and from each other. At least one and usually several are expected to be excited at saddle point and, therefore, to contribute to fission. The angular distributions of the symmetry axes of the compound nuclei in these states are presumed to lead to corresponding angular distributions for the fragments. Therefore, in principal measurements of fragment distributions can lead to energy level assignments at the saddle point.

Let $X^{\tau}_{\Omega}$ be the intrinsic wave function characterizing the particle state, $\Omega$ being the component of intrinsic angular momentum along the symmetry axis, and $\tau$ representing all other quantum numbers necessary to define X. The particle feels a deformed field which is however symmetric along z' and as a consequence $\Omega$ is a good quantum number. The collective rotation is much like that of a rigid rotator for which the wave function is simply $D^{I}_{MK}(\alpha\beta\gamma)$, the properties of which are given in Appendix D. Here I is the total angular momentum, M its z component, and K its z' component. Thus:

$$I^2 D^I_{MK} = I(I+1) D^I_{MK} ,$$

$$I_z D^I_{MK} = M D^I_{MK} ,$$

$$I_{z'} D^I_{MK} = K D^I_{MK} . \qquad (1)$$

The total angular momentum $\vec{I}$ consists of the intrinsic part $\vec{j}$ and the rotational part $\vec{R} = \vec{I} - \vec{j}$. The nuclear Hamiltonian is:

$$H = H_{intr}(r') + T_{rot} ,$$

$$T_{rot} = \sum_n (\hbar^2/2\mathcal{I}_n)(I_n - j_n)^2 = \frac{\hbar^2}{2\mathcal{I}} \left[ (\vec{I}-\vec{j})^2 - (I_3 - j_3)^2 \right] , \qquad (2)$$

where

$\mathcal{I}_n$ = moment of inertia about body axis n. (Axes 1,2,3 correspond to x'y'z' body-fixed axes.)

$$\mathcal{J} = \mathcal{J}_1 = \mathcal{J}_2 .$$

$$T_{rot} = T^{o}_{rot} + T_{coupl} . \tag{2a}$$

$$T^{o}_{rot} = \frac{\hbar^2}{2} (I^2 + j^2) - (I_3 - j_3)^2 . \tag{2b}$$

$$T_{coupl} = \frac{\hbar^2}{2}(-2\vec{I} + \vec{j}) . \tag{2c}$$

To the extent that the coupling term may be neglected the normalized eigenfunction of H is:

$$\psi = \sqrt{\frac{2I+1}{8\pi^2}}\, \chi^{\tau}_{\Omega}(r') D^{I}_{MK}(\alpha\beta\gamma) . \tag{3}$$

Axial symmetry demands invariance of $\psi$ with arbitrary rotations of the body-fixed reference frame about z'. Such a rotation, say through an angle $\phi$ transforms the Euler angles $\alpha\beta\gamma$ to $\alpha,\beta,\gamma + \phi$, and $D^{I}_{MK}(\alpha,\beta,\gamma+\phi) = e^{iK\phi} D^{I}_{MK}(\alpha\beta\gamma)$. Also $\chi^{\tau}_{\Omega} \rightarrow e^{-i\Omega\phi}\chi^{\tau}_{\Omega}$, the signs in the exponents being opposite because D is the wave function of the body coordinates in the laboratory system while $\chi$ is the intrinsic wave function in the body (x'y'z') system. Invariance under this rotation requires therefore that $K = \Omega$.

If the nucleus is a spheroid it is also invariant for a rotation of $\pi$ about any axis in the x'y' plane. Such a rotation, call it R', transforms $\alpha\beta\gamma$ to $\alpha \pm \pi$, $\pi-\beta$, $\gamma'$, where $\gamma'$ depends on the choice of axis. Then $D^{I}_{MK} \rightarrow e^{i\pi I} e^{i\delta} D^{I}_{M,-K}(\alpha\beta\gamma)$. (If R' is about x', $\gamma'=-\gamma$ and $\delta=2\pi M$ or 0 depending on the direction of the first Euler rotation. If R' is about y' then $\gamma' = \pm\pi-\gamma$ and $\delta = \pi(2M\pm K)$ or $\pi K$. The multiple choices arise from

the $4\pi$ periodicity of $\alpha$ and $\gamma$ when the quantum numbers are half integer. Note that they coalesce for integer numbers.) Writing $\chi_{\Omega}^{\tau} = \sum_j c_j \chi_{\Omega}^{\tau j}$ and using the same argument as in the first symmetry relation and writing $\Omega=K$:

$$\chi_{\Omega}^{\tau} \rightarrow e^{-i\pi j}\, e^{-i\delta}\, \chi_{-\Omega}^{\tau j} \quad , \tag{4}$$

where $c_j$ = probability amplitude for state j.

$$\psi = \sqrt{\frac{2I+1}{16\pi^2}} \left[ \chi_K^{\tau}(r') D_{MK}^{I} + (-1)^{I-j} \chi_{-K}^{\tau}(r') D_{M,-K}^{I} \right] , \tag{5}$$

where the term $(-1)^j$ must act separately on each j component of $\chi$. Note that for $K = 0$, $\psi$ vanishes unless I is even (ground state rotational spectra of even-even nuclei show this to be true).

The above argument is not directly applicable to fissioning nuclei at the saddle point because although the nucleus is still axially symmetric so that $K = \Omega$, it is not symmetric on reflection but is believed to be more or less pear shaped from the fact that the most probable mass ratios for fragments differ substantially from unity, particularly near the fission threshold. The axially symmetric pear shape, let p (for pear) be a shape-parameter characterizing this, can vibrate along z' into its reflection (-p) and clearly $H(p) = H(-p)$ and such a shape inversion from p to -p will have the same effect on $\psi$ as a rotation R' of $\pi$ about x' or any other axis in the x'y' plane. The lack of reflection symmetry relieves the parity restriction on I for even-even nuclei to the extent that now for any given K, I may have all

values, K, K+1, K+2, etc., but there will be an energy gap between the even series and the odd series of I values, the width of this gap being equal to the energy associated with the tunneling frequency of vibration between p and -p.

Odd mass nuclei are discussed to some extent in Ke59. The sequence of levels for a given K band is K, K+1, K+2, etc. with parity equal to that of the particle wave function. In general the separation between the different Kπ rotational bands is large compared to that between levels within a band. The asymmetric rotational spectra that one would expect at the saddle point are not ordinarily encountered for low excitations, so have received only passing mention in the literature. However, the wave functions should be of the form:

$$\psi \propto D^{I}_{MK}(\alpha\beta\gamma)\chi^{\tau}_{\Omega} = D^{I}_{MK}(\alpha\beta\gamma)\Sigma_{\ell j} c_{\ell j\Omega}\chi^{\tau}_{\ell j\Omega} \quad , \tag{6}$$

where $\ell$ is the orbital component of j in the expansion of $\chi^{\tau}_{\Omega}$ into its angular momentum eigenstates.

The angular distribution of the z' axis may be found from $\int \psi^{*}\psi d\tau$ where integration is over nuclear space, and using the orthogonality relation,

$$\int \chi^{*}_{\ell j\Omega}\chi_{\ell' j'\Omega'} d\tau = \delta_{\ell\ell'}\delta_{jj'}\delta_{\Omega\Omega'} \cdot \tag{7}$$

Then it follows that $\psi^{*}\psi \propto \left| D^{I}_{MK} \right|^{2}$. For neutrons on even-even nuclei this becomes $\left| D^{I}_{\pm 1/2,K} \right|^{2}$ and from symmetry one can visualize that the fragment angular distribution will be independent of the sign of M.

Neglecting the coupling term between the intrinsic states and collective rotation, the energy levels for the rotational band associated with a given intrinsic ($K\pi$) state are easily obtained.

$$E_k(I) = E_K^o + \frac{\hbar^2}{2\mathcal{J}} I(I+1) \quad . \tag{8}$$

For the special case of $K = 1/2$ however, the coupling of the intrinsic motion with the collective rotation is not the same for all levels within a band as is the case to first order for $K \neq 1/2$. The coupling arises from the axial symmetry of the nuclear potential, this potential coupling to the particle orbital angular momentum $\ell$. For $K = 1/2$, $\ell_z$, may be zero part of the time resulting in a partial decoupling. This is described in Ke59. The energy level spacings are found to be:

$$E_I = E_{1/2}^o + \frac{\hbar^2}{2\mathcal{J}} \left[ I(I+1) + \delta_{K,1/2}\, a(-1)^{I+1/2}(I+1/2) \right] , \tag{8a}$$

where the decoupling factor, $\underline{a}$ is:

$$a = - \sum_j |c_{j1/2}|^2 \, (-1)^{j+1/2}(j+1/2) , \tag{8b}$$

and $|c_{j1/2}|^2$ is the probability of finding the intrinsic wave function in state j.

For heavy nuclei with large deformations such as exist at the saddle point, $\underline{a}$ should be either +1 or -1, but not enough has been learned about the nature of the particle levels at these great deformations to predict which. Nuclei with asymmetries of the order of $\Delta R/R_o \simeq .3$ will show very strong coupling between intrinsic and

collective motions. The nuclear potential will resemble that of an anisotropic axially symmetric harmonic oscillator and wave functions calculated using this potential will reproduce energy states with good accuracy (Mo59).

The quantity $\frac{\hbar^2}{2\mathcal{I}}$ has been found to be about 7 kev near equilibrium deformation, but near saddle point is expected to be near 5 kev. Then for the K = 3/2 band, levels should run (to first order) taking the I = 3/2 level as zero; $E_I = 5\left[I(I+1) - (3/2)(5/2)\right] = 0, 25, 60, 105$ kev. For the K = 1/2 band, $E_I = 5\left[I(I+1) - 3/4 + a(-1)^{I+1/2}(I+1/2)\right]$, and if a = +1 the band spectrum should run 0, 30, 30, 100, 100 kev, and if -1 it should run 0, 0, 50, 50, 145 kev.

## II. RELATION BETWEEN ANGULAR DISTRIBUTION AND OTHER ASPECTS OF THE FISSION PROCESS

Although this work is concerned primarily with fragment angular distributions, it should be borne in mind that correlations will generally exist between these distributions and some of the other aspects of fission. For example, fissioning through two pure states differing only in parity would be expected to give rise to interference terms in the spatial distribution of fragment intensity, leading to a loss of symmetry about ninety degrees. That no such asymmetry has been observed can be ascribed to the fact that measurements made only on the number of fragments per se in a given solid

angle necessarily average over many other aspects, such as mass number, spin, charge, kinetic, and excitation energy of the fragments.

The spin of the compound nucleus is shared between fragment intrinsic spin and angular momentum, of which only the latter appears in the angular distribution. Fragment intrinsic spins have not been measured directly but would be expected to be small for excitations not far from the top of the barrier, as can be understood by visualizing the sequence of events leading up to passage over the saddle point. Energy brought in by the projectile is shared among many modes, intrinsic and collective, of motion available to the highly excited compound nucleus. Coupling exists between these modes, the constantly changing shape of the nuclear surface altering potentials within the boundaries, thereby shifting intrinsic energy levels as well as the collective ones. A sort of churning motion continues, wherein the energy associated with any given mode of motion varies with time, although the total excitation remains constant, until passage over the barrier takes place. This will occur when sufficient of the energy concentrates in potential energy of deformation to allow the nucleus to reach the saddle point configuration. If this requires a large fraction of the total excitation, then other modes must be absorbing a minimum of energy at the moment of passage over the barrier. Now there is no angular momentum associated with this deformation, yet spin of the compound nucleus must remain a constant at all times. Therefore, the most favorable conditions for fission will coincide with the energy necessarily associated with this spin being as small

as possible, which clearly indicates a collective rotation rather than intrinsic, since the moment of inertia of such a mode is much larger than for a single nucleon, even though the motion may be primarily irrotational resulting in a moment of inertia much less than that of rigid body motion. At the moment of scission then, the intrinsic spins of the prenascent fragments are expected to be small. Following scission the fragments will be highly excited, but their spins are presumed to have already been determined. Hence, fragment spins are probably low for excitations not too far above the top of the barrier, but experimental confirmation would be valuable.

The possibility of formation of high-spin fragments at low excitation has been considered by Strutinski (St60b). If scission takes place in a slightly asymmetric manner relative to the major axis of symmetry, and if there is a substantial amount of material in the neck, let us say equal to the difference between the most probable masses for light and heavy fragments, then when scission takes place there will be a transverse component of coulomb force which will cause the fragments to spin in opposite directions. It would also appear that if, instead of postulating asymmetry relative to the major axis, that a migration of mass along the neck parallel to the major axis were to take place in the spinning compound nucleus just prior to and right up to the moment of scission, this would also produce transverse forces causing the fragments to spin in opposite directions, an effect which would be further enhanced by the resulting transverse component of coulomb force between the stubs, or between one stub and the other

fragment, depending upon just where scission occurred.

At high bombarding energies where much angular momentum is brought in as for particle-induced fission, and there is an excess of energy available above that required to produce fission, it is quite logical to expect more frequent formation of high-spin fragments, and indeed Coffin and Halpern (Co58) have found indirect evidence for this. They bombarded Th-232 with 43-Mev alpha particles, under which condition $\bar{L}$, the average orbital angular momentum brought in by the projectile, is 14, but an analysis of the fragment angular distribution failed to show terms higher than $P_6$, where P is the Legendre polynomial. They conclude, therefore, that eleven units of angular momenta were distributed between the fragments, although a small amount may have been carried off by neutrons evaporated prior to fission. On the other hand, the fragment spins will probably not be parallel to each other, so their individual spins might be quite high. Strutinski (St60b) has pointed out that the existence of fragment spins will show up in an angular correlation between fragment direction and gamma quanta emitted during deexcitation of the fragments, and indicates that there is a little experimental evidence to support this. However, more work is definitely needed to settle this matter. The picture of just what happens between saddle point and scission, and whether any substantial migration of mass along the neck can occur, are matters that are still far from clear. Undoubtedly shell effects play a role, but how important a one cannot now be judged. Energy levels are greatly altered by the extreme shape distortions prevailing in this region. However,

as enough becomes known to allow Nilsson-type energy level diagrams to be extended into this region of distortion, better estimates of the effect of shells on the fission process will become possible.

There may be a correlation between mass asymmetry and angular anisotropy. At least experiments with gamma- and charged particle-induced fission would seem to show a fairly linear increase in the degree of angular anisotropy with increase in the degree of mass asymmetry, i.e., the ratio of heavy to light fragment mass, for even-even target nuclei. Odd-mass targets exhibit angular isotropy (Ba59). Unfortunately, these experiments have been performed only at medium energies where evaporation of one or more neutrons can take place prior to fission. Halpern (Ha59a) has pointed out that for this reason the correlation may be fortuitous. Consider gamma-induced fission. The cross section for formation of a compound nucleus by electric dipole absorption sufficiently outweighs higher multipole cross sections that this mode probably remains dominant at all energies. Therefore, the average compound nuclear spin, $\underline{I}$, will remain very nearly constant with energy, but more internal states of higher intrinsic excitation from which fission may occur will become available as photon energy is increased, resulting in a washing out of angular anisotropies. At the same time, for reasons that have not been clearly established, fission from states of high excitation favor a higher probability of mass-symmetric division. Now, if neutrons are evaporated from the compound nucleus prior to fission, the excitation energy will be reduced, and both angular and mass asymmetry from fission of the resulting nuclear

species will be enhanced. What is urgently needed here, then, is an experiment carried out with a maximum incident photon energy of around ten Mev with an even-even target such as U-238, and using a technique which will identify fragment masses coming off at different angles. A method such as that employed by Winhold (Wi53) at higher energies would be suitable, although the advent of the new barrier counters may offer a better line of attack.

Turning now to charged particle-induced fission, the observed correlation between angular and mass asymmetry may be explained in part at least by a similar line of reasoning which, however, will differ as to detail. In the first place, the coulomb barrier rules out any possibility of making observations near threshold. Secondly, compound nucleus formation increases with increasing angular momentum of the incoming particle over quite a range of L values, with the result that fission occurs from compound nuclei with rather large average spin, the higher the incident energy the higher the average spin will be, and the evaporation of neutrons ahead of fission will change the spin very little as such neutrons carry away but little angular momentum. (Even in the heavy nuclei the centrifugal barrier has a pronounced effect on evaporated neutrons, causing a strong preference for s-wave emission.) However, evaporated neutrons do carry away energy, with the result that subsequent fission will proceed from compound nuclei with lower average excitations and therefore with lower average K. Statistical analyses due to Strutinski (St57b) and to Griffin (Gr59) show that the degree of forward peaking depends on a factor $(\bar{I}/\bar{K})^2$, the square of the ratio of average compound nuclear

spin to its component along the symmetry axis at saddle point. Therefore, it can be seen that neutron evaporation before fission favors both angular and mass asymmetry.

The situation in regard to neutron-induced fission has not as yet been investigated. Similar results are to be expected at medium energies where one or more neutrons may be given off without reducing compoung nuclear excitation below the fission threshold. It would be very worth while to investigate the correlation between mass and angular asymmetry with neutrons of from two to five Mev from both even-even and even-odd targets.

For charged particle-induced fission a correlation has been found for fixed bombarding energy, between the degree of angular anisotropy and the so-called fissionability parameter, $Z^2/A$, the distribution tending towards isotropy as $Z^2/A$ increases. An explanation for this has been suggested by Halpern and Strutinski (Ha58) in terms of the increase in $\Gamma_f/\Gamma_n$ with $Z^2/A$. $\Gamma_f/\Gamma_n$ is larger for high $Z^2/A$, causing a larger fraction of fissions to take place ahead of neutron emission and hence from highly excited compound nuclei. For this reason $\overline{K}$ will be large, and the parameter $\overline{I^2}/\overline{K^2}$ will be small. If the fissionability parameter is small, conditions will be the reverse. Several neutrons will be evaporated ahead of fission, causing greater angular anisotropy. For charged particle-induced fission, the nature of the particle will influence the degree of anisotropy in ways which can be explained, qualitatively at least, by taking into account the fact that the average amount of angular momentum contributed by the

particle at a given energy increases with the square root of its mass. In some cases the nature of the compound nucleus which is formed will make itself felt. This is true in particular for the lighter less fissionable nuclei where rapid changes in fissionability may be found between nearby nuclear species.

Very little will be said about fission induced by high energy particles, say over 50 or 60 Mev in energy, because the picture becomes beclouded with other effects which make it difficult to draw any worthwhile conclusions from the results, at least as far as fission modes are concerned. However, a few general remarks are in order as they bear on angular distributions. Up to 50 Mev or so it seems safe to assume that practically all the energy of the incoming particle is absorbed in the compound nucleus (Me58). As energy is increased, however, the target nucleus becomes increasingly transparent, with the result that reactions between the projectile and one or more single nucleons take place, followed by the chance that the projectile may then leave with a substantial part of its original energy. Those struck nucleons which move in directions nearly normal to the beam will have low energy and so will be more effective in producing fission. Halpern (Ha59b) has suggested this as an explanation for the observed dependence of fragment angular anisotropy on proton energy. For uranium, forward peaking reaches a maximum around 50 Mev and then decreases steadily with increasing energy, becoming isotropic near 150 Mev, and increasingly peaked sidewise, normal to the beam, for higher energies. Lighter, less fissionable nuclei, such as bismuth

for example, behave quantitatively somewhat differently because of their lower fissionability.

## III. ANGULAR CORRELATIONS FROM NEUTRON-INDUCED FISSION

The neutron's lack of charge permits formation of compound nuclei with excitation energies down to the binding energy of the neutron -- of the order of five or six Mev. Fission characteristics for even-even target nuclei can be observed down to, and below, the thresholds. However, to carry out observations on the odd-neutron, or so-called "fissionable" nuclei, which undergo fission upon absorption of a thermal neutron, it is necessary to resort to a subterfuge as was done by Stokes, Northrop, and Boyer (St59). They bombarded targets of Pu-239, U-233, U-235, and U-238 with deuterons and recorded fission events which occurred coincidentally with detection of fast protons, which signified that a stripping reaction had taken place wherein a neutron was deposited in a target nucleus which then underwent fission. This technique allowed exploration of the so-called "negative energy region," that region below the binding energy of the neutron in the target nucleus. Fission probability as a function of excitation energy was measured down to, and below, the thresholds for these four nuclei.

The authors pointed out that this method could be extended by use of the (d,t) or ($He^3$,$He^4$) reaction to study fission from nuclei not otherwise obtainable; for example, by bombarding U-233, fission from U-232 might be studied. Although the method has not been applied

to investigations of fragment angular distributions, it does offer an excellent opportunity for observing distributions from even-even nuclei excited to energies close to the top of the fission barrier. It would be instructive to compare such distributions with those obtained from photon-induced fission of the same even-even nuclei.

Fragment angular distributions from odd-A targets show fore-and-aft peaking to a mild degree which varies only slowly with neutron energy. There remains one anomaly which has not yet been satisfactorily resolved. Such nuclei will have spins oriented randomly with respect to the neutron beam and so the larger the spin the greater would be the expected tendency towards isotropy. Therefore, U-233 with a spin of 5/2 should show less anisotropy at a given neutron bombarding energy than Pu-239, which has a spin of only 1/2. However, measurements (Si60) show the anisotropy, defined as the ratio of fragment intensity at zero degrees to that at ninety degrees, to average about two per cent greater for U-233 than for Pu-239 in the energy range below four Mev. In addition, U-235, in spite of its spin of 7/2, is found to have a still greater anisotropy by about two per cent than U-233 over the same range of energy. Comparisons with U-235 are complicated by the fact that its threshold lies about 0.9 Mev above that of U-233 and Pu-239 which have nearly identical thresholds. For like densities of intrinsic states this would cause $\overline{K}$ for a given bombarding energy to be lower in U-235 than in either of the other two, favoring fore-and-aft peaking. However, the similarity of the differences in distributions between U-235 versus U-233 and U-233

versus Pu-239 would suggest that this effect is quite small.

Another small effect tending to account for part of the discrepancy between theory and experiment is connected with the dependence of $\Gamma_f/\Gamma_n$ on the spin of the compound nucleus (Si60). The energy necessarily associated with spin is inversely proportional to the moment of inertia, and so is less at saddle point than for any other configuration within the barrier. This means that less energy is subtracted from that available for fission than from that available for neutron emission. Assuming the angular momentum of the incoming neutron to combine randomly with the target spin, then there will be a series of equally populated states, of which those with the highest spins will have the greatest probability of fissioning instead of emitting a neutron. If the K distribution is determined by excitation energy alone, subject only to the condition that it not exceed I, then these highest spin states will enhance the fore-and-aft peaking. This selective effect will be greater the larger the spin of the target nucleus. Although in the correct direction, the magnitude of this effect as estimated by Halpern (Ha59a) amounts to only about $1.5\ I^2$ kev for the change in relative barrier height for neutrons versus fission fragments. For d-wave neutrons this causes only about a 12-kev differential between the n-f barrier shift in U-235 and the n-f barrier shift in Pu-239. Since these barriers are not sharp, and the energy spread in the neutron beam can be expected to be several times this, it is doubtful that there would be any observable effects on the angular distributions.

Griffin (Gr59) has pointed out that on strictly geometrical grounds there is reason to expect an ellipsoidal nucleus to present a greater capture cross section to a beam of neutrons when its major axis lies in a plane normal to the beam than when parallel to it. For a deformation such that the difference between major and minor axes is equal to half the average radius, he estimates that this effect can account for about half the discrepancy between theory and experiment for the U-233 versus Pu-239 anisotropy, although more detailed quantum mechanical calculations might alter this somewhat. The point is that compound nuclei are formed with a preference for the $M \cong 0$ state, where M is the component of compound nuclear spin, I, along the beam axis. The maximum value of I may be considered to be proportional to the maximum extension of the radius of the target nucleus normal to the beam. Therefore, the formation of compound nuclei with larger $\bar{I}^2$ and small M will be favored, more particularly for the higher spin target nuclei, and these will enhance the anisotropy of the fragment distribution. However, the whole matter deserves further study.

As pointed out by A. Bohr (Bo55), anisotropy should be smaller for odd-even targets (odd proton, even neutron) than for either even-odd or even-even, for the reason that neither M nor K is restricted to small values. Also, the compound nucleus being odd-odd will have a greater level density than e-e, e-o, or o-e. M is restricted to $\pm$ 1/2 for even-even targets. Even-odd targets will form even-even compound nuclei, which are expected to have large spacings between intrinsic levels, tending to suppress large K values. Odd-odd targets

are of course not available, but might be studied by the indirect method previously discussed. Anisotropies of the same order as for the odd-even would be expected. The fragment distribution of Np-237 (spin of 5/2) has been measured as a function of energy and found to be quite similar to that from U-233 in reasonable accord with predictions (Si60, Go59). The anisotropy did not seem to be smaller, however, so it may be that the density of intrinsic levels near saddle point has an unexpectedly small effect on the distribution. The extreme distortion of the compound nucleus in the neighborhood of saddle point makes any accurate description of level densities most difficult. It seems reasonable to expect a substantial increase in level spacing in even-even compound nuclei near saddle point, over the spacing existent in other nuclear species, particularly between the ground state and first intrinsic state. Just how substantial an increase is another matter. Further angular distribution measurements from odd-even targets such as Pa-231 and Am-241 would be valuable.

It is instructive to observe angular distributions obtained with somewhat higher neutron energies, say up to about ten Mev. There is little to be gained by going beyond this, as the situation becomes increasingly complicated without bringing in any novel features worthy of study. Between five and seven Mev the heavy nuclei, those with $Z \geq 90$, reach a second threshold where the (n,n'f) process becomes possible. At higher energies of course the possibility of (n,xn'f) processes arise, where $x_{max} \cong E_n/6$ with $E_n$ equal to the incident neutron energy in Mev. When a neutron of six or more Mev is captured

by an even-even nucleus it may have roughly an even chance of emitting a neutron and then fissioning. In this case the fissioning species will be even-even, restricted to $M = \pm 1/2$, and for $E_n$ just above the n'f threshold, $\overline{K}$ will be expected to be small. $\overline{I}$ will be quite large, however, so theory predicts fragment distributions to become quite peaked parallel to the beam, and this is what actually happens. Any detailed comparison between theory and experiment is difficult because the ratio of first- to second-chance fissions can only be estimated, and also because not enough is known as yet about energy distribution within the compound nucleus to permit a proper calculation of $\overline{K}$, especially for the second-chance fissions. Similar, but not as striking effects have been found for other species of target nuclei around the n'f thresholds. An excellent discussion of this subject is to be found in Griffin (Gr59).

Mention should be made of the results, rather preliminary as yet, from a very interesting but difficult line of experimentation, fission from nuclei aligned at low temperature. This work was initiated several years ago at the Oak Ridge National Laboratory by Roberts, Dabbs, et al., from which at the present time results are available from fission of U-233 and U-235 induced by thermal neutrons (Da60). The spatial distribution of the alpha particles was also measured using the same setup except for the absence of the neutron beam. In addition, Hanauer (Ha60) has reported on the angular distribution measurements of alpha particles from Np-237 under the same conditions of low-temperature alignment.

The collective model of Hill and Wheeler (Hi53) predicts that alpha emission will be quite strongly enhanced parallel to the symmetry axis, for the reason that the nuclear barrier is weakest in this direction. This is what has been observed; both alpha and fission fragments preferring to come out parallel to the nuclear symmetry axis. The effect is directly measurable for the alpha emission, directional correlation increasing linearly with the reciprocal of the absolute temperature. The fission mechanism itself clearly assures this to be the case for fission fragments. Proceeding on this basis then, and using the concepts introduced by A. Bohr (Bo55) it is possible to deduce from the measured distribution, some conclusions about the channels (denoted here by K, I, $\pi$, where $\pi$ stands for parity) involved. Unfortunately, since both U-233 and U-235 have high spins, there will be many possibilities; in addition to the two I values there will be several possibilities for K also, which makes it impossible to draw definite conclusions. The fragments from U-233 were found to be emitted isotropically, that is, without regard to the direction of the symmetry axis of the excited compound nucleus, at least within experimental accuracy. From this, the authors concluded that either the channel (2,3, +) was responsible, or else a combination of more than one, and that in either case, channels with smallest possible K do not strongly predominate.

A small anisotropy was found for U-235, from which the conclusion was drawn that low K levels are favored here, but that the level with lowest K is not the only contributor. These findings are in

qualitative agreement with theory, but it appears that a strong preference for the low K levels is lacking. Similar experiments with nuclei having spins of only 1/2, such as Pu-239, would be very worthwhile since only two channels could contribute to anisotropy, and these have strikingly different characteristic distributions.

In addition to studies with aligned nuclei, much can be learned from investigations of fission characteristics near threshold, fission being induced by a beam of reasonably monoenergetic neutrons. Relatively few channels are open near threshold so that statistical analyses can be avoided in favor of individual channel analyses. If more intense beams of neutrons could be obtained in the 100 to 1000 kev decade, energy and angle resolutions could be improved, which would facilitate identification of individual channels. The new surface barrier particle detectors may turn out to offer the same possibility in a different manner.

Because of the well-known difficulties encountered in this energy region, little work has been done on angular distributions near threshold, and only one individual channel analysis is known to have been attempted. Henkel and Brolley (He56) measured the angular distribution of fragments from Th-232 and found very striking fluctuations near threshold, which seemed to correlate with wide fluctuations in fission cross section. In particular, at 1.60 Mev a peak occurs in the cross section and also a very strong sidewise peaking of fragment distribution, the intensity being roughly three times as great at ninety degrees as at zero degrees. Measurements were made at 0, 15, 30, 60, and 90

degrees. A channel analysis was carried out by Wilets and Chase (Wi56), who found that a good fit could be had from a series of terms up to I = 7/2 in the K = 3/2- band. Their expression is:

$$W(\Theta)=0.34+0.63W(3/2,3/2,-)+0.18W(3/2,5/2,-)+0.33W(3/2,7/2,-) \qquad (9)$$

where the $W(K,I,\pi)$ are derived from the symmetric top wave functions, the so-called D functions denoted here by D(K,I,M), by taking into account the equal probability of occurrence of states with M = +1/2 and M = -1/2, and opposite signs of K. Thus:

$$W(K,I,\pi) = \text{constant} \int \left[ \left| D(+K,I,\pm 1/2) \right|^2 + \left| D(-K,I,\pm 1/2) \right|^2 \right], \qquad (10)$$

since from the symmetry of the system it is clear that the measured distributions must be independent of the signs of M and K. Normalization is such that:

$$\int_{-1}^{+1} W(K,I,\pi) d(\cos\Theta) = 1 \ . \qquad (10a)$$

They conclude that the large I = 7/2 term is probably due to f-wave neutrons rather than g, since $kR_o$, the product of neutron wave number and average radius of the thorium nucleus, is about 2.4. Then the I = 5/2 channel would be fed by f-wave neutrons, and the I = 3/2 by p-wave. The s- and d-wave neutrons would not contribute to fission through this particular rotational band because of parity.

If data could be obtained to higher accuracy it would be of interest to compare the coefficients of the Ws with calculations of partial wave cross sections for compound nucleus formation using an

optical model potential. Such a potential gives peaks at various energies for the separate angular momenta, and might help to explain the large W(3/2,7/2) compared to the W(3/2,5/2) contribution, the statistical factor of 4/3 not being sufficient to do so. The compilation of Emmerich (Em58), which is based on a Saxon well, is appropriate and useful for this purpose.

# CHAPTER III

## EXPERIMENTAL EQUIPMENT AND METHODS

In chapter II several areas were pointed out where further experimentation might prove fruitful. Of these the equipment available at the Oak Ridge High Voltage Laboratory was best suited to pursue a study of neutron-induced fission near threshold. This required a "non-fissionable" (to thermal neutrons) target, that is, one with an even number of neutrons. If individual channels were to be recognized, then a minimum number should be open to fission in the region of excitation energy under investigation, which indicated that the number of protons should be even also, hence an even-even target. The number of possible channels is further restricted if the angular momentum contributed by the incident neutrons is small. Thus the field narrows to an even-even nucleus with a low threshold for neutron-induced fission. Since counting rates will be low at best, the cross section for fission should be as high as possible.

U-234 fulfills the above conditions admirably. Furthermore, previous measurements (La55) had shown structure in the total fission cross section at around an Mev neutron energy. Current concepts call for a smoothly increasing cross section, followed by a slow leveling off, but not a decrease. The structure had to be explainable in terms of competition, presumably from neutron emission, if present theories were to apply. This, then, seemed an appropriate region to investigate, in view also of the fortunate circumstance that suitable foils of U-234 were on

hand from the above-mentioned work.

This chapter will indicate the measurements which were made and describe the methods and equipment used. The detailed results will be left for a later chapter. Procedures used in modern fast neutron experimentation have been well described elsewhere (Ma60); consequently, techniques and apparatus which are standard for the trade will only be mentioned by name. Additional remarks will be added when a significant departure was made.

## I. MEASUREMENT OF TOTAL FISSION CROSS SECTION

The total fission cross section of U-234 was measured once again with improved resolution and higher statistical accuracy than previous measurements (La55) in order to discover any additional structure which might be present, as well as to define more precisely the shape of the curve in the region of 1-Mev neutron energy. The same foils, apparatus, and procedure were used, but in regions where the cross section showed strong variations with energy, resolution was improved and more counts taken. Additional data were also taken over the initial rising portion of the curve, using solid ZrT and also Li targets for neutron production in order to guard against any chance of energy errors. A gas target will produce a higher neutron flux but energy errors can creep in more readily, usually because of changes in pressure or composition of the gas in the tritium cell. The Li target permitted cross-section measurements to be carried down to around 150 kev with targets of reasonable thickness without risk of errors arising from the backwardly direct-

ed (in the center-of-mass coordinate system) neutrons. At energies below 120 kev such neutrons would impinge upon the fission foils with energies of only a few kev. Since the U-234 foil contained a few per cent of U-235 impurity, appreciable error could then arise for which in practice an accurate allowance would be extremely difficult. Therefore, estimates of the cross section below about 150 kev are very rough. A definite effect was observable, however, for neutrons as low as the 60-kev energy region.

Additional structure was found at around 260 kev but the cross section here is so low that angular distribution measurements would be impractical. Therefore, the original decision to confine the investigation primarily to the energy region around 800 to 1200 kev was not altered.

## II. ANGULAR DISTRIBUTION MEASUREMENTS

Measurements of fragment angular distribution were made in much the same way as those of total fission cross section; the only difference being the addition of a collimator over each foil, and improved angular resolution obtained by greater distance between counter and neutron source. The U-235 foil was of course replaced by another of U-234, so that the counter contained two nearly identical foils, back-to-back, each covered with a collimator. Particles traversing a collimator were detected by an ionization chamber of precisely the same geometry as before. In fact, the same counter was used for the angular distribution measurements as for the cross-section work, the support

posts merely being lengthened to accommodate the two collimators.

Figure 1 is a schematic drawing (not to scale) of the arrangement of counters relative to the neutron beam. This same arrangement was adhered to for each separate run, irrespective of whether the 3- or the 5-Mv Van de Graaff was being used. However, the long counters differed from run to run and their sensitivities were markedly different. During any given run, however, the long counter was not changed, and furthermore its gain was closely monitored by use of a standard Po-Be neutron source. The threshold counter was used to measure target thickness and also to determine the energy loss of the protons in the beam due to traversing the nickel foils in the gas target. (This target will be described in some detail in a separate paragraph.) The threshold counter was placed close to the tritium cell of the gas target and on the beam axis when being used for such measurements. The rest of the time it was moved back as shown in the figure so that its reading could serve as a rough check on the performance of the long counter.

Construction details of long counters have been more or less standardized and are described in Ma60. Experience has shown them not to be as energy independent in response as was originally thought. There is also a noticeable response to room-scattered neutrons despite the shield which surrounds the paraffin moderating cylinder and counter. As employed in this work, however, these two factors did not affect the accuracy of the measurements.

The fission detector containing the two foils, and with collimator holes in the two collimators oriented at 90 degrees to each other,

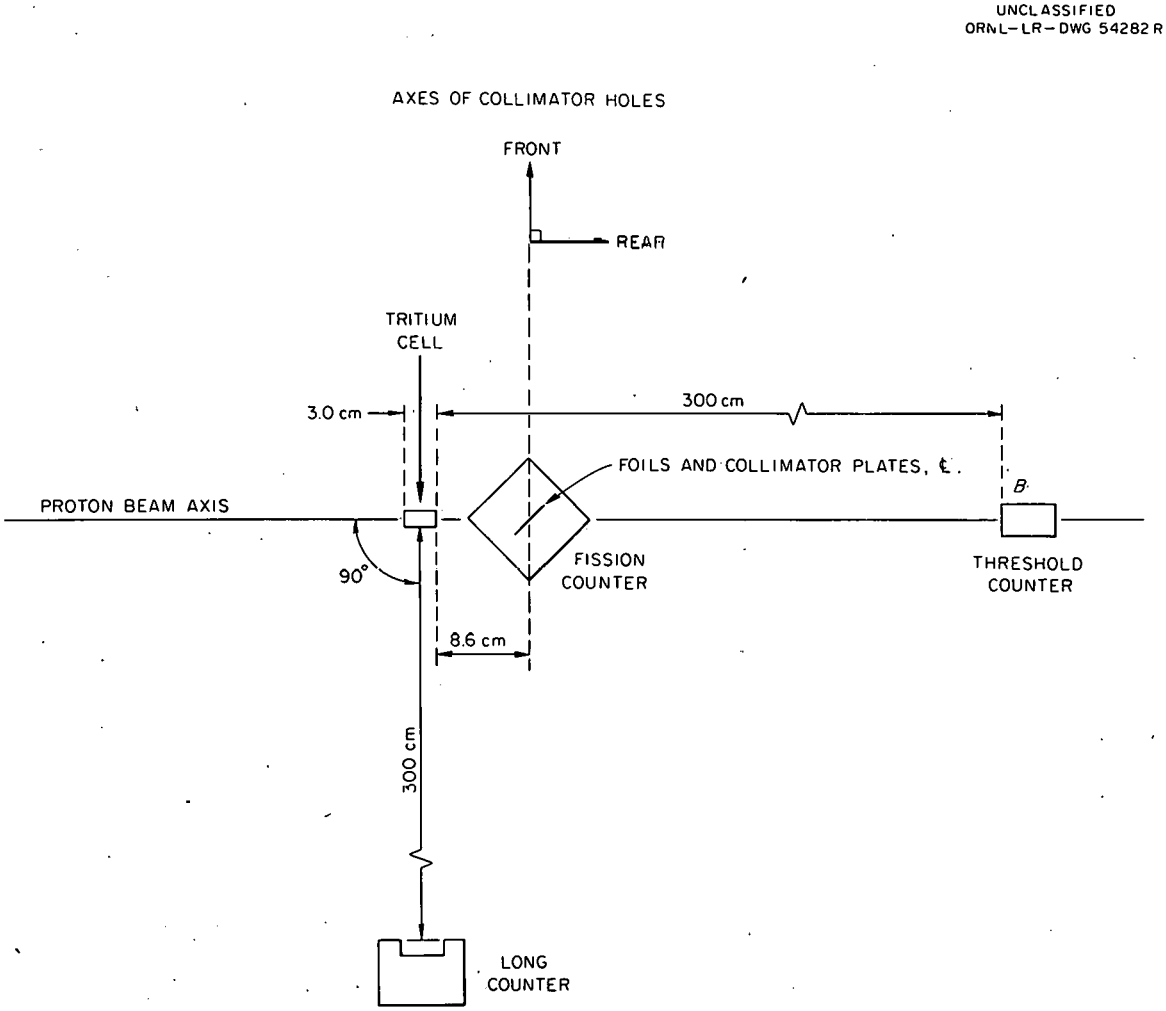


Fig. 1. Schematic of Counter and Gas Target Locations.

was capable of providing the ratio of fragment densities at any two angles differing by ninety degrees merely by appropriate orientation of the counter relative to the beam axis. The ratio of fragment emission parallel and perpendicular to the beam was obtained for many neutron energies between 400 and 3500 kev, and for these points the long counter reading had no direct bearing on the results. However, it was noted at occasional intervals along with the integrated beam current, as the ratio of these two provided a convenient running check on the quantity of tritium remaining in the gas target.

The premium on generator time led to periods of continuous operation frequently in excess of 24 hours and in one case exceeding 80 hours by a single experimenter. Under such circumstances it is useful for the individual to be able to absent himself from the control room from time to time. This proved possible since the running time at a given counter and energy setting varied from one to several hours. A microphone placed near the magnetic counters and connected either to the telephone system or the building annunciator permitted this freedom, as it allowed the experimenter to maintain a check on the progress of the work from any place within the building. The relative counting rates of the various counters served for this purpose, and were readily ascertained since no two magnetic counters sounded alike.

More complete investigations were undertaken at three neutron energies where the fragment intensity ratio (30/120) degrees, equivalent to the (30/60) degree ratio, was also measured. In order to normalize this ratio to the (0/90) ratio, the long counter reading was

required. During such a run care was exercised to see that the scattering geometry in the target area remained unchanged; that is, no equipment was moved which might alter the percentage of neutrons scattered into the long counter. Under these conditions, and with frequent checks of relative counting efficiency, it was felt that negligible error was introduced by use of the long counter as a monitoring device.

The threshold detector consisted of a short, thick $B^{10}F_3$ counter tube surrounded by paraffin moderator and a cadmium shield. Its small size made it convenient for checking target and foil thicknesses, at which times it was placed in the position shown for the fission counter.

Figure 2 is a schematic diagram of the electronic equipment which was kept as simple as possible. Identical channels served to amplify, clip, discriminate, and record pulses from the two ion chambers in the double fission counter. The low count rates led to some departures from standard techniques in order to reduce background counts from noise, or loss of data by electronic failures. To this end special preamplifiers were built with high signal-to-noise level, and with positive output pulses so that a long cable could be driven without overloading the last tube. A rather high amplification, of around 100, was employed in order to reduce the chance of noise pickup in the cables between the preamplifiers and the amplifiers, as it was necessary for these cables to be quite long. A clipping time of about 0.38 microsecond was incorporated in each preamplifier.

Power was supplied through a 2 kv-a isolation transformer with a grounded electrostatic shield. It was found by trial that the best

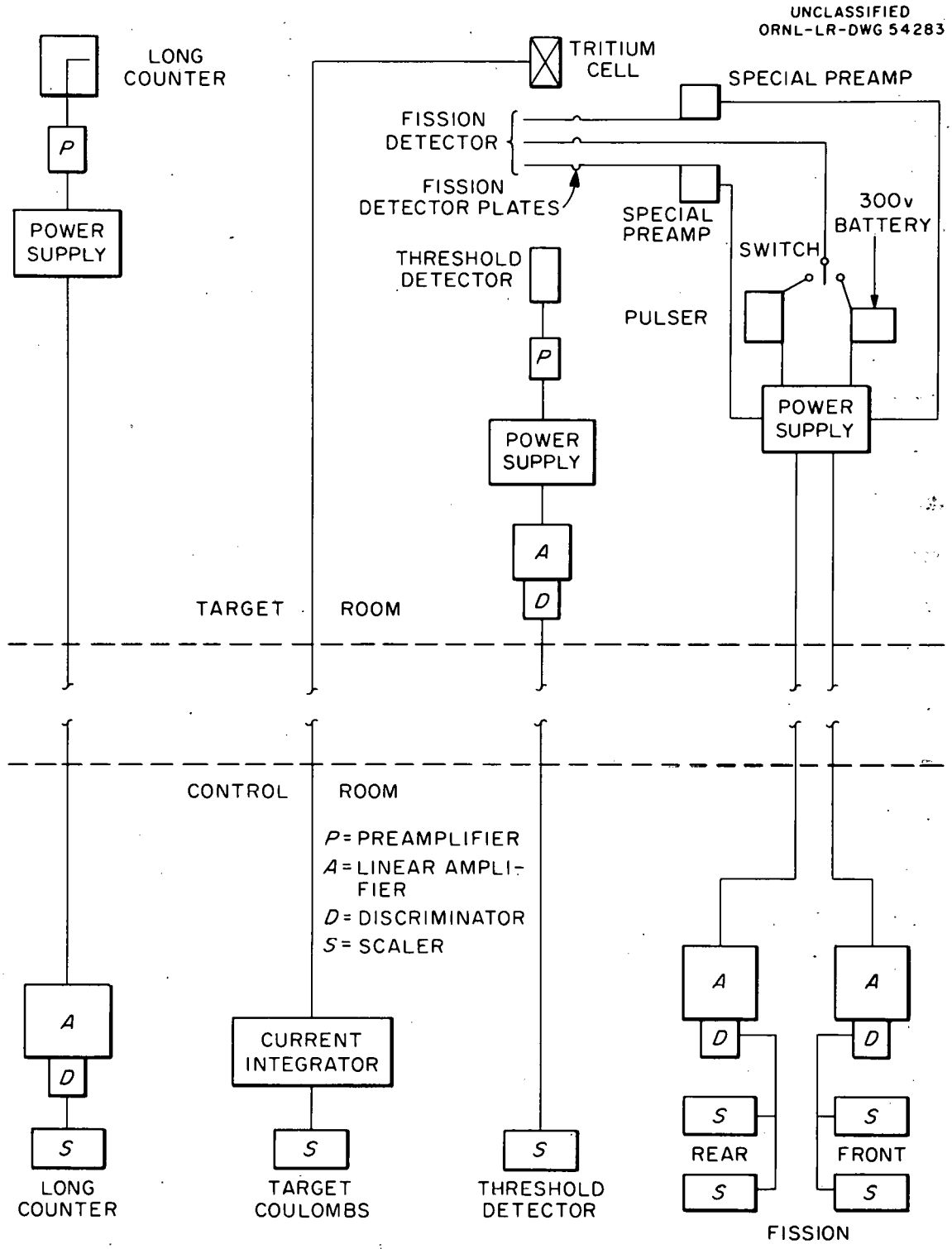


Fig. 2. Block Diagram of Electronics.

grounding arrangement resulted from grounding the special preamplifiers directly to the metal floor of the target room, and that some further benefit was derived from also grounding their electronic power supply. This is of interest since it is often stated that a single ground is best for freedom from noise. Although a very good starting assumption, this experience showed that sometimes small additional gains can be realized by additional grounds, due no doubt to the complicated interplay of the many widely distributed and unavoidable capacitive and magnetic couplings to various external sources of noise. That this method was indeed effective was shown by the fact that the system could be left for several days at a time without picking up a single noise count in either fission channel. Alpha pulses came in only below 15 volts on the discriminators, whereas all data were taken at 30. Therefore, errors from these two sources were deemed negligible. Thorough background checks were, however, made at intervals not exceeding 8 hours apart.

The rest of the electronic circuitry was quite standard. Most of it had been developed in the laboratory for other purposes at various times. The current integrator was designed by Floyd Glass of Oak Ridge National Laboratory in 1953 (Gl53), and deserves special mention for its outstanding precision, dependability, and stability.

Data were taken in a series of 12 runs from one to two weeks duration. These usually alternated between the 3- and 5-Mv generators, and were separated by periods of several weeks during which times the equipment was thoroughly checked, and the fission counter, with its

foils and collimators undisturbed, was immersed in a bath of thermal neutrons for normalization. The small percentage (2.82%) of U-235 impurity present in the U-234 foils made this possible. The same normalization figure was attained each time, that is, the relative counting rates of the two foils remained constant from run to run. Dividing the data between runs afforded a partial check on possible systematic error. To derive the greatest advantage from this, the total data on any single energy point was always divided among several runs, the results always being found consistent within statistical limits.

The fission counter was mounted so that it could be rotated about a vertical axis which passed through the center of the foils along a diameter. It could also be rotated about its own axis, which passed through the centers of the foils normal to their surfaces. By means of proper rotations about these two axes it was possible to orient the collimator holes at any angle from 0 to 360 degrees relative to the neutron beam. Data for each point were further divided in roughly equal proportions about the 360 degrees. That is, for a point where only the (0/90) degree ratio was desired, the front collimator assumed angles of 0, 90, 180, and 270, while the rear one differed by 90 degrees. For the three points where data were taken at 0, 30, 60, and 90 degrees, the same system was followed; the actual data being taken at 30 degree intervals around the entire circle, with roughly equal statistics for each position of the counter. This technique proved that symmetry in the angular distribution existed about 90 degrees, so that for analysis, all data could be folded back into the

first quadrant. It also showed the absence of aberrations from possible asymmetry in counter design or foil mounting. A comparison of the data at any given energy also served to check the accuracy of the normalization, and showed that the thermal normalization was indeed correct for the fast flux to within counting statistics. Conversely, by appropriate averaging of the data it was possible to eliminate the need for the normalization figure entirely.

A further check was carried out from time to time against the possibility of systematic electronic errors. On a given counter settings, leads were interchanged at the back of the fission counter so that part of the data was obtained with reversed channels. These checks always gave the same results, showing freedom from electronic bias. Occasional visual checks of pulse shapes from the linear amplifier outputs were carried out with fast oscilloscopes. These always showed the pulses to be clean, unadorned with noise effects, as would be expected from the fact that the noise level always remained well below 5 volts, usually 1 or 2, whereas the fission pulses were of the order of 80 volts. Frequent checks were made of gain stability of the fission channels. A drift of one volt difference between the two channels would cause an error of 0.8% due to the slope of the bias curves. However, drifts rarely exceeded one-fourth of this amount, so errors from this source were also considered to be negligible. A bias curve is shown in Fig. 3, taken for fission fragments from the thermal fission of U-235, with collimator and counter conditions identical to those prevailing during the fast neutron measurements.

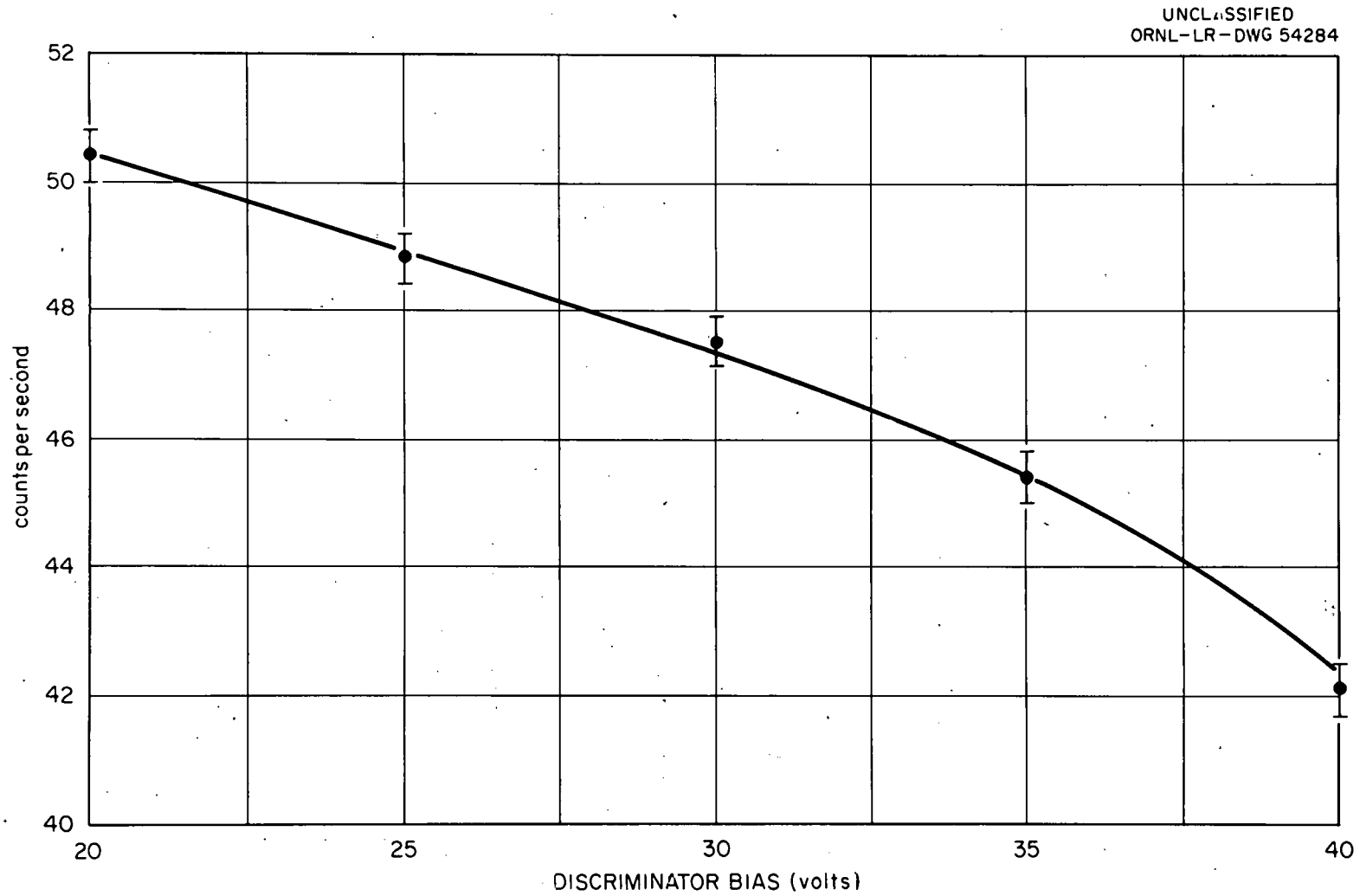


Fig. 3. Collimated Fission Detector Bias Curve.

The foregoing considerations indicate that errors from electronic sources, noise, and alpha particles are negligible, and that no aberrations were introduced by counter asymmetries. Thermal flux normalizations were consistent, and so many counts were taken that statistical uncertainty was only of the order of 0.1% and so could be neglected. Where the long counter was used to normalize between angle ratios the errors were believed to be negligible, and statistical accuracy dependent only on the fission counts since the long counter count rate was extremely rapid, over 1000 times that of the fission counters.

Other possible sources of error as well as energy and angular resolution are discussed in the next two sections which deal more specifically with the fission counter and the gas target.

The Collimated Fission Detector. Figure 4 shows the construction of the fission chamber with the two collimators in place. The foils have been described in detail in La55. Each contained 4.00 mg of uranium in the form of the oxide, mostly $U_3O_8$, plated over the area of a one-inch diameter circle on one side of a 0.002 inch thick nickel foil 2.13 inches in diameter. The isotopic composition was:

$$\text{U-234} = 96.16\% \pm .03\% ,$$

$$\text{U-235} = 2.82\% \pm .03\% ,$$

$$\text{U-238} = 1.02\% \pm .02\% .$$

These foils were placed back-to-back between the two collimators, with spacing of 0.015 inch between the plated surface and collimator surface. They were identified by the numbers, 24K12, which faced towards the front of the counter, and 24K11, which faced the rear during all the

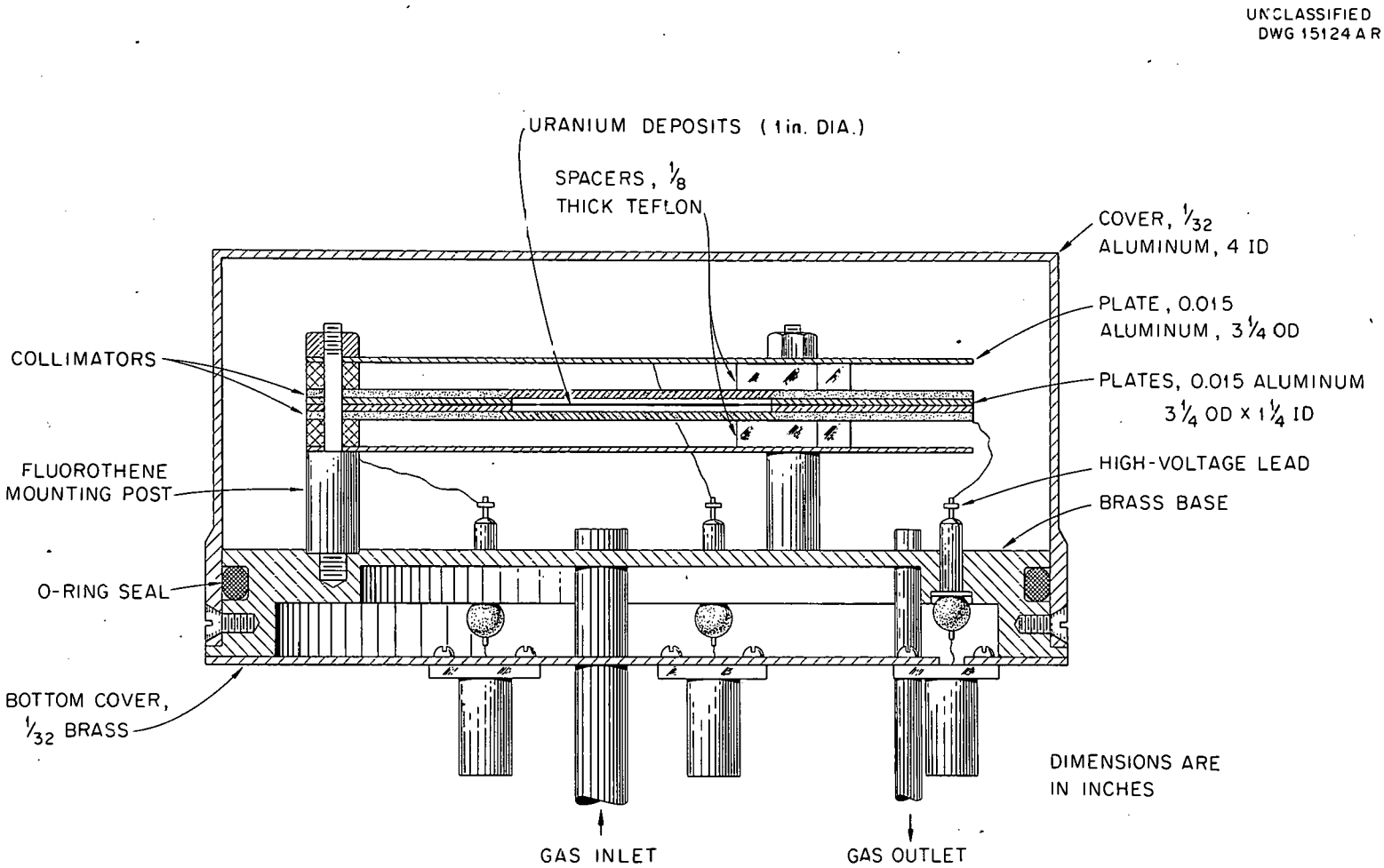


Fig. 4. The Collimated Fission Detector.

measurements with fast neutrons. Deposition densities could easily have varied by as much as 20% from the average of 0.8 mg per $cm^2$ over the plated area, and this coupled with self-absorption effects and collimator hole locations could account for the departure of 12% from unity in the normalization factor.

Normalization measurements were carried out as follows: Since absorption of thermal neutrons in the foil backings was not negligible, a measurement was first made with foil and collimator assembly in their reversed order, followed by a similar measurement with them in their normal order (that order which prevailed during the runs with fast neutrons). Collimators and foils were handled as a single unit when the order was changed, so that no relative motion took place between them. The results from the first normalization measurements were as follows:

Reversed order (24K11, 24K12): F/R = 1.145

Normal order (24K12, 24K11): R/F = 1.060

Average = 1.102

where F = front foil count, R = rear foil count, and the quantities in parentheses refer to foil positions in the sequence (F,R). The average value was considered correct for fast neutrons since their absorption in the foils was negligible. Subsequent normalization checks consisted in merely remeasuring the R/F count ratio with the normal order, avoiding the necessity of disturbing the arrangement.

After some preliminary runs with fast neutrons the counter was disassembled, the uranium foils removed, and clean aluminum foils

substituted. The counter was then exposed to the fast neutron beam at an energy of 3.7 Mev for a half hour at normal intensity. The resulting count of zero for each channel proved that there was no background, such as might have existed if any fissionable material had become loosened from one of the foils and lodged near the sensitive areas of the counter.

Following this background check the foils of uranium were replaced and renormalized with thermal neutrons, this time giving a value of 1.12 for the ratio, (R/F), to be applied to results obtained from subsequent data with fast neutrons. The foils and collimators were not disturbed again and all subsequent checks confirmed the constancy of this figure throughout the duration of the experiment.

Each collimator consisted of a flat disc of aluminum 0.060" thick, with 0.020" (No. 76 drill) diameter holes bored through it at 45 degrees to the normal over the area of a 1.375 inch diameter, centrally located circle. Holes were spaced 0.0396" apart along rows, with rows spaced 0.028" apart, resulting in 1340 holes per collimator. The drilling of so many small holes at 45 degrees to the normal required great care and still greater patience. One man worked several months to complete the two. Figure 5 shows one in the process of construction, and Fig. 6 shows the completed article.

A collimator reduced the fission counting rate by a factor of 275 compared to the rate without it ($2\pi$ geometry). Particles which succeeded in traversing the holes without colliding with the walls were limited to a maximum departure of $13.2^{\circ}$ from the axis of collimation,

UNCLASSIFIED
PHOTO 18774

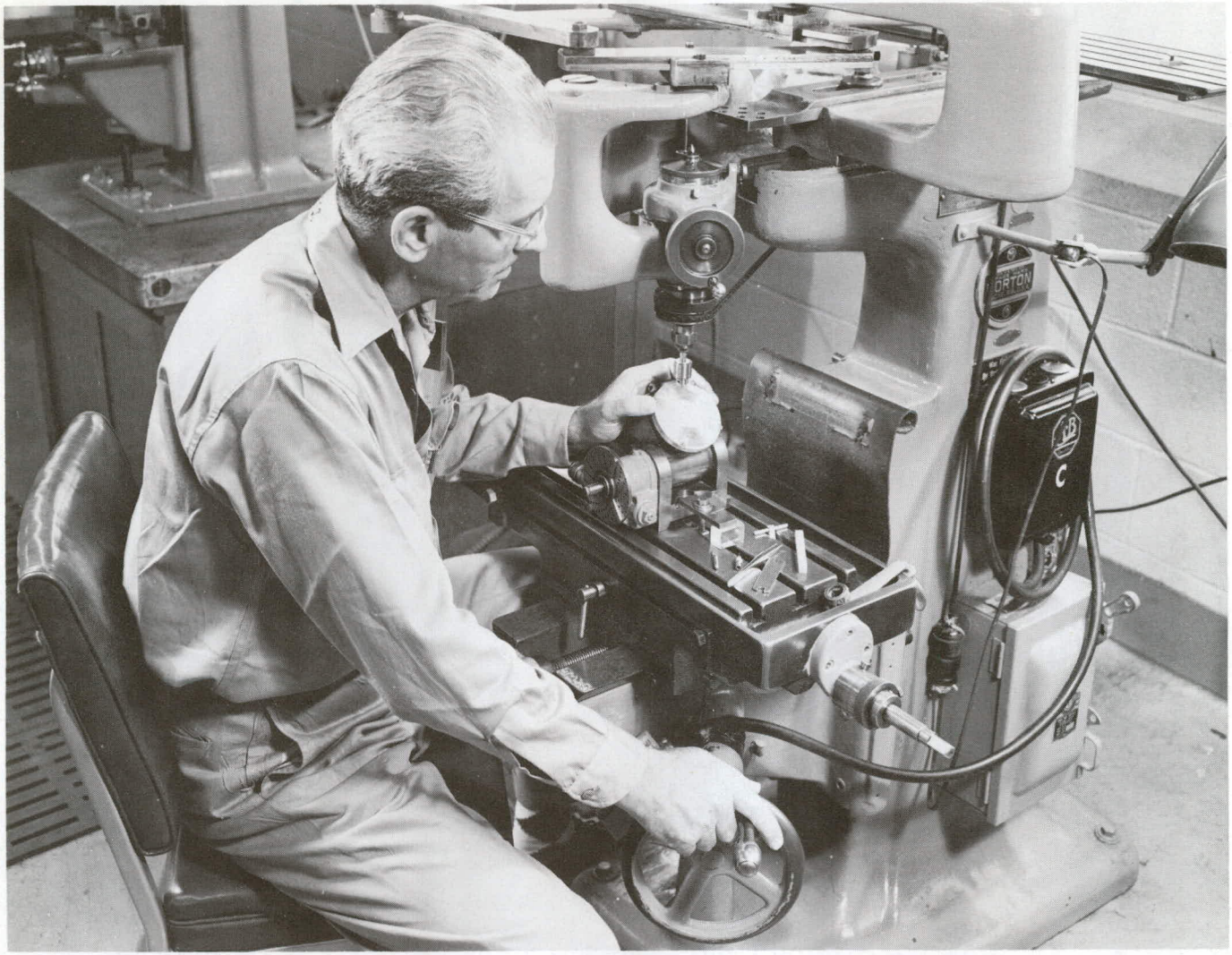

Fig. 5. Collimator Under Construction.

UNCLASSIFIED
PHOTO 18773

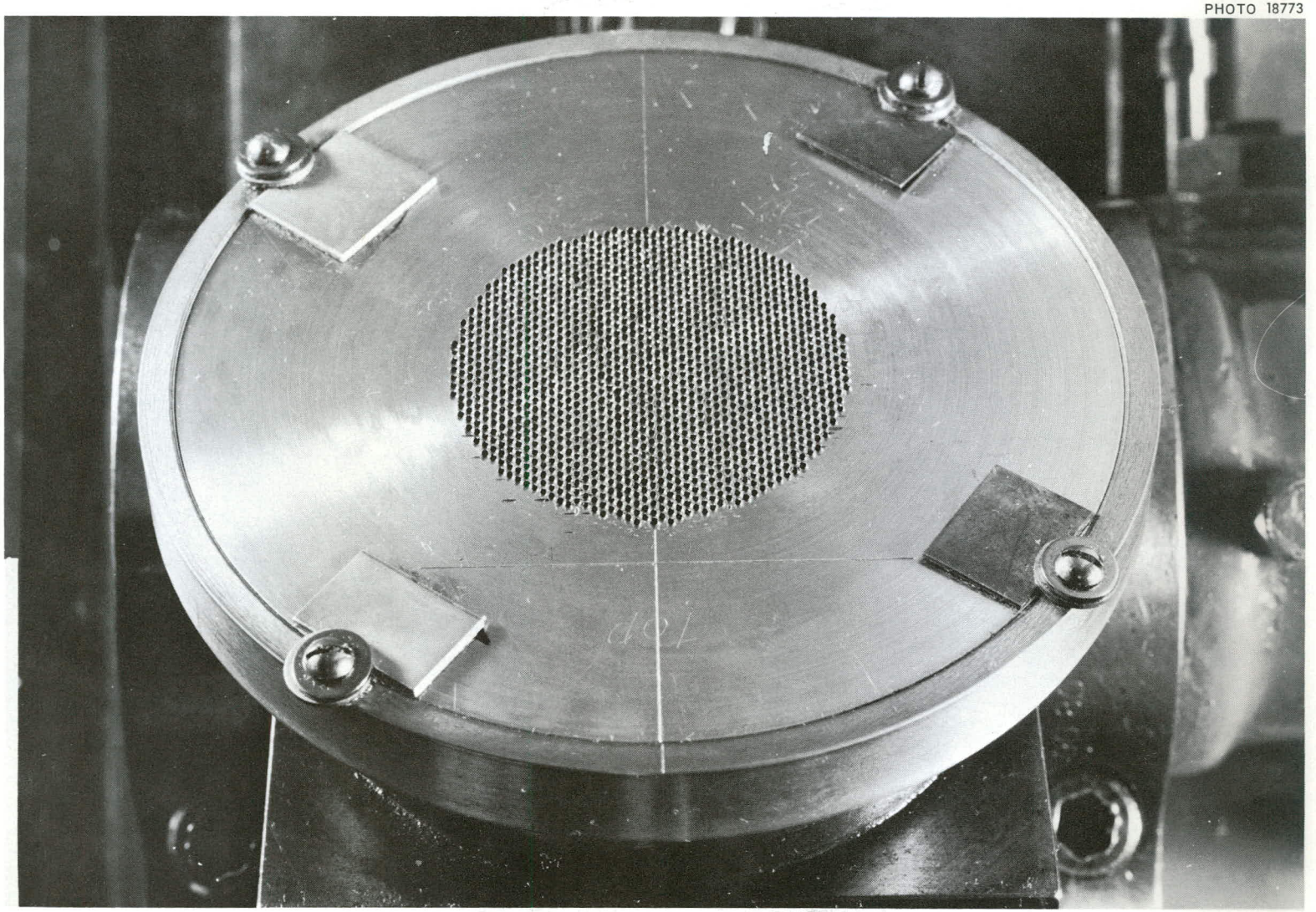

Fig. 6. Collimator Surface After Completion of Drilling.

and an average departure of $5.1^{\circ}$. Calculations to this effect are contained in the Appendix.

Of those particles which struck the walls by far the majority penetrated into the aluminum and were lost. However, a very small percentage scattered out into the ion chamber. Most of these retained insufficient energy to be counted, but a few had sufficient energy remaining to cause pulses in excess of the discriminator setting. The characteristics of coulomb scattering are such that these particles deviated only slightly from the direction of the collimator axis, on the average, and so did not impair the angular resolution. Arguments in support of this conclusion may be found in the Appendix.

Neutrons from the primary beam were scattered by the collimator and other parts of the counter, as well as from nearby objects outside the counter. Below one Mev these collisions were nearly all elastic, and infrequent enough so that only single scattering needed to be considered. There was present at the foils then, a secondary flux very nearly random in direction and with energy only a few per cent below that of the primary beam. This enhanced the observed isotropic part of the fragment angular distribution sufficiently to warrant a correction. Its magnitude is energy dependent, and has been estimated in the Appendix for the three energies at which the more complete angular distribution analyses were carried out.

The two ion chambers were identical, designed to take full advantage of the difference in the specific ionization versus range characteristics of alpha particles and fission fragments. The counting

gas was a mixture of 97% argon plus 3% $CO_2$ at one atmosphere absolute. The distance between the plated surface and collector plate measured along the direction of collimation amounted to 7.2 mm. The range of the 4.78-Mev alpha particle from U-234 was 33 mm, so only the early portion of this range, where specific ionization density is fairly low, lay within the counting volume, after which the particles buried themselves in the collector. Range of a medium heavy (60 Mev) fission fragment is 20 mm. Its high initial charge, gradually lost as it progresses along its path, causes the early part of the track to yield high ionization density, and much of this lay within the counting volume. The foils were fairly thin compared to these ranges. A particle starting at the bottom of the deposit and traveling in the direction of collimation was obliged to traverse on the average, 1.13 $mg/cm^2$ of uranium, equivalent to a range of 2.4 mm in the gas. Such a particle would strike the collector with a residual range of 52%. Fission fragments, unlike alpha particles, have a continuous distribution of energy, but very few have energies below 40 Mev and even these would produce a count in the chamber. However, a few do occur with lower energies, and some are added by scattering from the collimator walls and serve to account for the slight slope of the fission bias curve (Fig. 3).

This chamber, designed as it was, to discriminate against pulses from alpha particle pile-up, was used in the initial measurements of $\sigma_f$(U-234), where this feature was required since the $2\pi$ counting geometry allowed many alpha particles to be emitted within the resolving

time of chamber and amplifier. The addition of collimation made this a matter of less importance due to the reduction of 275 in the count rate. The preamplifiers had a clipping time of 0.38 microsecond, and electron collection time in the chamber was 0.08 microsecond. A collection voltage of 300 volts (center plate negative) was furnished by a small "Minimax" battery which proved to be the ideal power supply. About 170 volts (E/p = 0.65 volt/cm/mm Hg) was estimated to be adequate for saturation (Ma60, p. 471), and once saturated the change in pulse size with collection potential was very small, so that ordinary changes in battery voltage were of no importance.

Gas was continuously supplied to the counter from a cylinder and reducer at a rate of about 0.1 standard cubic foot per hour. Between runs the counter was not connected to the tank and so quite soon became filled with air. It was found by several trials that flushing with counter gas at a rate of one cubic foot per hour for 15 minutes always served to restore pulses to their full height. Prior to starting a run the counter was always flushed for at least 30 minutes to insure proper pulses. Back diffusion of air into the chamber was inhibited by connecting to the exit port a line of 1/8 inch copper tubing about 15 feet in length which led back to a small flow meter mounted at the supply tank. Materials within the counter were limited to clean metal, teflon, and fluorothene (for mounting posts and insulators). However, an ungreased rubber O-ring was used to seal the cover and was found not to be detrimental to pulse size. The gas flow could

be stopped for several hours before any noticeable diminution occurred in pulse size or count rate.

The Tritium Gas Target. Conventional tritium gas targets employ a single thin foil for admitting the proton beam to the gas cell. They are limited to currents of the order of 2 microamperes (at 2-Mev proton energy) by excessive diffusion of tritium through the hot foil, or actual melting of the foil by the beam. With such a limitation this experiment would have been impractical. A good rotating lithium target can accommodate currents up to about 8 microamperes without excessive evaporation of the lithium deposit. Table I gives the relative neutron yields at zero degrees for tritium and lithium targets at the same beam current and target thickness. After the resonance in the Li(p,n) reaction has been passed, the ratio rapidly and continuously improves in favor of the tritium.

TABLE I

RELATIVE NEUTRON YIELD OF TRITIUM AND LITHIUM TARGETS AT ZERO DEGREES FOR THE SAME BEAM CURRENT AND THE SAME TARGET THICKNESS IN KILOVOLTS

| Neutron Energy in Mev | Ratio of Neutron Yield Tritium/Lithium |
|---|---|
| 400 | 2.8 |
| 450 | 1.0 |
| 500 | 0.69 |
| 550 | 0.54 |
| 600 | 0.60 |

The lithium target was deemed unsuitable due to its low yield over the energy region of interest, and also because of the added burden of corrections for the effects of the second group of neutrons which would have been present over this region. Consequently a new tritium gas target was built which permitted much larger beam currents to be used.

The tritium cell was separated from the evacuated beam tube by a second narrow cell through which helium was pumped at high velocity. This cell, 7.0 mm in length, was separated from the vacuum system by means of a 0.0001" thick nickel foil, and from the tritium cell by a similar foil. These foils were unsupported over a 3/16" diameter circle through which the proton beam passed. A pressure differential of one atmosphere could be maintained with safety across each of the two foils. The helium entered the cell through two slits, 0.015" x 0.194", inclined at a grazing angle of $20^{\circ}$ to the foil surfaces. The gas was circulated by means of a two-horsepower, hermetically-sealed, Copeland refrigeration compressor which had a free gas capacity of about 10 cubic feet per minute. The pressure at the inlet of the compressor was somewhat below atmospheric so that only about 6 or 7 cfm were actually circulated. (A word of warning: Helium has a very low electrical breakdown voltage. The windings of a hermetically-sealed motor-compressor unit are immersed in the gas at inlet pressure. In some of the earlier work a single-phase, 208-volt motor with a capacitor in series with the second, or split-phase winding was used but soon developed trouble from electrical flashover as the capacitor winding

operated at potentials in the neighborhood of 400 volts from ground. Its replacement by a three-phase, 208-volt motor, wye-connected, with the neutral grounded ended the trouble, since no potential exceeded 120 volts with respect to ground.) Assuming a pressure of one atmosphere absolute to exist at the exits of the slits in the helium cooling cell and 6 cfm to be circulated, the velocity would be 2480 ft/sec, or 84% of sonic.

Figure 7 shows the gas target in place on the end of the proton beam tube, and the fission counter sitting out in front of it. Figure 8 is a block diagram of the gas-handling system, not to scale. Figure 9 shows the construction of the gas target and an expanded view of the helium cooling cell. Considerable oil left the high-pressure outlet of the compressor with the gas, and it was imperative that this be removed before the gas entered the cooling cell, as otherwise it would have become carbonized by the beam and have formed a coating over the two thin nickel foils. This would have interfered with cooling and also increased the energy loss in the beam, and led to foil burnout. It was effectively removed by use of two conventional oil traps in series, followed by two filters with cotton fiber elements, and finally a charcoal trap. The little safety valve was made vacuum tight and served to bypass the gas from the high to the low side of the pumping unit when the pressure differential exceeded a preset amount of about 50 pounds per square inch. This permitted the compressor to be started, and then the gas flow through the target to be increased slowly and carefully in order to avoid undue strain on the foils.

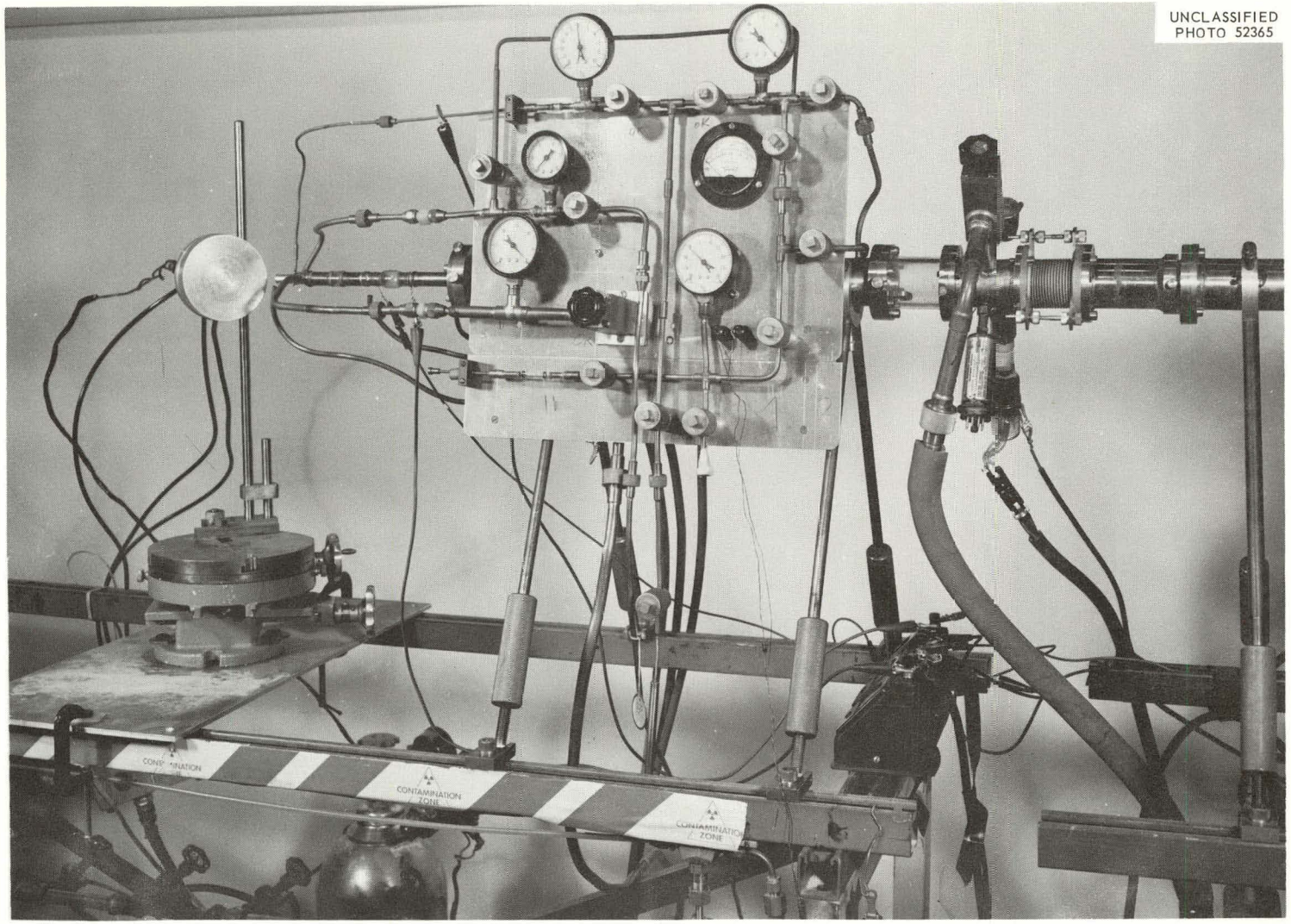


Fig. 7. Fission Counter and Gas Target Setup.

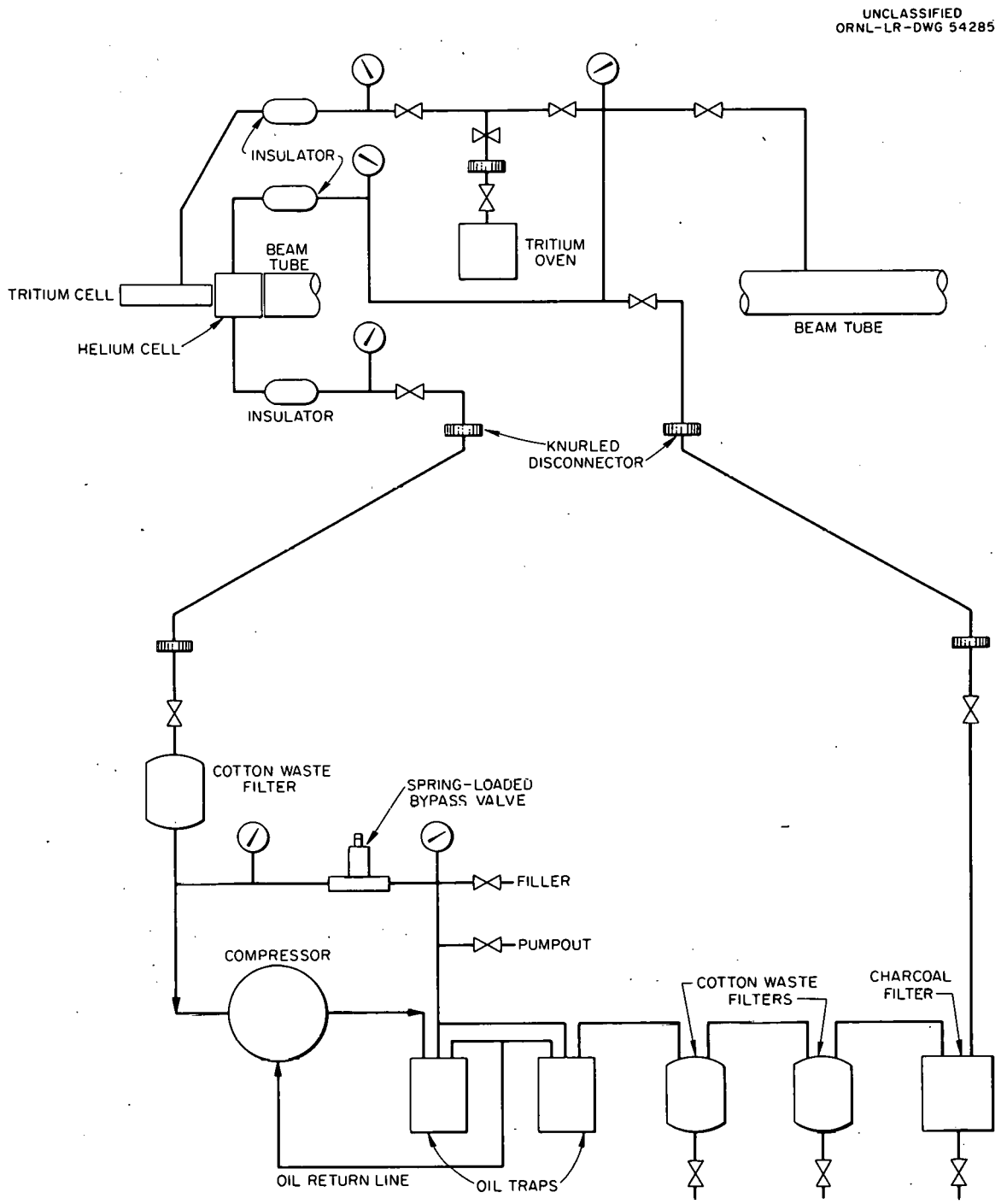


Fig. 8. Block Diagram of Tritium and Helium Systems.

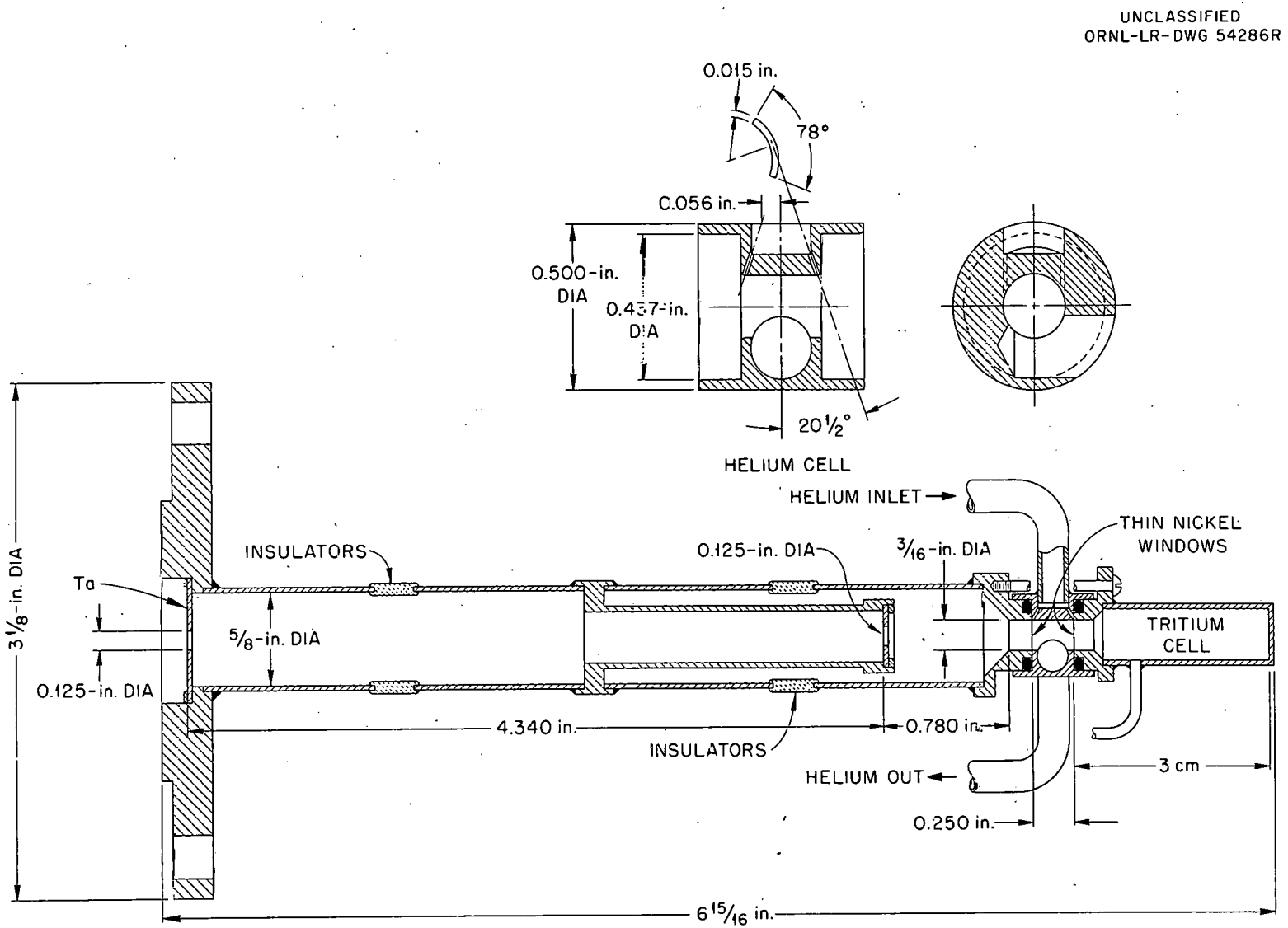


Fig. 9. Tritium Gas Target, Showing Expanded View of Helium Cell.

The entire system was made vacuum tight to helium leak detector standards. This was essential since with use the helium became highly contaminated with tritium. The permeability of a metal foil to a gas is an exponential function of temperature. The nickel foils ordinarily ran at a dull red heat, under which condition very little gas transfer took place between the tritium and helium cells, but local hot spots, which might approach the melting point of the nickel, were prone to develop from time to time usually due to instability of the beam diameter. Under these conditions transfer of helium and tritium would occur through the foil. Actual breakage took place quite frequently causing the loss of the tritium into the helium circulating system. Since this had been anticipated in its design, no harm was done other than the time lost in replacing the foil and recharging the tritium cell.

The foil on the vacuum side of the helium cell ruptured occasionally, permitting the contaminated helium to escape into the beam tube. A fast-operating magnetic vacuum valve was installed in the tube about three feet from the gas target, set to slam shut in response to a signal from an ion gauge which was located closer to the target. This ion gauge was connected to a meter and an electronic unit in the control room. Any sudden increase in pressure served to close the valve and also to remove the charging current from the Van de Graaff belt. This system worked so rapidly and well that a foil failure would not disturb the vacuum in the accelerator tube, and the operator was not required to take any action until he was ready to replace the foil.

The two 1/8" diameter beam collimators ahead of the gas cell were electrically isolated and connected through meters to ground. Current readings on these meters compared to that from the gas cell served as a fairly good check on alignment and also on the sharpness of focus. The importance of the sharpness of focus of the proton beam can be illustrated by the fact that foils which would operate perfectly at 22 microamperes with a properly diffuse beam would blow in a few seconds at 3 microamperes with a sharply focussed beam.

The current handling ability of the target depended on the effectiveness with which the foils could be cooled and also on the extent to which the beam could be made uniform in current density over a circle 1/8" in diameter. Both factors could undoubtedly be greatly improved. The geometry of the cooling cell was predicated largely on intuition. A more sophisticated program of development would almost certainly yield substantial improvement. No effort whatever was made to improve beam optics. Strong-focus lenses of the type commonly used nowadays on long beam tubes (one was used in this experiment) are notorious for the magnitudes of their aberrations. Improvement in beam uniformity would seem to offer considerable potential for improvement in current handling ability of the target. Developments along these lines were not pursued, however, since there were indications that future work might well be restricted to the 5-Mv generator which at the present time is not capable of producing even 22 microamperes with any sustained reliability. It is a matter of record that the target once operated at 33 microamperes for ten minutes without foil burnout. This

was, of course, on the small generator where beam optics are known to be superior. A 50 microampere target would seem to be a distinct possibility. However, to utilize this on the large generator would require drastic re-design of the entire optical system, probably even including electrode shapes in the upper half of the accelerator tube.

Summary. The equipment and methods of experimentation were designed to minimize the occurrence of systematic errors. An analysis of all known sources of such errors has been presented, from which the conclusion is drawn that all are negligible compared to statistical uncertainties with the exception of a small isotropic contribution to the angular distribution contributed by neutrons scattered from component parts of the counter, and the magnitude of this effect has been estimated in the Appendix.

There exist, of course, additional uncertainties arising from the finite spread in energy of the neutron beam and from the lack of sharpness in the angular distribution measurements. This angular spread amounted to a $5.2^{\circ}$ average angular uncertainty from the collimator, $4.5^{\circ}$ from the neutron beam, and an estimated $2^{\circ}$ in alignment of counter with the beam axis, all of which compounds to a total angular uncertainty of $7.1^{\circ}$.

A gas target was constructed which is capable of handling ten times the current of a conventional single-foil target. It can produce up to $1.2 \times 10^{10}$ neutrons per second at an average energy of 2.2 Mev and total energy spread of 60 kev.

# CHAPTER IV

## EXPERIMENTAL RESULTS

The original data taken during the course of these investigations comprised some 250 pages of observations of fission fragment angular distributions from U-235 and U-234 as well as total fission cross section measurements on U-234. They have been combined and grouped in Tables III to IX.

Table II lists absolute fission cross section measurements made on U-235 by B. C. Diven (Di57a) in the energy region between 400 and 1600 kev. This was a comparison experiment wherein the fission cross section was compared to the n-p scattering cross section by use of a double ionization chamber. The presently accepted values for U-235 in the Mev region as shown in Fig. 11 are based on these values and on others which have been normalized to them within this energy bracket. The rise in the cross section occurring at around 900 kev was investigated further by Diven (Di57b) with better neutron energy resolution, which showed that it is actually much more abrupt than the smoothed curve given in the Brookhaven Compilation, BNL-325 (Hu58). The rise must be interpreted as signifying the onset of fission through one or more new channels which become available at this energy. According to current theories this should (except for a rare coincidence) lead to a small change in the fragment angular distribution, and for this reason the (0/90) degree ratio of fragment intensities was measured over the energy range between 850 and 1050 kev with the best resolution

TABLE II

ABSOLUTE MEASUREMENTS OF $\sigma_f$(U-235) (Di57a)

| $E_n$(kev) | $\sigma_f$(barns) |
|---|---|
| 1620 ± 30 | 1.31 ± 0.05 |
| 1545 ± 32 | 1.30 ± 0.05 |
| 1424 ± 35 | 1.27 ± 0.04 |
| 1272 ± 35 | 1.27 ± 0.04 |
| 1171 ± 37 | 1.27 ± 0.04 |
| 1095 ± 39 | 1.27 ± 0.04 |
| 1025 ± 39 | 1.26 ± 0.05 |
| 944 ± 39 | 1.27 ± 0.05 |
| 865 ± 39 | 1.23 ± 0.06 |
| 770 ± 40 | 1.19 ± 0.06 |
| 673 ± 41 | 1.17 ± 0.06 |
| 562 ± 39 | 1.27 ± 0.07 |
| 513 ± 39 | 1.24 ± 0.07 |
| 403 ± 39 | 1.28 ± 0.08 |

obtainable from the gas target. No definite change was discernible within the limits of accuracy imposed by energy spread and counting statistics, but the points did seem to exhibit somewhat more marked deviations from the norm than did those lying outside this region of energy. This may be indicative of the presence of small fluctuations in angular distribution, closely spaced energywise, so that their true shape was obscured by the energy spread in the neutron beam. This would be logical, since the amplitudes of the fluctuations ought to be small because of the presence of many other channels already open to fission, and if the rise in cross section is abrupt the fluctuations should be close together in energy. However, the data are not adequate to support any conclusions other than to state that no large fluctuations take place.

The total fission cross section of U-234 was measured by comparison with U-235 in a double fission chamber (the one shown in Fig. 4 but without the collimators). Some of these measurements have already been described (La55), but for the purpose of more precisely determining the shape of the curve, many more measurements have been made, and Table V lists all measurements. The curve is presented in Fig. 12 with points omitted since their inclusion would, by their very number, obscure some of the detail in regions of interest.

The angular distribution measurements on U-235 as well as those on U-234 required corrections for a flux of neutrons scattered from components of the fission detector. This is discussed in the Appendix, and following the procedure outlined therein the magnitude of the

effective flux as a percentage of the primary flux is plotted as a function of energy in Fig. 10. As recounted in the Appendix the difference between the curve for U-235 and that for U-234 stems from the fact that some of the scattering was inelastic, and so degraded in energy below the fission threshold for U-234. The cross sections for computation of these curves were taken from the compilation of Howerton (Ho59) with some smoothing to allow for the neutron energy spread extant in this work. This spread was greater for the primary flux integrated over scattering objects than for the same flux incident on the fission foils since the scattering objects subtended a greater range of beam angle than did the foils.

Tables III and IV list the combined data on angular distributions from all runs on U-235. The tabulated counts have been normalized for foil inequalities by dividing the counts obtained from the rear (heavier) foil by the normalizing factor of 1.093. Counting statistics were calculated after normalization and so are slightly conservative. These and other uncertainties are expressed in per cent standard deviations. A 20% uncertainty is assumed to exist in the scattering correction so that where this correction alters the angular distribution by 1% an additional uncertainty of 0.2% is presumed to be introduced into the measurements by the inadequate knowledge of the nature of this scattered flux. This stems largely from lack of accurate knowledge of scattering cross sections. The source of error is unimportant for U-235 but for U-234 at 843 kev it becomes substantial.

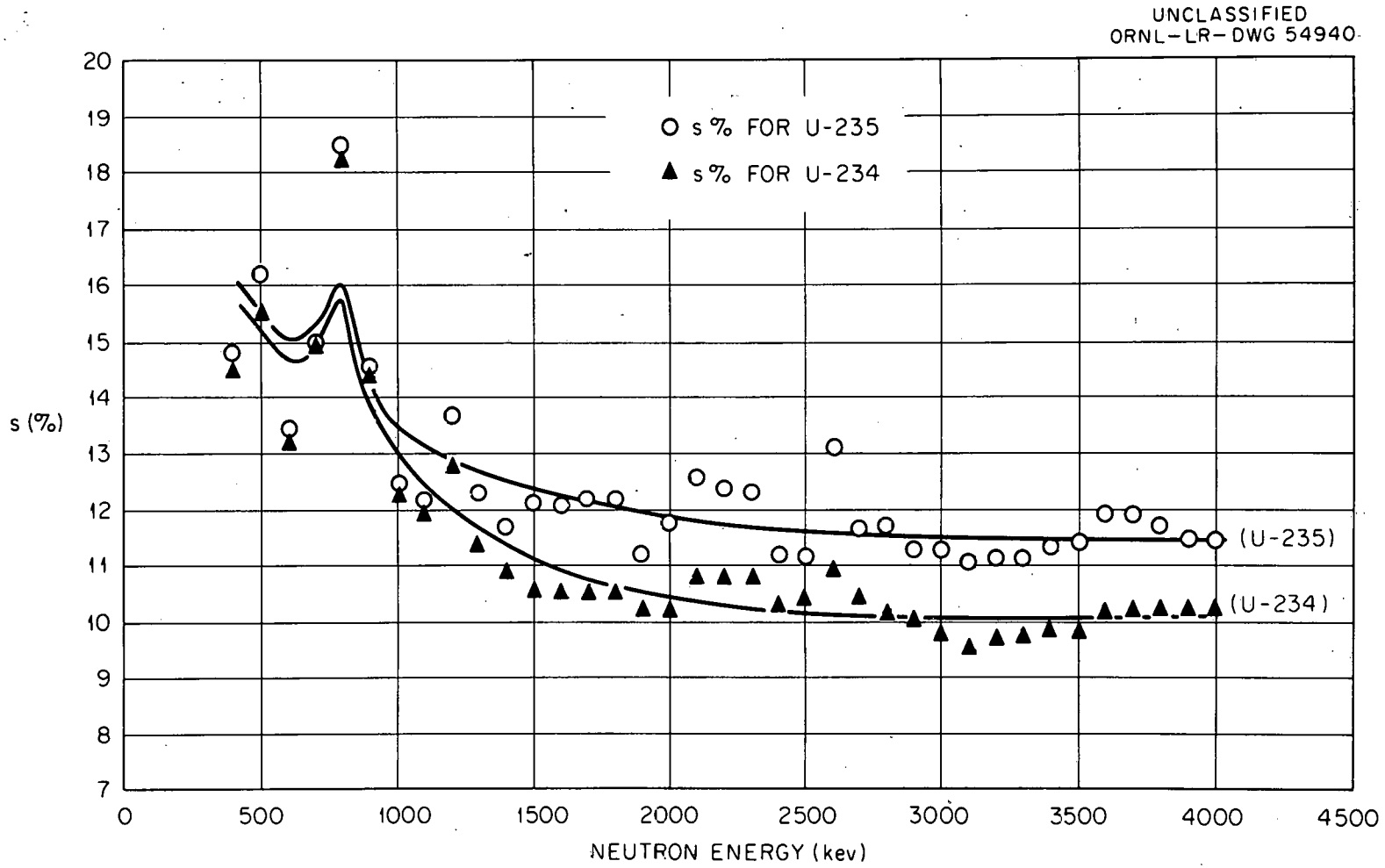


Fig. 10. Neutron Flux Scattered by Counter Components, and Effective in Causing Fission in the Uranium Foils. Expressed as a Percentage of the Primary Flux Incident on the Foils.

TABLE III

MEASUREMENTS OF FRAGMENT ANGULAR DISTRIBUTIONS FROM U-235 FISSION

| $E_n$(kev) | Fragment intensity ratio, R | | | | Per cent[a] uncertainties |
|---|---|---|---|---|---|
| | Observed | | Corrected for scattering | | |
| | (0/90) | (30/60) | (0/90) | (30/60) | |
| 424 ± 80 | 1.03 | | 1.04 | | 1.5 |
| 506 ± 75 | 1.05 | | 1.06 | | 1.7 |
| 617 ± 70 | 1.09 | | 1.10 | | 2.3 |
| 655 ± 65 | 1.07 | | 1.08 | | 2.3 |
| 698 ± 65 | 1.08 | | 1.09 | | 2.3 |
| 742 ± 68 | 1.08 | | 1.09 | | 1.7 |
| 805 ± 60 | 1.11 | | 1.13 | | 2.5 |
| 845 ± 62 | 1.07 | | 1.08 | | 2.2 |
| 845 ± 31 | 1.13 | 1.04 | 1.15 | 1.05 | 2.3 |
| 881 ± 31 | 1.13 | | 1.15 | | 2.5 |
| 940 ± 29 | 1.08 | | 1.09 | | 1.5 |
| 980 ± 31 | 1.13 | | 1.15 | | 2.4 |
| 1020 ± 59 | 1.10 | | 1.12 | | 1.7 |
| 1052 ± 30 | 1.13 | 1.06 | 1.15 | 1.07 | 2.5 |
| 1089 ± 50 | 1.10 | | 1.12 | | 2.4 |
| 1212 ± 57 | 1.10 | | 1.11 | | 1.7 |
| 1552 ± 55 | 1.13 | | 1.15 | | 2.3 |
| 1932 ± 49 | 1.13 | | 1.15 | | 2.4 |
| 2370 ± 46 | 1.13 | | 1.15 | | 2.4 |
| 3011 ± 37 | 1.14 | | 1.16 | | 1.5 |
| 3690 ± 39 | 1.14 | 1.03 | 1.16 | 1.04 | 1.7 |

[a] In these measurements the additional uncertainty introduced by the scattering correction is negligible in comparison with the statistical uncertainty so that this represents the totality of known sources of error. It is expressed in per cent standard deviations.

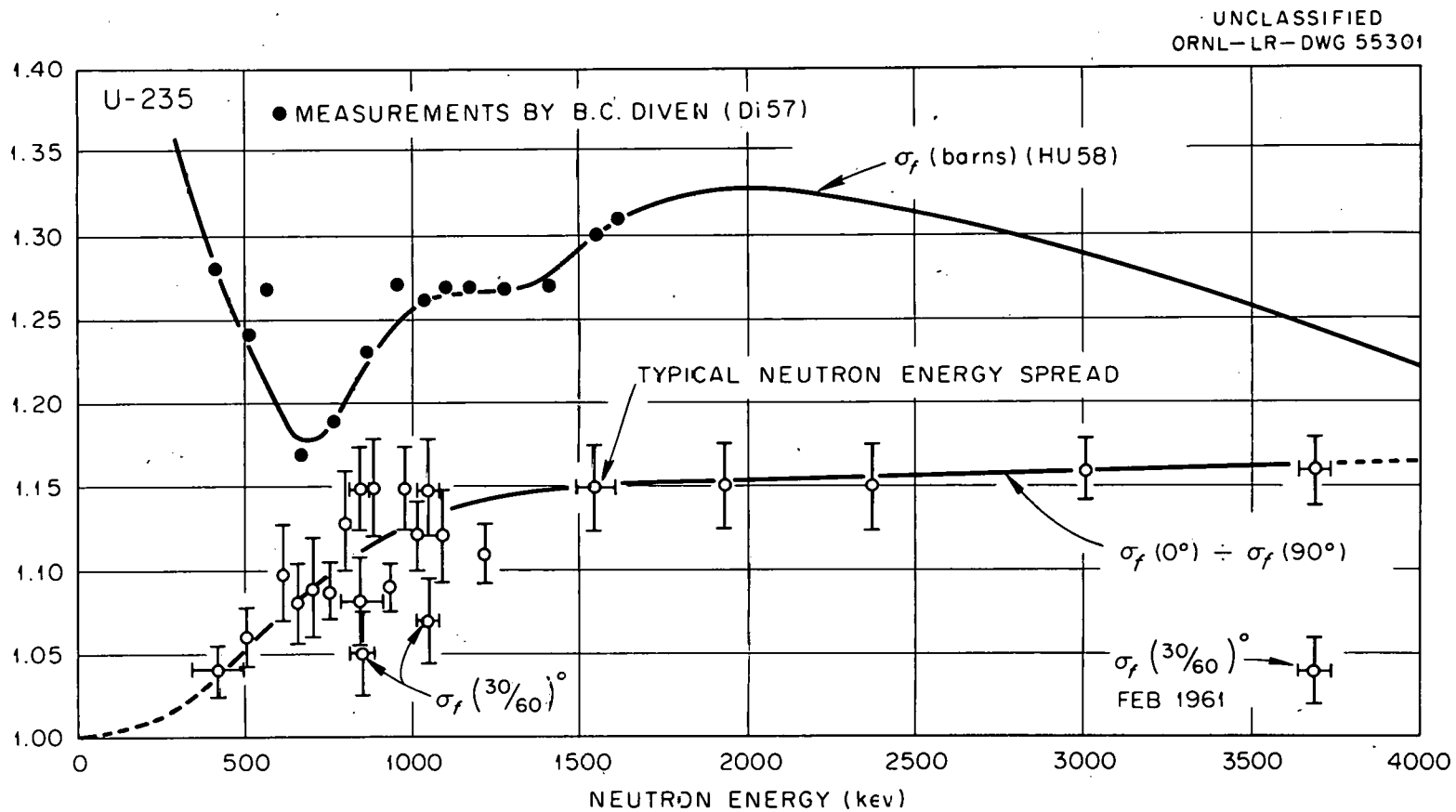


Fig. 11. Total Fission Cross Section, and Fragment Angular Distribution for $U^{235}$ Obtained from Neutron Induced Fission. The Lower Curve Shows the Ratio of Fragments Emitted at 0° to those Emitted at 90° with the Neutron Beam. The 3 Points so Marked are the Ratios of Fragments Emitted at 30° to those at 60°.

TABLE IV

NORMALIZED FOUR-POINT ANGULAR DISTRIBUTIONS FOR U-235 AT NEUTRON ENERGIES OF 844, 1052, AND 3690 KEV

| θ | Fission counts ÷ 64 | Monitor counts ÷ 40960 | Normalized ratios | Corrected for scattering | % uncertainties | | |
|---|---|---|---|---|---|---|---|
| | | | | | Counting | Scattering | Total |
| | | For 844 ± 42 kev incident neutrons | | | | | |
| 0 | 125.5 | 4821 | 1.100 | 1.115 | 1.12 | 0.30 | 1.16 |
| 30 | 57.5 | 2228 | 1.091 | 1.105 | 1.65 | 0.28 | 1.67 |
| 60 | 55.2 | 2228 | 1.047 | 1.054 | 1.68 | 0.14 | 1.69 |
| 90 | 114.1 | 4821 | 1.000 | 1.000 | 1.17 | 0 | 1.17 |
| | | For 1052 ± 30 kev incident neutrons | | | | | |
| 0 | 51.3 | 1998 | 1.125 | 1.142 | 1.75 | 0.34 | 1.79 |
| 30 | 49.2 | 1974 | 1.092 | 1.104 | 1.79 | 0.24 | 1.81 |
| 60 | 46.2 | 1974 | 1.025 | 1.028 | 1.84 | 0.06 | 1.84 |
| 90 | 45.6 | 1998 | 1.000 | 1.000 | 1.85 | 0 | 1.85 |
| | | For 3690 ± 39 kev incident neutrons | | | | | |
| 0 | 108.3 | 965.6 | 1.138 | 1.154 | 1.20 | 0.32 | 1.24 |
| 30 | 105.8 | 983.2 | 1.091 | 1.101 | 1.22 | 0.20 | 1.24 |
| 60 | 103.1 | 983.2 | 1.064 | 1.071 | 1.23 | 0.14 | 1.24 |
| 90 | 95.2 | 965.6 | 1.000 | 1.000 | 1.28 | 0 | 1.28 |

The U-234 angular distribution data required an additional correction for the small percentage of U-235 contaminant. This was always small and the error introduced thereby is negligible in comparison with counting statistics. The data from all runs have been collected and tabulated in Table VI after this simple correction was made. Tables VII, VIII, and IX list in greater detail the results for the three energies at which more complete angular distribution measurements were made. Normalization against the long counter monitor permits intensities at all angles to be related to that at 90 degrees which has been arbitrarily set equal to unity. The point at 843 kev was further corrected for the effect of neutron energy spread in reducing the observed value of the peak in the distribution below its true height. Since the actual shape of the peak is not known, only an approximate correction can be made. A sine shape was assumed with a peak at 843 kev and zero amplitude at 643 and 1043 kev for the plot of

$$A = \frac{\sigma_f(\theta)^\circ - \sigma_f(90)^\circ}{\sigma_f(90)^\circ},$$

then

$$A = A_o \sin \frac{\pi}{400} (E - 643).$$

Averaging over a neutron energy spread of $\pm$ 39 kev about the peak shows that the measured A was 1% below the true value, $A_o$. Although the actual shape of the curve is probably not sinusoidal it is felt that the inclusion of a correction of this form brings the results

TABLE V

MEASUREMENTS OF THE FISSION CROSS SECTION OF U-234 TO 4054 KEV

| $E_n$ (kev) | $\frac{\sigma_f(\text{U-234})}{\sigma_f(\text{U-235})}$ | $\sigma_f$(U-235)[a] in barns | $\sigma_f$(U-234) in barns | Per cent[b] counting statistics |
|---|---|---|---|---|
| | Run No. 1. Neutrons from Li(p,n) reaction | | | |
| 50 ± 25[c] | 0.014 | | | 10 |
| 136 ± 14 | 0.021 | 1.64 | 0.034 | 8.7 |
| 163 ± 14 | 0.025 | 1.57 | 0.039 | 7.7 |
| 186 ± 14 | 0.030 | 1.51 | 0.045 | 6.8 |
| 211 ± 14 | 0.034 | 1.47 | 0.050 | 6.2 |
| 235 ± 14 | 0.041 | 1.44 | 0.059 | 5.3 |
| 258 ± 14 | 0.048 | 1.40 | 0.067 | 4.6 |
| 280 ± 14 | 0.068 | 1.37 | 0.093 | 2.5 |
| 302 ± 14 | 0.102 | 1.35 | 0.138 | 1.9 |
| 325 ± 14 | 0.121 | 1.32 | 0.160 | 1.8 |
| 348 ± 14 | 0.118 | 1.31 | 0.154 | 1.8 |
| 369 ± 14 | 0.143 | 1.30 | 0.186 | 1.6 |
| 390 ± 14 | 0.180 | 1.28 | 0.231 | 1.4 |
| 412 ± 14 | 0.216 | 1.28 | 0.276 | 1.3 |
| 433 ± 14 | 0.266 | 1.27 | 0.338 | 1.1 |

[a] These values are from the second edition (1958) of BNL-325 (Hu58) and were up to date as of January, 1961.

[b] These are believed to reflect the accuracy to which the cross section ratios were measured, other known sources of error being small by comparison (La55). However, the possibility of systematic error cannot be excluded, but would not be expected to exceed one per cent. The uncertainty in the U-234 cross section is therefore defined principally by that of U-235, which is of the order of five per cent.

[c] This "point" was obtained by bombarding Li-7 with protons just enough above threshold (1882 kev) to give a maximum neutron energy of 68 kev. Due to center-of-mass motion they are not mono-energetic at this low energy.

TABLE V (continued)

| $E_n$ (kev | $\frac{\sigma_f(U\text{-}234)}{\sigma_f(U\text{-}235)}$ | $\sigma_f(U\text{-}235)$ in barns | $\sigma_f(U\text{-}234)$ in barns | Per cent counting statistics |
|---|---|---|---|---|
| 455 ± 14 | 0.329 | 1.26 | 0.415 | 1.1 |
| 476 ± 14 | 0.367 | 1.25 | 0.459 | 1.0 |
| 487 ± 14 | 0.385 | 1.25 | 0.481 | 1.3 |
| 498 ± 14 | 0.428 | 1.25 | 0.535 | 0.9 |
| 509 ± 14 | 0.455 | 1.24 | 0.564 | 1.3 |
| 520 ± 13 | 0.510 | 1.24 | 0.633 | 0.9 |
| 531 ± 13 | 0.531 | 1.24 | 0.659 | 1.2 |
| 542 ± 13 | 0.578 | 1.23 | 0.711 | 0.9 |
| 553 ± 13 | 0.577 | 1.23 | 0.710 | 1.2 |
| 563 ± 13 | 0.595 | 1.22 | 0.726 | 0.8 |
| 574 ± 13 | 0.598 | 1.22 | 0.730 | 1.1 |
| 584 ± 13 | 0.623 | 1.21 | 0.754 | 0.8 |
| 595 ± 13 | 0.635 | 1.21 | 0.768 | 1.1 |
| 606 ± 13 | 0.644 | 1.20 | 0.773 | 1.1 |
| Run No. 2. Neutrons from T(p,n) reaction. Zrt target. | | | | |
| 501 ± 21 | 0.398 | 1.25 | 0.497 | 1.4 |
| 604 ± 21 | 0.610 | 1.20 | 0.732 | 1.1 |
| 655 ± 22 | 0.729 | 1.20 | 0.874 | 1.1 |
| 706 ± 22 | 0.832 | 1.19 | 0.990 | 1.0 |
| 756 ± 22 | 1.032 | 1.18 | 1.22 | 1.0 |
| Run No. 3. Neutrons from T(p,n) reaction. Gas target. | | | | |
| 565 ± 30 | 0.543 | 1.22 | 0.662 | 1.2 |
| 583 ± 31 | 0.573 | 1.21 | 0.693 | 1.2 |
| 600 ± 31 | 0.602 | 1.20 | 0.722 | 1.2 |
| 617 ± 31 | 0.629 | 1.20 | 0.755 | 1.1 |
| 637 ± 32 | 0.665 | 1.20 | 0.798 | 1.1 |
| 656 ± 32 | 0.725 | 1.20 | 0.870 | 1.1 |
| 675 ± 32 | 0.754 | 1.19 | 0.897 | 1.1 |
| 692 ± 32 | 0.820 | 1.19 | 0.976 | 1.0 |
| 711 ± 33 | 0.828 | 1.19 | 0.985 | 1.0 |
| 730 ± 33 | 0.904 | 1.18 | 1.07 | 1.0 |

TABLE V (continued)

| $E_n$(kev) | $\frac{\sigma_f(\text{U-234})}{\sigma_f(\text{U-235})}$ | $\sigma_f$(U-235) in barns | $\sigma_f$(U-234) in barns | Per cent counting statistics |
|---|---|---|---|---|
| 750 ± 32 | 0.937 | 1.18 | 1.11 | 0.7 |
| 773 ± 30 | 1.02 | 1.17 | 1.19 | 0.6 |
| 790 ± 32 | 1.05 | 1.17 | 1.23 | 1.0 |
| 810 ± 26 | 1.07 | 1.17 | 1.25 | 0.7 |
| 830 ± 31 | 1.07 | 1.17 | 1.25 | 1.0 |
| 848 ± 26 | 1.06 | 1.17 | 1.24 | 0.7 |
| 868 ± 31 | 1.06 | 1.18 | 1.25 | 1.0 |
| 888 ± 25 | 1.03 | 1.19 | 1.23 | 1.0 |
| 907 ± 30 | 0.986 | 1.20 | 1.18 | 1.0 |
| 925 ± 25 | 0.953 | 1.21 | 1.15 | 1.0 |
| 945 ± 30 | 0.939 | 1.23 | 1.15 | 1.0 |
| 965 ± 24 | 0.917 | 1.24 | 1.14 | 1.0 |
| 986 ± 30 | 0.884 | 1.24 | 1.10 | 1.0 |
| 1003 ± 27 | 0.901 | 1.24 | 1.12 | 1.0 |
| 1025 ± 29 | 0.865 | 1.24 | 1.07 | 1.0 |
| 1041 ± 27 | 0.875 | 1.25 | 1.09 | 1.0 |
| 1066 ± 29 | 0.896 | 1.25 | 1.12 | 1.0 |
| 1083 ± 26 | 0.921 | 1.25 | 1.15 | 1.0 |
| 1105 ± 29 | 0.941 | 1.26 | 1.18 | 1.0 |
| 1127 ± 26 | 0.952 | 1.26 | 1.20 | 1.0 |
| 1147 ± 28 | 0.957 | 1.27 | 1.21 | 1.0 |
| 1169 ± 32 | 0.952 | 1.27 | 1.21 | 1.0 |
| 1188 ± 29 | 0.962 | 1.27 | 1.22 | 1.0 |
| 1206 ± 32 | 0.962 | 1.27 | 1.23 | 1.0 |
| 1224 ± 31 | 0.958 | 1.27 | 1.22 | 1.0 |
| 1246 ± 31 | 0.954 | 1.28 | 1.22 | 1.0 |
| 1265 ± 31 | 0.975 | 1.28 | 1.25 | 1.0 |
| 1286 ± 32 | 0.981 | 1.28 | 1.25 | 0.8 |
| 1304 ± 31 | 0.972 | 1.28 | 1.24 | 1.0 |
| 1326 ± 32 | 0.992 | 1.28 | 1.27 | 1.0 |

TABLE V (continued)

| $E_n$(kev) | $\frac{\sigma_f(\text{U-234})}{\sigma_f(\text{U-235})}$ | $\sigma_f$(U-235) in barns | $\sigma_f$(U-234) in barns | Per cent counting statistics |
|---|---|---|---|---|
| 1348 ± 31 | 1.00 | 1.28 | 1.28 | 1.0 |
| 1369 ± 33 | 0.991 | 1.28 | 1.27 | 1.0 |
| 1390 ± 30 | 1.00 | 1.29 | 1.29 | 1.0 |
| 1411 ± 32 | 1.01 | 1.29 | 1.30 | 1.0 |
| 1493 ± 32 | 1.04 | 1.29 | 1.34 | 1.0 |
| 1516 ± 30 | 1.03 | 1.30 | 1.34 | 1.0 |
| 1535 ± 32 | 1.06 | 1.30 | 1.38 | 1.0 |
| 1557 ± 31 | 1.07 | 1.30 | 1.39 | 1.0 |
| 1579 ± 32 | 1.09 | 1.30 | 1.42 | 1.0 |
| 1602 ± 31 | 1.10 | 1.31 | 1.44 | 1.0 |
| 1624 ± 32 | 1.12 | 1.31 | 1.47 | 0.7 |
| 1644 ± 31 | 1.12 | 1.31 | 1.47 | 1.0 |
| 1668 ± 30 | 1.13 | 1.31 | 1.48 | 1.0 |
| 1689 ± 31 | 1.13 | 1.31 | 1.48 | 1.0 |
| 1774 ± 30 | 1.13 | 1.32 | 1.49 | 1.0 |
| 1797 ± 31 | 1.14 | 1.32 | 1.50 | 1.0 |
| 1817 ± 31 | 1.15 | 1.32 | 1.52 | 1.0 |
| 1861 ± 31 | 1.16 | 1.32 | 1.53 | 1.0 |
| 1908 ± 31 | 1.16 | 1.33 | 1.54 | 1.0 |
| 1952 ± 31 | 1.16 | 1.33 | 1.54 | 1.0 |
| 1996 ± 32 | 1.15 | 1.33 | 1.53 | 1.0 |
| 2062 ± 34 | 1.13 | 1.33 | 1.50 | 1.0 |
| 2108 ± 28 | 1.12 | 1.33 | 1.49 | 1.0 |
| 2152 ± 28 | 1.13 | 1.33 | 1.50 | 1.0 |
| 2200 ± 28 | 1.12 | 1.33 | 1.49 | 1.0 |
| 2249 ± 28 | 1.13 | 1.32 | 1.49 | 1.0 |
| 2297 ± 29 | 1.12 | 1.32 | 1.48 | 1.0 |
| 2343 ± 29 | 1.12 | 1.32 | 1.48 | 1.0 |
| 2390 ± 29 | 1.13 | 1.32 | 1.49 | 1.0 |
| 2438 ± 30 | 1.13 | 1.32 | 1.49 | 1.0 |

TABLE V (continued)

| $E_n$(kev) | $\frac{\sigma_f(U\text{-}234)}{\sigma_f(U\text{-}235)}$ | $\sigma_f(U\text{-}235)$ in barns | $\sigma_f(U\text{-}234)$ in barns | Per cent counting statistics |
|---|---|---|---|---|
| 2487 ± 30 | 1.13 | 1.32 | 1.49 | 1.0 |
| 2537 ± 30 | 1.14 | 1.31 | 1.49 | 1.0 |
| 2587 ± 30 | 1.16 | 1.31 | 1.52 | 1.0 |
| 2636 ± 31 | 1.15 | 1.31 | 1.51 | 1.0 |
| 2688 ± 31 | 1.17 | 1.30 | 1.52 | 1.0 |
| 2735 ± 31 | 1.18 | 1.30 | 1.53 | 1.0 |
| 2785 ± 32 | 1.17 | 1.30 | 1.52 | 1.0 |
| 2835 ± 32 | 1.17 | 1.30 | 1.52 | 1.0 |
| 2887 ± 32 | 1.17 | 1.30 | 1.52 | 1.0 |
| 2939 ± 33 | 1.18 | 1.29 | 1.52 | 1.0 |
| 2990 ± 33 | 1.18 | 1.29 | 1.52 | 1.0 |
| Run No. 4. Neutrons from T(p,n) reaction. Gas target. | | | | |
| 1451 ± 45 | 1.02 | 1.29 | 1.32 | 0.36 |
| 1739 ± 41 | 1.14 | 1.31 | 1.49 | 0.36 |
| 1910 ± 41 | 1.16 | 1.33 | 1.54 | 0.90 |
| 2034 ± 39 | 1.15 | 1.33 | 1.53 | 0.36 |
| 2305 ± 36 | 1.13 | 1.32 | 1.49 | 0.90 |
| 2697 ± 39 | 1.14 | 1.30 | 1.48 | 0.90 |
| 2834 ± 45 | 1.17 | 1.30 | 1.52 | 0.36 |
| 3184 ± 44 | 1.19 | 1.28 | 1.52 | 0.90 |
| 3222 ± 50 | 1.20 | 1.28 | 1.53 | 0.36 |
| 3595 ± 47 | 1.22 | 1.25 | 1.52 | 0.90 |
| 3807 ± 54 | 1.22 | 1.24 | 1.51 | 0.36 |
| Run No. 5. Neutrons from T(p,n) reaction. Gas target. | | | | |
| 1430 ± 32 | 1.02 | 1.29 | 1.32 | 2.1 |
| 1485 ± 32 | 1.03 | 1.29 | 1.33 | 2.8 |
| 1524 ± 32 | 1.09 | 1.30 | 1.42 | 2.0 |
| 1616 ± 32 | 1.13 | 1.31 | 1.48 | 2.6 |
| 1712 ± 33 | 1.15 | 1.31 | 1.51 | 2.8 |
| 1760 ± 33 | 1.12 | 1.32 | 1.48 | 2.7 |
| 1807 ± 34 | 1.11 | 1.32 | 1.47 | 2.8 |
| 1854 ± 34 | 1.21 | 1.32 | 1.60 | 2.8 |

TABLE V (concluded)

| $E_n$(kev) | $\frac{\sigma_f(\text{U-234})}{\sigma_f(\text{U-235})}$ | $\sigma_f$(U-235) in barns | $\sigma_f$(U-234) in barns | Per cent counting statistics |
|---|---|---|---|---|
| 1902 ± 34 | 1.17 | 1.33 | 1.56 | 2.7 |
| 1953 ± 34 | 1.19 | 1.33 | 1.58 | 2.7 |
| 2004 ± 34 | 1.19 | 1.33 | 1.58 | 2.7 |
| 2104 ± 35 | 1.13 | 1.33 | 1.50 | 2.8 |
| 2200 ± 36 | 1.14 | 1.33 | 1.52 | 2.7 |
| 2251 ± 37 | 1.14 | 1.32 | 1.51 | 2.8 |
| 2302 ± 38 | 1.11 | 1.32 | 1.47 | 2.1 |
| 2353 ± 38 | 1.12 | 1.32 | 1.48 | 2.7 |
| 2404 ± 38 | 1.13 | 1.32 | 1.49 | 2.8 |
| 2506 ± 40 | 1.11 | 1.31 | 1.45 | 2.1 |
| 2609 ± 41 | 1.16 | 1.31 | 1.52 | 2.7 |
| 2719 ± 43 | 1.16 | 1.30 | 1.51 | 1.6 |
| 2822 ± 44 | 1.16 | 1.30 | 1.51 | 2.8 |
| 2876 ± 44 | 1.15 | 1.30 | 1.50 | 2.7 |
| 2929 ± 44 | 1.21 | 1.29 | 1.56 | 2.1 |
| 2982 ± 44 | 1.19 | 1.29 | 1.54 | 2.7 |
| 3035 ± 45 | 1.20 | 1.29 | 1.55 | 2.1 |
| 3090 ± 45 | 1.19 | 1.29 | 1.54 | 2.7 |
| 3145 ± 46 | 1.16 | 1.28 | 1.49 | 2.1 |
| 3200 ± 47 | 1.21 | 1.28 | 1.55 | 2.7 |
| 3255 ± 48 | 1.19 | 1.28 | 1.52 | 2.0 |
| 3365 ± 48 | 1.21 | 1.27 | 1.54 | 2.7 |
| 3479 ± 49 | 1.21 | 1.26 | 1.53 | 2.7 |
| 3591 ± 50 | 1.23 | 1.25 | 1.54 | 2.7 |
| 3703 ± 51 | 1.21 | 1.24 | 1.50 | 2.7 |
| 3761 ± 52 | 1.16 | 1.24 | 1.44 | 2.5 |
| 3819 ± 52 | 1.18 | 1.24 | 1.46 | 2.1 |
| 3878 ± 52 | 1.22 | 1.23 | 1.50 | 2.7 |
| 3936 ± 53 | 1.20 | 1.23 | 1.48 | 2.1 |
| 3995 ± 53 | 1.18 | 1.23 | 1.45 | 2.8 |
| 4054 ± 54 | 1.20 | 1.22 | 1.46 | 2.8 |

TABLE VI

MEASUREMENTS OF FRAGMENT ANGULAR DISTRIBUTIONS FROM U-234 FISSION

| $E_n$(kev) | Fragment intensity ratio, R: Observed (0/90) | Observed (30/60) | Corrected for scattering (0/90) | Corrected for scattering (30/60) | % uncertainties[a]: Counting | Scattering | Total |
|---|---|---|---|---|---|---|---|
| 410 ± 40 | 0.70 | | 0.65 | | 2.42 | 1.54 | 2.9 |
| 503 ± 37 | 0.57 | | 0.50 | | 1.97 | 2.80 | 3.4 |
| 615 ± 30 | 0.93 | | 0.92 | | 2.23 | 0.22 | 2.3 |
| 644 ± 36 | 0.97 | | 0.96 | | 3.16 | 0.21 | 3.2 |
| 690 ± 34 | 1.08 | | 1.09 | | 1.71 | 0.19 | 1.8 |
| 750 ± 36 | 1.43 | | 1.50 | | 1.22 | 0.93 | 1.6 |
| 805 ± 30 | 1.63 | | 1.73 | | 1.57 | 1.16 | 2.0 |
| 843 ± 30 | 1.70 | 1.34 | 1.80 | 1.39 | 1.06 | 1.11 | 1.53 |
| | | | | | | 0.72 | 1.28 |
| 887 ± 30 | 1.62 | | 1.70 | | 1.50 | 0.94 | 1.8 |
| 944 ± 31 | 1.48 | | 1.54 | | 1.53 | 0.78 | 1.8 |
| 988 ± 31 | 1.28 | | 1.32 | | 1.63 | 0.61 | 1.8 |
| 1020 ± 35 | 1.11 | | 1.13 | | 1.66 | 0.36 | 1.7 |
| 1051 ± 28 | 1.11 | 1.06 | 1.13 | 1.07 | 1.15 | 0.36 | 1.20 |
| | | | | | | 0.19 | 1.17 |
| 1081 ± 34 | 1.09 | | 1.11 | | 1.68 | 0.36 | 1.7 |
| 1206 ± 42 | 1.14 | | 1.16 | | 1.74 | 0.35 | 1.8 |
| 1542 ± 42 | 1.20 | | 1.22 | | 1.72 | 0.33 | 1.8 |
| 1915 ± 43 | 1.20 | | 1.22 | | 1.75 | 0.33 | 1.8 |
| 2345 ± 38 | 1.18 | | 1.20 | | 1.67 | 0.33 | 1.7 |
| 3008 ± 28 | 1.18 | | 1.20 | | 1.64 | 0.33 | 1.7 |
| 3735 ± 28 | 1.19 | 1.09 | 1.21 | 1.10 | 1.00 | 0.33 | 1.05 |
| | | | | | | 0.18 | 1.02 |

[a]The scattering and total uncertainties for the (30/60) degree ratios are listed directly below those for the (0/90) degree ratios.

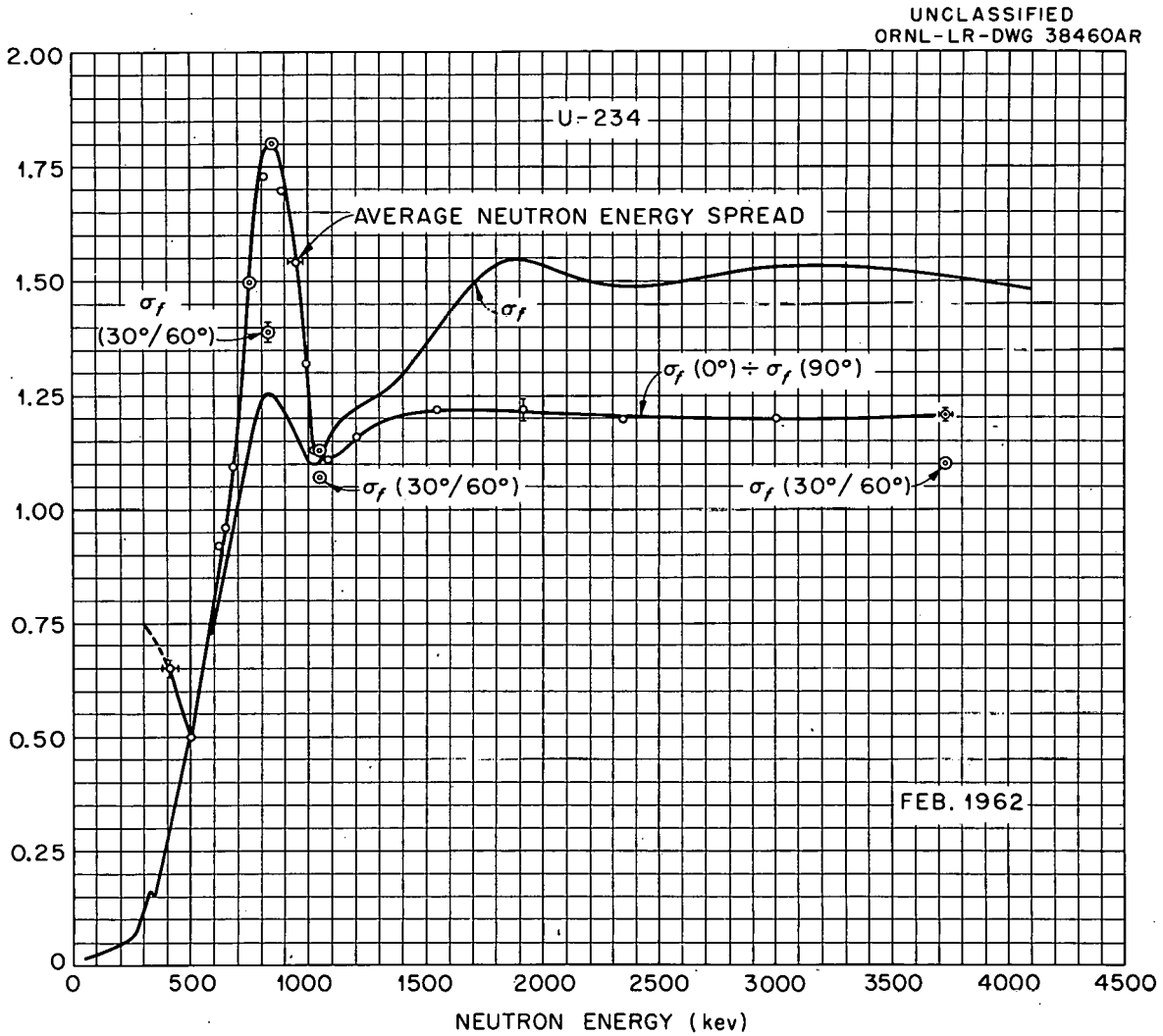


Fig. 12. Total Neutron-Induced Fission Cross Section, and Ratio of Fragments Emitted at 0° to those Emitted at 90° to Neutron Beam Axis. The Three Points so Marked are the Ratios of Fragments Emitted at 30° to those Emitted at 60°.

TABLE VII

FOUR-POINT ANGULAR DISTRIBUTION FOR U-234 AT 843 KEV

| | Run S3 | | | Run L5 | | | Total |
|---|---|---|---|---|---|---|---|
| θ | Fission counts ÷ 64 | Monitor counts ÷ 40960 | Normalized ratios | Fission counts ÷ 64 | Monitor counts ÷ 40960 | Normalized ratios | fission counts ÷ 64 |
| 0 | 176.1 | 4978 | 1.655 | 178.7 | 2012 | 1.673 | 354.8 |
| 30 | 151.6 | 4931 | 1.438 | 156.5 | 2010 | 1.467 | 308.1 |
| 60 | 116.0 | 4931 | 1.101 | 117.8 | 2010 | 1.104 | 233.8 |
| 90 | 106.4 | 4978 | 1.000 | 106.8 | 2012 | 1.000 | 213.2 |

| | Net normalized fission ratios | Corrected for | | | % uncertainties | | | |
|---|---|---|---|---|---|---|---|---|
| θ | | U-235 | Neutron energy spread | Scattering | Counting | Energy spread | Scattering | Total |
| 0 | 1.664 | 1.679 | 1.686 | 1.786 | 0.66 | 0.42 | 1.12 | 1.37 |
| 30 | 1.453 | 1.463 | 1.468 | 1.536 | 0.71 | 0.34 | 0.89 | 1.20 |
| 60 | 1.102 | 1.103 | 1.104 | 1.119 | 0.82 | 0.10 | 0.27 | 0.87 |
| 90 | 1.000 | 1.000 | 1.000 | 1.000 | 0.86 | 0 | 0 | 0.86 |

TABLE VIII

FOUR-POINT ANGULAR DISTRIBUTION FOR U-234 AT 1051 KEV

| | Run S4 | | Run L4 | | | Run L6 | | |
|---|---|---|---|---|---|---|---|---|
| θ | Fission counts ÷ 64 | Normalized ratios | Fission counts ÷ 64 | Monitor counts ÷ 40960 | Normalized ratios | Fission counts ÷ 64 | Monitor counts ÷ 40960 | Normalized ratios |
| 0 | 52.7 | 1.079 | 103.6 | 1735 | 1.098 | 114.3 | 1988 | 1.137 |
| 30 | 0 | | 99.7 | 1712 | 1.070 | 109.9 | 1976 | 1.100 |
| 60 | 0 | | 93.2 | 1712 | 1.001 | 104.1 | 1976 | 1.042 |
| 90 | 48.9 | 1.000 | 94.4 | 1735 | 1.000 | 100.5 | 1988 | 1.000 |

| θ | Net normalized fission ratios | Corrected for | | % uncertainties | | |
|---|---|---|---|---|---|---|
| | | U-235 | Scattering | Counting | Scattering | Total |
| 0 | 1.110 | 1.110 | 1.124 | 0.65 | 0.28 | 0.71 |
| 30 | 1.085 | 1.085 | 1.096 | 0.86 | 0.22 | 0.89 |
| 60 | 1.022 | 1.022 | 1.025 | 0.89 | 0.06 | 0.89 |
| 90 | 1.000 | 1.000 | 1.000 | 0.90 | 0 | 0.90 |

TABLE IX

FOUR-POINT ANGULAR DISTRIBUTION FOR U-234 AT 3735 KEV

| | Run L1 | | | Run L3 | | | Run L4 | | |
|---|---|---|---|---|---|---|---|---|---|
| θ | Fission counts ÷ 64 | Monitor counts ÷ 40960 | Normalized ratios | Fission counts ÷ 64 | Monitor counts ÷ 40960 | Normalized ratios | Fission counts ÷ 64 | Monitor counts ÷ 40960 | Normalized ratios |
| 0 | 107.2 | 839.2 | 1.193 | 109.4 | 733.2 | 1.178 | 117.0 | 1013 | 1.199 |
| 30 | 105.9 | 839.6 | 1.178 | 106.1 | 741.4 | 1.130 | 110.1 | 1023 | 1.117 |
| 60 | 95.9 | 839.6 | 1.067 | 98.8 | 741.4 | 1.052 | 102.5 | 1023 | 1.040 |
| 90 | 89.9 | 839.2 | 1.000 | 92.9 | 733.2 | 1.000 | 97.6 | 1013 | 1.000 |

| | | | Corrected for | | % uncertainties | | |
|---|---|---|---|---|---|---|---|
| θ | Total counts ÷ 64 | Net normalized fission ratios | U-235 | Scattering | Counting | Scattering | Total |
| 0 | 333.6 | 1.190 | 1.191 | 1.210 | 0.69 | 0.34 | 0.77 |
| 30 | 322.2 | 1.141 | 1.142 | 1.156 | 0.70 | 0.24 | 0.74 |
| 60 | 297.2 | 1.053 | 1.053 | 1.058 | 0.73 | 0.09 | 0.73 |
| 90 | 280.4 | 1.000 | 1.000 | 1.000 | 0.75 | 0 | 0.75 |

closer to reality and also serves to indicate the order of magnitude of error to be expected from this source. A true evaluation would involve runs with successively thinner targets and an extrapolation of shape to zero energy spread, which is impractical due to the smallness of the effect and the low count rate obtainable.

The possibility of thermalized room-scattered neutrons affecting the angular distribution measurements on U-235 was considered, and to check on this the counter was surrounded with a 0.020 inch thick shield of cadmium. Ratios of $\sigma_f(0/90)^\circ$ were measured at energies of 424, 506, 742, 845, 940, and 1020 kev and compared to similar measurements without the cadmium. Agreement was within statistics and the averaged ratios with and without cadmium both amounted to 1.07. Consequently this effect, although certainly present, was too small to be detected. It would lie in a direction to make the measured ratios closer to unity than they should be.

These results are subjected to further analyses in the next chapter.

# CHAPTER V

## COMPARISON OF RESULTS WITH THEORY

An effort will be made in this chapter to determine the channels contributing to the fission of U-234 near threshold and also to assign very approximate relative strengths to them. This is accomplished by combining theory and experiment in a manner which correlates the experimental results as closely with the theory as possible subject to the requirement that the results make sense. (For example a negative magnitude for a channel strength does not make sense.)

In addition to the shape of the angular distribution it is also possible to make quantitative estimates of the maximum possible contribution which can be made by a given channel. Such limiting values are found by calculating a differential cross section, $\sigma_K(\Theta)$, for formation of a compound nucleus with angular momentum component K along the symmetry axis z', which is oriented at an angle $\Theta$ with respect to the laboratory z axis, taken as the direction of the beam of neutrons incident on the U-234 target. The method of accomplishing this is on fairly solid ground, the major inaccuracy resting with the neutron transmission factors, $T_\ell^+$ (Pe62). The differential cross section obtained in this way may be integrated to find the reaction cross section, $\sigma_r$.

$$\sigma_r = \sigma_f + \sigma_{nn'} + \sigma_{ce} + \sigma_\gamma \simeq \sigma_f + \sigma_n \ ,$$

where:

$\sigma_f$ = total fission cross section.

$\sigma_{nn'}$ = cross section for inelastic neutron scattering.

$\sigma_{ce}$ = compound-elastic cross section (neutron leaves the compound nucleus by its entrance channel).

$\sigma_{\gamma}$ = absorption cross section. Negligible for fast neutrons in comparison with $\sigma_f$ or $\sigma_n$.

$\sigma_n \equiv \sigma_{nn'} + \sigma_{ce}$.

$\sigma_f$ is available to good accuracy from experiment, so $\sigma_n$ can be found from this and the calculated $\sigma_r$. $\sigma_{ce}$ is not needed for the channel analysis. It can be obtained by a Hauser-Feshbach (Ha52) analysis once $\sigma_n$ has been calculated. It will be of the order of a barn at one Mev but will fall rapidly as the excitation energy increases since additional channels come in ever more rapidly. The ratio $\sigma_f/\sigma_n$, which is usually referred to in the literature as $\Gamma_f/\Gamma_n$, is of direct interest to the channel analysis. It is this factor and the calculated angular distributions for the various K bands that are combined with the experimental angular distribution to delineate the modes contributing to fission. Most unfortunately however the $\Gamma_f/\Gamma_n$ calculated above is an average over all channels whereas what is desired is this ratio for each separate channel. This is not obtainable with any reasonable accuracy and herein lies the point of greatest uncertainty in the evaluation of fission level strengths. Only very crude estimates can be made of $\gamma \equiv \Gamma_f/\Gamma_t = \Gamma_f/(\Gamma_f + \Gamma_n)$ for the individual channels at this stage of our knowledge. This should be kept clearly in mind in what is to follow as it is for this reason that the estimates of channel strengths must be regarded as indicative only of sensible, but not unique assignments.

For a U-234 target no attempt is made to recognize individual channels above a bombarding energy of 1050 kev, and not at all for U-235 since statistical methods would need to be resorted to, and in order to obtain useful information from such methods it is necessary to have a large amount of information on one or more nuclei. Statistical methods differ sharply from those found useful for single channel analyses so are not discussed in this paper. Some excellent experimental work at higher neutron bombarding energies where such a method applies has been carried out by Simmons and Henkel (Si61). Analyses of this and other work have been made by various authors, notably in the works of Griffin, Halpern, and Strutinski listed in the Bibliography.

The non-local optical potentials of Perey and Buck (Pe62) have been used to obtain transmission factors, $T_\ell^{\pm}$, for neutron energies of 500, 850, and 1050 kev. Through the courtesy of F. Perey machine calculations were carried out which yielded the scattering matrix S.

$$S_\ell = (S_r + iS_i)_\ell \,. \tag{11}$$

$$|S^{\pm}|_\ell^2 = |S_r^{\pm}|_\ell^2 + |S_i^{\pm}|_\ell^2 \,. \tag{11a}$$

$$T_\ell^{\pm} = 1 - |S^{\pm}|_\ell^2 \,. \tag{11b}$$

$$\sigma_r = \pi\lambda^2 \sum_\ell \left[(\ell+1)T_\ell^{+} + \ell T_\ell^{-}\right] = \pi\lambda^2 \sum_\ell (2\ell+1)\gamma_\ell \,, \tag{12}$$

where

$$\gamma_\ell \equiv \frac{1}{2\ell+1}\left[(\ell+1)T_\ell^{+} + \ell T_\ell^{-}\right] . \tag{12a}$$

The $\gamma_\ell$ is a statistical average of $T_\ell^{+}$ and $T_\ell^{-}$ and can be compared directly with the more usual $T_\ell$ factors such as those of Emmerich (Em58). The more sophisticated $T_{\ell I}$ (for reactions where channel spin

has only a single value, such as for neutrons on spin-zero targets where this can be written simply as $T_{\ell}^{+-}$) include the effects of spin-orbit coupling and should therefore be somewhat more accurate, particularly for differential cross sections. Note that the cross section for formation of a compound nucleus with spin I may be written:

$$\sigma_I = \frac{\pi\lambda^2}{2} \sum_{\ell} (2I+1) T_{\ell I} \ . \tag{13}$$

The partial reaction cross sections $\sigma_c(\ell)$ are shown on Fig. 13. The strong p-wave interaction is characteristic of the fissionable nuclei under neutron bombardment.

## I. DERIVATION OF K-BAND DIFFERENTIAL CROSS SECTIONS

To derive the differential cross section consider now a plane wave of spinless (spin will be introduced later on) particles traveling in the z direction. Such a wave has the form $e^{ikz}$, which for $kr >> \ell$ approaches the asymptotic expression:

$$\frac{1}{kr} \sum_{\ell} \sqrt{\pi(2\ell+1)}\, i^{\ell+1} \left\{ \exp\left[-i\left(kr - \frac{\ell\pi}{2}\right)\right] - \exp\left[i\left(kr - \frac{\ell\pi}{2}\right)\right] \right\} Y_{\ell,o}(\theta) =$$
$$\frac{1}{kr} \sum_{\ell} \sqrt{\pi(2\ell+1)}\, i^{\ell+1} \left\{ A_i - A_o \right\} Y_{\ell,o}(\theta). \tag{14}$$

The outgoing part, $A_o$, of this wave will be modified by collision with the target nucleus so that the result will be:

$$\psi_r = \frac{1}{kr} \sum_{\ell} \sqrt{\pi(2\ell+1)}\, i^{\ell+1} \left\{ A_i - \eta_\ell A_o \right\} Y_{\ell,o}(\theta). \tag{15}$$

Along the z axis ($\theta=0$), using the relation

$$Y_{\ell m}(o,\phi) = \sqrt{\frac{2\ell+1}{4\pi}}\, \delta_{m,o} \ ,$$

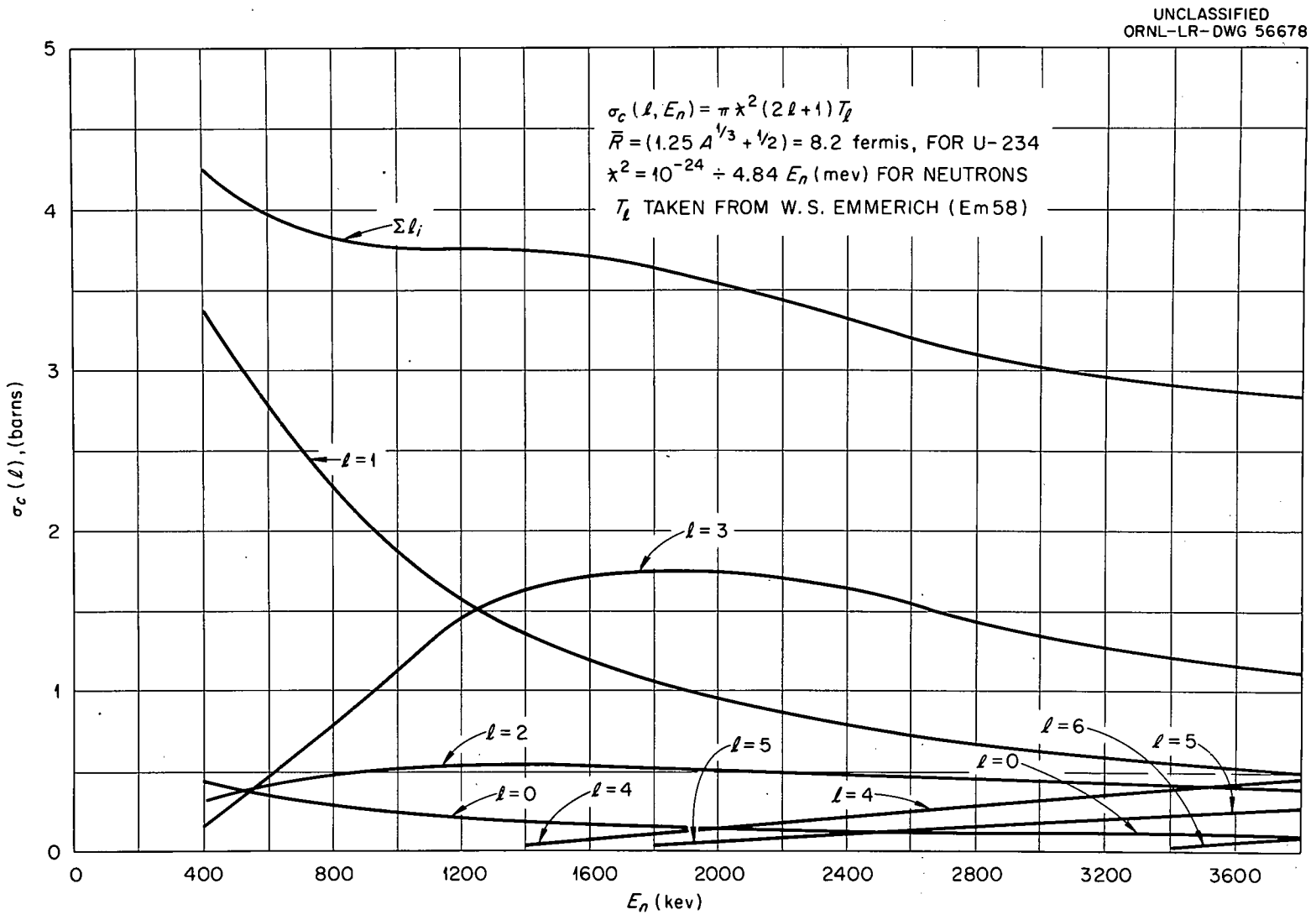


Fig. 13. Partial Cross Section for the Formation of Compound Nucleus by Neutrons on $U^{234}$.

this becomes:

$$\psi_r(0) = \frac{\lambda\!\!\!^{-}}{2r} \sum_{\ell} (2\ell+1) i^{\ell+1} \left\{ A_i - \eta_\ell A_o \right\} . \tag{15a}$$

The compound nucleus formed by the absorption of a neutron will in general be deformed. Consider axes to be fixed in this nucleus such that z' is along the major symmetry axis, and take $\beta$ to be the angle between the z and z' axes. Then the orientation of the body-fixed (primed) axes relative to the laboratory (unprimed) axes is defined by the D function, $D^I_{MK}(\alpha\beta\gamma)$ (See Appendix D), so that

$$\psi_r(\beta) = \psi_r(0) D^I_{MK}(\alpha\beta\gamma) . \tag{15b}$$

Let the incident flux be $N = v = \hbar/M\lambda\!\!\!^{-}$, and the absorbed flux be $N_r$. Then $\sigma_r = N_r/N$ and (Bℓ52, page 321):

$$d\sigma_r = - \frac{M\lambda\!\!\!^{-}}{\hbar} \frac{\hbar}{2iM} \left[ \frac{\partial \psi'_r}{\partial r} \psi_r^* - \frac{\partial \psi'^*_r}{\partial r} \psi_r \right] r^2 d\Omega . \tag{16}$$

$$\sigma_r(\beta) = - \frac{\lambda\!\!\!^{-2}}{8i} \sum_{\ell} (2\ell+1)^2 \left[ -ik(A_i + \eta_\ell A_o)(A_i^* - \eta_\ell^* A_o^*) - ik(A_i^* + \eta_\ell^* A_o)(A_i - \eta_\ell A_o) \right] D^I_{MK}(\alpha\beta\gamma) D^{*I}_{MK}(\alpha\beta\gamma) =$$

$$\frac{\lambda\!\!\!^{-2}}{4} \sum_{\ell} (2\ell+1)^2 \left[ 1 - |\eta_\ell|^2 \right] D^* D . \tag{17}$$

The specific nuclear factors are contained in the $\eta_\ell$.

$$1 - |\eta_\ell|^2 = \sum_{Ijm} |\langle IKM(R) j\ell mo \rangle|^2$$

$$= \sum_{Ijm} |\langle IK(R) j\ell \rangle \, C^{j\ell I}_{moM}|^2$$

$$= \sum_{Ijm} \frac{2I+1}{(2j+1)(2\ell+1)} \, T_{\ell I} \, |C^{j\ell I}_{mom}|^2 \, . \qquad (18)$$

The effect of the channel spin, j, having z component m now appears for the first time, whereas in a rigorous development it would have been introduced at the very beginning, which would have immensely complicated the development without changing the result. The reason that its introduction can be postponed until this point is that the cross section is an <u>average</u> over incoming spin states and such an average is independent of the choice of reference axes. This is discussed in Bl52 but can be easily visualized without recourse to mathematics. It would of course <u>not</u> be true for cases where polarization or alignment exists, thus rendering certain m values more probable than others. Buck and Satchler (Bu62) have derived the cross section for compound nucleus formation in terms of the transmission factors by the more detailed method wherein channel spin is introduced at the outset. In addition the spin functions are orthogonal so that:

$$\int \chi^j_\Omega \, \chi^{j'}_{\Omega'} \, d\tau = \delta_{jj'} \, \delta_{\Omega\Omega'} \, , \qquad (19)$$

where integration extends over the nuclear volume.

In the general case it is however necessary at this point to take account of possible interference effects between different orbital

angular momenta, $\ell$, as these being part of the same wave are coherent. But in the special but very commonly occurring case where spin-half particles are incident on spin-zero targets, such as is the situation here, there will be no interference between $\ell$ values because parity effects insure that only a single $\ell$ wave can contribute to a given compound state, $(I\pi)$. Therefore, bearing in mind that the equation is specifically for even-even targets one can write:

$$\sigma(\beta) = \frac{\lambda^2}{4} \sum_{Ijm\ell} \frac{(2I+1)(2\ell+1)}{2j+1} T_{\ell I} \left| C^{j\ell I}_{mom} \right|^2 \left| D \right|^2 . \qquad (20)$$

$$\sigma(\beta) = \frac{\lambda^2}{8} \sum_{Im\ell} (2I+1)(2\ell+1)\, T_{\ell I} \left| C^{1/2\ell I}_{mom} \right|^2 \left| D \right|^2 . \qquad (20a)$$

But (Ro57):

$$\left| D \right|^2 = (-1)^{m-K} D^I_{-m,-K}(\alpha\beta\gamma) D^I_{mK}(\alpha\beta\gamma) = (-1)^{m-K} \sum_{\lambda} C^{II\lambda}_{mmo} C^{II\lambda}_{-KKo} P_\lambda(\cos\beta). \qquad (20b)$$

So:

$$\sigma_K(\beta) = \frac{(-1)^{-K}\lambda^2}{8} \sum_{xI\ell m} (2I+1)(2\ell+1) T_{\ell I} C^{IIx}_{-KKo} P_x (-1)^m C^{IIx}_{-mmo} \left| C^{1/2\ell I}_{mom} \right|^2 \qquad (20c)$$

From Appendix D:

$$\sum_m (-1)^m C^{j\ell I}_{mom} C^{j\ell' I}_{mom} C^{IIx}_{-mmo} = (-1)^{x-j} (2I+1) C^{\ell\ell' x}_{ooo} W(\ell\ell' II; xj). \qquad (20d)$$

$$C^{\ell\ell' x}_{ooo} W(\ell\ell' II; xj) = \frac{Z(\ell I \ell' I, jx)}{(2I+1)\sqrt{(2\ell+1)(2\ell'+1)}} (-1)^{1/2(x+\ell'-\ell)}$$

$$= \frac{\bar{Z}(\ell I \ell' I, jx)}{(2I+1)\sqrt{(2\ell+1)(2\ell'+1)}} . \qquad (20e)$$

So:

$$\sigma_K(\beta) = \frac{(-1)^{-K-1/2}\lambda^2}{8} \sum_{xI\ell} (-1)^{x/2}(2I+1)T_{\ell I}C^{IIx}_{-KKo}Z(\ell I\ell I,1/2x)P_x$$

$$= \frac{(-1)^{-K-1/2}\lambda^2}{8} \sum_{xI\ell} (2I+1)T_{\ell I}C^{IIx}_{-KKo}\bar{Z}(\ell I\ell I,1/2x)P_x$$

$$= \frac{\lambda^2}{4} \sum_{\ell I} (2I+1)T_{\ell I}W(KI) \ , \qquad (21)$$

where

$$W(KI) \ \frac{(-1)^{-K-1/2}}{2} \sum_x (-1)^{x/2}C^{IIx}_{-KKo}Z(\ell I\ell I,1/2x)P_x \ . \qquad (21a)$$

Clearly the W(KI) must be closely related to the square of the D functions and must involve a sum over possible m values ($m = \pm 1/2$), and further it must depend only on $\beta$ and hence on the small d function, $d^I_{MK}(\beta)$. The relation is:

$$W(KI) = (1/4)(2I+1)\left[\left|d^I_{1/2,K}(\beta)\right|^2 + \left|d^I_{-1/2,K}(\beta)\right|^2\right] . \qquad (21b)$$

The angle $\beta$ is the second Euler angle in the rotation $\alpha\beta\gamma$ and so corresponds to $\theta$ in the notation $(\phi\ \theta\Psi)$ and since it is usual to express angular distributions in terms of $\theta$, henceforth $\beta$ will be replaced with $\theta$, recalling that this angle refers to the probability distribution of the symmetry axis of the spheroidal compound nucleus, and thus to the direction of fragment emission.

Interference effects will not be observed among the outgoing fragments because each exit channel as defined here by what a simple ion chamber measures contains many modes which are summed over, thereby washing out the interference effects from close-lying $I\pi$ levels, and

yielding the symmetry about 90° which is characteristic of fission fragment angular distributions. Consequently only even powers of x appear in the summation in terms of the Legendre polynomials, $P_x(\cos\Theta)$. Now replace $T_{\ell_I}$ by $T_\ell^{\pm} \equiv T(\ell, I=\ell \pm 1/2)$. Then the expressions pertinent to channel analysis may be written in an easily remembered array which brings out the physical significance of the parameters with clarity. The $\sigma_{K\pi}(\Theta)$ are the cross sections for formation of a compound nucleus with a component, K of angular momentum along the major symmetry axis, and with that axis oriented at an angle $\Theta$ with the neutron beam, i.e., a K-band differential cross section. The angular dependence for the band as a whole does depend on parity because the relative strengths of the levels within a band depend on the transmission factors. These factors for even $\ell$ values will be found only in the even parity K bands and those with odd $\ell$ in the odd parity bands.

$$
\begin{aligned}
\sigma(\Theta)_{1/2-} &= \frac{\lambda^2}{2}\left[T_1^- W(\tfrac{1}{2}\,\tfrac{1}{2}) + 2T_1^+ W(\tfrac{1}{2}\,\tfrac{3}{2}) + 3T_3^- W(\tfrac{1}{2}\,\tfrac{5}{2}) + 4T_3^+ W(\tfrac{1}{2}\,\tfrac{7}{2}) + \ldots\right],\\
\sigma(\Theta)_{1/2+} &= \frac{\lambda^2}{2}\left[T_0 W(\tfrac{1}{2}\,\tfrac{1}{2}) + 2T_2^- W(\tfrac{1}{2}\,\tfrac{3}{2}) + 3T_2^+ W(\tfrac{1}{2}\,\tfrac{5}{2}) + \ldots\right],\\
\sigma(\Theta)_{3/2-} &= \frac{\lambda^2}{2}\left[2T_1^+ W(\tfrac{3}{2}\,\tfrac{3}{2}) + 3T_3^- W(\tfrac{3}{2}\,\tfrac{5}{2}) + 4T_3^+ W(\tfrac{3}{2}\,\tfrac{7}{2}) + \ldots\right],\\
\sigma(\Theta)_{3/2+} &= \frac{\lambda^2}{2}\left[2T_2^- W(\tfrac{3}{2}\,\tfrac{3}{2}) + 3T_2^+ W(\tfrac{3}{2}\,\tfrac{5}{2}) + \ldots\right],\\
\sigma(\Theta)_{5/2-} &= \frac{\lambda^2}{2}\left[3T_3^- W(\tfrac{5}{2}\,\tfrac{5}{2}) + 4T_3^+ W(\tfrac{5}{2}\,\tfrac{7}{2}) + \ldots\right],\\
\sigma(\Theta)_{5/2+} &= \frac{\lambda^2}{2}\left[3T_2^+ W(\tfrac{5}{2}\,\tfrac{5}{2}) + \ldots\right],\\
\sigma(\Theta)_{7/2-} &= \frac{\lambda^2}{2}\left[4T_3^+ W(\tfrac{7}{2}\,\tfrac{7}{2}) + \ldots\right].
\end{aligned}
\qquad (22)
$$

TABLE X

THE W(KI) AS FUNCTIONS OF $\theta$

| $\theta^\circ$ | $W(\frac{1}{2}\ \frac{3}{2})$ | $W(\frac{1}{2}\ \frac{5}{2})$ | $W(\frac{1}{2}\ \frac{7}{2})$ | $W(\frac{3}{2}\ \frac{3}{2})$ | $W(\frac{3}{2}\ \frac{5}{2})$ | $W(\frac{3}{2}\ \frac{7}{2})$ | $W(\frac{5}{2}\ \frac{5}{2})$ | $W(\frac{5}{2}\ \frac{7}{2})$ | $W(\frac{7}{2}\ \frac{7}{2})$ |
|---|---|---|---|---|---|---|---|---|---|
| 0 | 1.0000 | 1.5000 | 2.0000 | 0 | 0 | 0 | 0 | 0 | 0 |
| 5 | .9943 | 1.4773 | 1.9437 | .0057 | .0226 | .0560 | .0001 | .0003 | .0000 |
| 10 | .9774 | 1.4112 | 1.7839 | .0226 | .0879 | .2111 | .0009 | .0050 | .0000 |
| 15 | .9498 | 1.3075 | 1.5464 | .0502 | .1883 | .4296 | .0042 | .0236 | .0003 |
| 20 | .9123 | 1.1747 | 1.2679 | .0877 | .3124 | .6622 | .0128 | .0682 | .0018 |
| 25 | .8660 | 1.0240 | .9882 | .1340 | .4461 | .8573 | .0299 | .1483 | .0062 |
| 30 | .8125 | .8672 | .7427 | .1875 | .5742 | .9741 | .0586 | .2661 | .0171 |
| 35 | .7533 | .7160 | .5555 | .2467 | .6826 | .9915 | .1015 | .4141 | .0389 |
| 40 | .6901 | .5806 | .4360 | .3099 | .7594 | .9123 | .1600 | .5745 | .0771 |
| 45 | .6250 | .4688 | .3789 | .3750 | .7969 | .7617 | .2344 | .7227 | .1367 |
| 50 | .5599 | .3852 | .3678 | .4401 | .7920 | .5793 | .3228 | .8319 | .2210 |
| 55 | .4967 | .3312 | .3805 | .5033 | .7467 | .4086 | .4221 | .8804 | .3304 |
| 60 | .4375 | .3047 | .3960 | .5625 | .6680 | .2856 | .5273 | .8569 | .4614 |
| 65 | .3840 | .3009 | .3991 | .6160 | .5666 | .2303 | .6325 | .7644 | .6061 |
| 70 | .3377 | .3129 | .3839 | .6623 | .4561 | .2423 | .7310 | .6206 | .7531 |
| 75 | .3002 | .3332 | .3540 | .6998 | .3507 | .3028 | .8161 | .4549 | .8883 |
| 80 | .2726 | .3541 | .3191 | .7274 | .2641 | .3810 | .8818 | .3021 | .9978 |
| 85 | .2557 | .3694 | .2916 | .7443 | .2073 | .4446 | .9233 | .1948 | 1.0690 |
| 90 | .2500 | .3750 | .2813 | .7500 | .1875 | .4688 | .9375 | .1563 | 1.0938 |

NOTE: $W(KI) \equiv \frac{(-1)^{-K-1/2}}{2} \sum_x (-1)^{x/2} C^{IIx}_{-KKO} Z(\ell_I \ell_I, 1/2x) P_x(\cos\theta)$.

$\int_{-1}^{+1} W(KI)\,d(\cos\theta) = 1$. $W(\frac{1}{2}\ \frac{1}{2}) = 1/2$ for all angles.

The W(KI) are positive definite functions of $\Theta$ symmetrical about $90^{\circ}$. They have been tabulated up to K = I = 7/2 by Mrs. Nancy Dismuke of the ORNL Math. Group. Figure 14 shows a plot of these functions, and numerical values are listed in Table X. They may also be expressed simply in terms of the Legendre Polynomials, $P_x(\cos \Theta)$; the more common ones are given in Table XI.

TABLE XI

THE W(KI) EXPRESSED IN TERMS OF THE LEGENDRE POLYNOMIALS.

| | Coefficients of: | | | |
|---|---|---|---|---|
| W(KI) | $P_o$ | $P_2$ | $P_4$ | $P_6$ |
| $(\frac{1}{2},\frac{1}{2})$ | .5 | | | |
| $(\frac{1}{2},3/2)$ | .5 | .5 | | |
| (3/2,3/2) | .5 | -.5 | | |
| $(\frac{1}{2},5/2)$ | .5 | .571 | .429 | |
| (3/2,5/2) | .5 | .144 | -.644 | |
| $(\frac{1}{2},7/2)$ | .5 | .597 | .527 | .379 |
| (3/2,7/2) | .5 | .359 | -.176 | -.682 |

The W(KI) as defined above are automatically normalized so that:

$$\int_{-1}^{+1} W(KI)\, d\,(\cos \Theta) = 1.$$

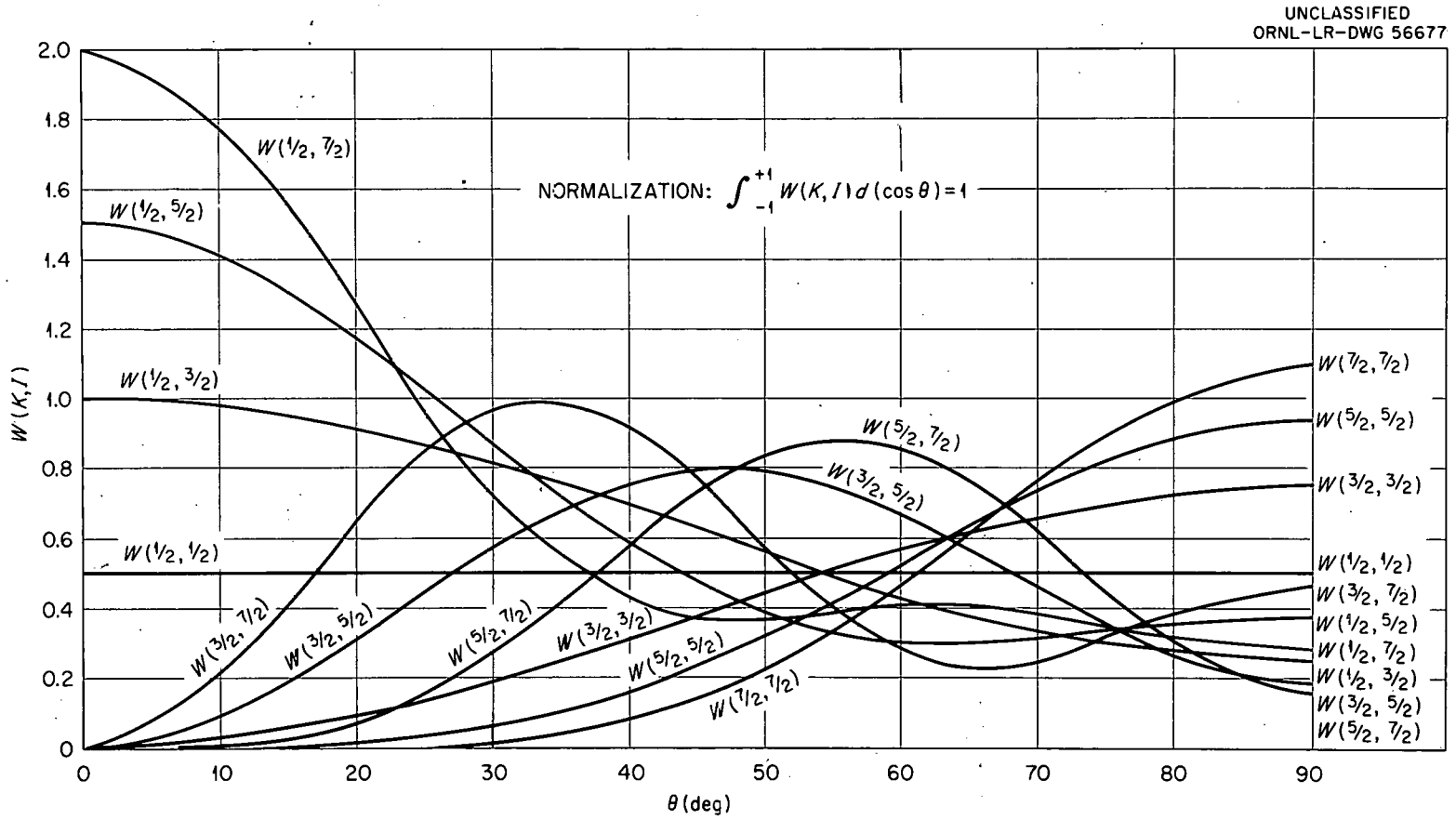


Fig. 14. Theoretical Fission Fragment Angular Distributions for Fission Through Pure Rotational States, W(K,I).

Consequently the integrated cross section becomes:

$$\sigma_{K\pi} = \pi \lambda\!\!\!^{-2} \left[\text{sum of coefficients of the } W(KI)\right]_{K\pi} . \quad (23)$$

$$\sigma_r \equiv \text{reaction cross section} = \sigma_{1/2+} + \sigma_{1/2-}$$

$$= \frac{\pi \lambda\!\!\!^{-2}}{2} \sum_{\ell I} (2I+1) T(\ell I) \delta(\ell I \tfrac{1}{2} = \Delta) = \pi \lambda\!\!\!^{-2} \sum_{\ell} (2\ell+1) \gamma_\ell , \quad (24)$$

where

$$\gamma_\ell \equiv \sum_I \frac{(2I+1)T(\ell I)}{(2j+1)(2\ell+1)} \xrightarrow[j=1/2]{=} \frac{(\ell+1)T_\ell^{+} + \ell T_\ell^{-}}{2\ell+1} . \quad (24a)$$

A partial cross section, $\sigma(\Theta)_{K\pi}$, would yield a fission fragment angular distribution directly only in the unlikely situation where all capture decayed by fission through the $(K\pi)$ band. Then the coefficients of the $W(KI)$ would give the relative probabilities of fission via the various $(KI\pi)$ levels within that band. The same would still be true if two bands differing in parity coexisted. If two bands of like parity coexisted then the coefficients of the $W(KI)$ of this common parity would equal the sum of the fission probabilities through the two levels of the same $(I\pi)$.

Actually however, neutron emission always competes very strongly ($\Gamma_n / \Gamma_f > 1$ usually) with fission and with unequal strengths for different levels. Accurate predictions of fission fragment angular distribution could in theory be made providing the locations of the first few K bands near saddle point were known along with the signs of the decoupling constants in the case of $K = 1/2$ bands, and if all levels open to neutron decay in the target nucleus were known as well as the laws

governing decay to such levels. Turning the thing about, experimental measurements of some of these things may yield information about others. For example, fission measurements may provide information on inelastic neutron scattering processes as well as on the relative locations of $(K\pi)$ bands in highly distorted nuclei.

## II. DECAY BY NEUTRON EMISSION

Neutron emission, by proceeding more readily from some compound states than others causes the relative level strengths for fission through a given K band to differ from the relative formation strengths. To make an estimate of this effect a modified HF analysis was carried out to find the relative ease of neutron emission, $P(I\pi)$, from each of the $(I\pi)$ levels. This was done for incident neutron energies of 500, 850, and 1050 kev. $P(I\pi) = \sum_{i'} T_{\ell'}(E_n')$ summed over all possible decay channels and, hopefully, to all available levels, i', in U-234. Table XII shows these levels. Note that three have been postulated on the basis of nuclear systematics. Decay to these three is comparatively light due either to their high spin or energy. Decay to the ground state gives rise to the so-called compound-elastic scattering. The $P(I\pi)$ include this, of course, but the relative probabilities of decay to the ground level were also separated out and used with other factors to compute $\sigma_{ce}$, the compound-elastic scattering cross section, a quantity which cannot be directly measured. As a matter of general interest the complete tabulation is given in Table XIII, whereas the summations used in the fission analysis are given in Table XIV. The transmission

factors used in their computation were those of Emmerich (Em58) since the PB factors are not yet available as functions of energy. For lack of better information, decay to the beta and octupole levels were treated on the same basis as decays to the ground state band.

Table XV lists a few nuclear parameters determined from combination of theory and the experimentally evaluated fission cross sections. The capture cross section is assumed to be negligible compared to fission and neutron emission. The total, scattering, and reaction cross sections have been obtained from machine calculations using the PB potentials through the courtesy of Francis Perey. The cross section for neutron emission, $\sigma_n$, is taken as the difference between this reaction cross section, $\sigma_r$, and the measured fission cross section, $\sigma_f$. Then $\Gamma_n/\Gamma_f$, a function pertinent to fission fragment angular distribution analysis, is simply $\sigma_n/\sigma_f$. This is, of course, the average over all channels. $\sigma_{ce}$ is obtained then from the HF analysis and $\sigma_n$.

One can see by inspection that neutron emission should not appreciably affect the relative intensities of fission from levels within any given K band except the two 1/2 bands. For these, the ground state levels would be expected to have higher $\Gamma_f/\Gamma_n$ than the average over all levels within the band. At 500 kev since $(\overline{\Gamma_n/\Gamma_f}) \gg 1$ the individual $\Gamma_f/\Gamma_t = \Gamma_f/(\Gamma_f + \Gamma_n)$ may be taken as very nearly in inverse proportion to the $P(I\pi)$. At the higher energies a somewhat more accurate but still quite approximate method is used.

The major sources of error are believed to lie with the assumptions. For example, it has been assumed that inelastic neutron scattering

TABLE XII

ENERGY LEVELS IN U-234 (Ga59, Wo60)

| E(kev) | K | Iπ | Type of Level | Comments |
|---|---|---|---|---|
| 984 | 0 | 5- | Octupole | Postulated |
| 952 | 0 | 4+ | Beta | Ditto |
| 858 | 0 | 3- | Octupole | Ditto |
| 854 | 0 | 2+ | Beta | Observed |
| 812 | 0 | 0+ | Beta | Ditto |
| 788 | 0 | 1- | Octupole | Ditto |
| 290 | 0 | 6+ | Gnd. state rot. band | Observed |
| 143 | 0 | 4+ | Ditto | Observed |
| 43 | 0 | 2+ | Ditto | Ditto |
| 0 | 0 | 0+ | Gnd. state | -- |

TABLE XIII

DECAY OF U-235* BY NEUTRON EMISSION[a]

| | | | | $E_n$ = 500 | | $E_n$ = 850 | | $E_n$ = 1050 | |
|---|---|---|---|---|---|---|---|---|---|
| $I\pi$ | $i'\pi$ | $j'$ | $\ell'$ | $E_n'$ | $T_{\ell'}$ | $E_n'$ | $T_{\ell'}$ | $E_n'$ | $T_{\ell'}$ |
| 1/2+ | 0+ | 1/2 | 0 | 500 | .29 | 850 | .35 | 1050 | .42 |
| | 2+ | 3/2 | 2 | 460 | .048 | 810 | .12 | 1010 | .18 |
| | 2+ | 5/2 | 2 | 460 | .048 | 810 | .12 | 1010 | .18 |
| | 0+ | 1/2 | 0 | | | 40 | .10 | 240 | .218 |
| | 1- | 3/2 | 1 | | | 60 | .14 | 260 | .512 |
| | 1- | 1/2 | 1 | | | 60 | .14 | 260 | .512 |
| | 2+ | 3/2 | 2 | | | | | 200 | .01 |
| | | 5/2 | 2 | | | | | 200 | .01 |
| | | | | | .39 | | .97 | | 2.04 |
| 1/2- | 0+ | 1/2 | 1 | 500 | .78 | 850 | .94 | 1050 | .98 |
| | 2+ | 3/2 | 1 | 460 | .75 | 810 | .93 | 1010 | .97 |
| | 2+ | 5/2 | 3 | 460 | .024 | 810 | .14 | 1010 | .32 |
| | 4+ | 7/2 | 3 | 360 | .01 | 710 | .10 | 910 | .20 |
| | 1- | 1/2 | 0 | | | 60 | .12 | 260 | .224 |
| | 1- | 3/2 | 2 | | | | | 260 | .016 |
| | 0+ | 1/2 | 1 | | | 40 | .10 | 240 | .48 |
| | 2+ | 3/2 | 1 | | | | | 200 | .41 |
| | 3- | 5/2 | 2 | | | | | 190 | .01 |
| | | | | | 1.56 | | 2.33 | | 3.61 |
| 3/2+ | 0+ | 1/2 | 2 | 500 | .056 | 850 | .13 | 1050 | .25 |
| | 2+ | 3/2 | 0 | 460 | .28 | 810 | .35 | 1010 | .38 |
| | 2+ | 3/2 | 2 | 460 | .048 | 810 | .12 | 1010 | .18 |
| | 2+ | 5/2 | 2 | 460 | .048 | 810 | .12 | 1010 | .18 |
| | 4+ | 7/2 | 2 | 360 | .031 | 710 | .098 | 910 | .14 |
| | 1- | 1/2 | 1 | | | 60 | .14 | 260 | .512 |
| | 1- | 3/2 | 1 | | | 60 | .14 | 260 | .512 |
| | 0+ | 1/2 | 2 | | | | | 240 | .014 |
| | 2+ | 3/2 | 0 | | | | | 200 | .200 |
| | 2+ | 3/2 | 2 | | | | | 200 | .01 |
| | 2+ | 5/2 | 2 | | | | | 200 | .01 |
| | 3- | 5/2 | 1 | | | | | 190 | .39 |
| | | | | | .46 | | 1.10 | | 2.78 |

TABLE XIII (continued)

| | | | | $E_n$ = 500 | | $E_n$ = 850 | | $E_n$ = 1050 | |
|---|---|---|---|---|---|---|---|---|---|
| $I\pi$ | $i'\pi$ | $j'$ | $\ell'$ | $E_n'$ | $T_{\ell'}$ | $E_n'$ | $T_{\ell'}$ | $E_n'$ | $T_{\ell'}$ |
| 3/2- | 0+ | 1/2 | 1 | 500 | .78 | 850 | .94 | 1050 | .98 |
| | 2+ | 3/2 | 1 | 460 | .75 | 810 | .93 | 1010 | .97 |
| | 2+ | 3/2 | 3 | 460 | .024 | 810 | .14 | 1010 | .32 |
| | 2+ | 5/2 | 1 | 460 | .75 | 810 | .93 | 1010 | .97 |
| | 2+ | 5/2 | 3 | 460 | .024 | 810 | .14 | 1010 | .32 |
| | 4+ | 7/2 | 3 | 360 | .01 | 710 | .10 | 910 | .20 |
| | 4+ | 9/2 | 3 | 360 | .01 | 710 | .10 | 910 | .20 |
| | 1- | 1/2 | 2 | | | | | 260 | .016 |
| | 1- | 3/2 | 0 | | | 60 | .12 | 260 | .224 |
| | 1- | 3/2 | 2 | | | | | 260 | .016 |
| | 0+ | 1/2 | 1 | | | 40 | .10 | 240 | .48 |
| | 2+ | 3/2 | 1 | | | | | 200 | .41 |
| | 2+ | 5/2 | 1 | | | | | 200 | .41 |
| | 3- | 5/2 | 2 | | | | | 190 | .01 |
| | 3- | 7/2 | 2 | | | | | 190 | .01 |
| | | | | | 2.35 | | 3.50 | | 5.54 |
| 5/2+ | 0+ | 1/2 | 2 | 500 | .056 | 850 | .13 | 1050 | .25 |
| | 2+ | 3/2 | 2 | 460 | .048 | 810 | .12 | 1010 | .18 |
| | 2+ | 5/2 | 0 | 460 | .28 | 810 | .35 | 1010 | .38 |
| | 2+ | 5/2 | 2 | 460 | .048 | 810 | .12 | 1010 | .18 |
| | 4+ | 7/2 | 2 | 360 | .031 | 710 | .098 | 910 | .14 |
| | 4+ | 9/2 | 2 | 360 | .031 | 710 | .098 | 910 | .14 |
| | 1- | 3/2 | 1 | | | 60 | .14 | 260 | .512 |
| | 0+ | 1/2 | 2 | | | | | 240 | .014 |
| | 2+ | 3/2 | 2 | | | | | 200 | .01 |
| | 2+ | 5/2 | 2 | | | | | 200 | .01 |
| | 2+ | 5/2 | 0 | | | | | 200 | .20 |
| | 3- | 5/2 | 1 | | | | | 190 | .39 |
| | 3- | 7/2 | 1 | | | | | 190 | .39 |
| | 4+ | 7/2 | 2 | | | | | 100 | .01 |
| | 4+ | 9/2 | 2 | | | | | 100 | |
| | | | | | .49 | | 1.06 | | 2.81 |

TABLE XIII (concluded)

| | | | | $E_n$ = 500 | | $E_n$ = 850 | | $E_n$ = 1050 | |
|---|---|---|---|---|---|---|---|---|---|
| Iπ | i'π | j' | ℓ' | $E_n'$ | $T_{\ell'}$ | $E_n'$ | $T_{\ell'}$ | $E_{\ell'}$ | $T_{\ell'}$ |
| 5/2- | 0+ | 1/2 | 3 | 500 | .033 | 850 | .165 | 1050 | .56 |
| | 2+ | 3/2 | 1 | 460 | .75 | 810 | .93 | 1010 | .97 |
| | 2+ | 3/2 | 3 | 460 | .024 | 810 | .14 | 1010 | .32 |
| | 2+ | 5/2 | 1 | 460 | .75 | 810 | .93 | 1010 | .97 |
| | 2+ | 5/2 | 3 | 460 | .024 | 810 | .14 | 1010 | .32 |
| | 4+ | 7/2 | 1 | 360 | .65 | 710 | .90 | 910 | .95 |
| | 4+ | 7/2 | 3 | 360 | .01 | 710 | .10 | 910 | .20 |
| | 4+ | 9/2 | 3 | 360 | .01 | 710 | .10 | 910 | .20 |
| | 6+ | 11/2 | 3 | 210 | - | 560 | .049 | 760 | .12 |
| | 1- | 1/2 | 2 | | | | | 260 | .016 |
| | 1- | 3/2 | 2 | | | | | 260 | .016 |
| | 2+ | 3/2 | 1 | | | | | 200 | .410 |
| | 2+ | 5/2 | 1 | | | | | 200 | .410 |
| | 3- | 5/2 | 0 | | | | | 190 | .197 |
| | 3- | 7/2 | 2 | | | | | 190 | .01 |
| | | | | | 2.25 | | 3.45 | | 5.67 |
| 7/2- | 0+ | 1/2 | 3 | 500 | .033 | 850 | .165 | 1050 | .56 |
| | 2+ | 3/2 | 3 | 460 | .024 | 810 | .14 | 1010 | .32 |
| | 2+ | 5/2 | 1 | 460 | .75 | 810 | .93 | 1010 | .97 |
| | 2+ | 5/2 | 3 | 460 | .024 | 810 | .14 | 1010 | .32 |
| | 4+ | 7/2 | 1 | 360 | .65 | 710 | .90 | 910 | .95 |
| | 4+ | 7/2 | 3 | 360 | .01 | 710 | .10 | 910 | .20 |
| | 4+ | 9/2 | 1 | 360 | .65 | 710 | .90 | 910 | .95 |
| | 4+ | 9/2 | 3 | 360 | .01 | 710 | .10 | 910 | .20 |
| | 6+ | 11/2 | 3 | 210 | - | 560 | .049 | 760 | .12 |
| | 6+ | 13/2 | 3 | 210 | - | 560 | .049 | 760 | .12 |
| | 1- | 3/2 | 2 | | | | | 260 | .016 |
| | 2+ | 5/2 | 1 | | | | | 200 | .41 |
| | 3- | 5/2 | 2 | | | | | 190 | .01 |
| | 3- | 7/2 | 0 | | | | | 190 | .197 |
| | 3- | 7/2 | 2 | | | | | 190 | .01 |
| | 4+ | 7/2 | 1 | | | | | 100 | .198 |
| | 4+ | 9/2 | 1 | | | | | 100 | .198 |
| | | | | | 2.15 | | 3.47 | | 5.75 |

[a] Relative intensities of neutron emission from the various (Iπ) states of the compound nucleus U-235* formed by neutrons of energy $E_n$ incident on U-234, if all decay proceeded by neutron emission.

TABLE XIV

RELATIVE FORMATION AND NEUTRON DECAY FACTORS FOR COMPOUND STATES[a]

| Compound level $I\pi$ | $P(I\pi)$ | | | $(2I+1)\,T_{\ell I}$ | | |
|---|---|---|---|---|---|---|
| $E_n$ = | 500 | 850 | 1050 | 500 | 850 | 1050 |
| 1/2+ | .39 | .97 | 2.04 | .72 | .86 | .92 |
| 3/2+ | .46 | 1.10 | 2.78 | .31 | .68 | .88 |
| 5/2+ | .49 | 1.06 | 2.81 | .41 | .95 | 1.24 |
| 1/2- | 1.56 | 2.33 | 3.61 | 1.40 | 1.74 | 1.83 |
| 3/2- | 2.35 | 3.50 | 5.54 | 3.24 | 3.79 | 3.91 |
| 5/2- | 2.25 | 3.45 | 5.67 | .11 | .61 | 1.13 |
| 7/2- | 2.15 | 3.47 | 5.75 | .26 | 1.26 | 2.15 |
| | | | | 6.45 | 9.89 | 12.06 |

[a]Summation of transmission factors for neutron emission from levels $(I\pi)$ in compound nucleus U-235 to the levels listed in Table XII for incident neutron energies of 500, 850, and 1050 kev. The last three columns give $\sigma_c(I\pi)2/\pi\lambda^2$.

TABLE XV

CROSS SECTIONS[a] FOR U-234 BOMBARDED BY NEUTRONS WITH ENERGIES OF 500, 850, AND 1050 KEV

| | $E_n$ (kev) | | |
|---|---|---|---|
| | 500 | 850 | 1050 |
| $\sigma_t$ | 9.80 | 8.05 | 7.51 |
| $\sigma_s$ | 5.52 | 4.18 | 3.68 |
| $\sigma_r$ | 4.27 | 3.87 | 3.83 |
| $\sigma_f$ | 0.50 | 1.26 | 1.10 |
| $\sigma_n$ | 3.77 | 2.61 | 2.73 |
| $\sigma_{ce}$ | 1.41 | 0.62 | 0.43 |
| $\Gamma_n/\Gamma_f$ | 7.5 | 2.1 | 2.5 |

[a]Deduced from calculations based on the non-local optical model potential of Perey and Buck, the Hauser-Feshbach analysis, and measured fission cross sections for neutrons incident on U-234 with energies of 500, 850, and 1050 kev. (Capture cross sections assumed negligible.)

probability is independent of whether the daughter state is a ground state rotational level or one built on a beta or octupole vibration. Intuitively one would not expect this to be so.

## III. DECAY BY FISSION

Figure 12 shows extrema in $\sigma_f(\theta)$ at neutron energies of approximately 500, 850, and 1050 kev. The counting rates at 500 kev were extremely low so that measurements were limited to a determination of the $(0/90)^\circ$ ratio. The scattering matrices obtained from the non-local potentials of Perey and Buck yielded the spin-dependent neutron transmission factors listed in Table XVI. From these the theoretical $K\pi$ band angular distributions are calculated and compared with results of measurements at the above three energies. Crude estimates of the effects of neutron competition based on the computations of the preceding paragraph are made in each case in order to assist in arriving at approximate partial cross sections for fission through the contributing $KI\pi$ channels.

Figures 15 and 16 show the angular distributions at 850 and 1050 kev and the least squares fits to the data points. These fits are given on the curves in terms of the Legendre polynomials.

Analysis at 500 kev. At this energy maximum sidewise peaking occurs with a fragment intensity ratio, $\sigma_f(0/90)^\circ = 0.50$. The fission cross section is 0.5 barn, and the calculated reaction cross section is 4.27 barns. Plugging the transmission factors obtained from the PB scattering matrix into the equations for $\sigma_{K\pi}(\theta)$, one obtains:

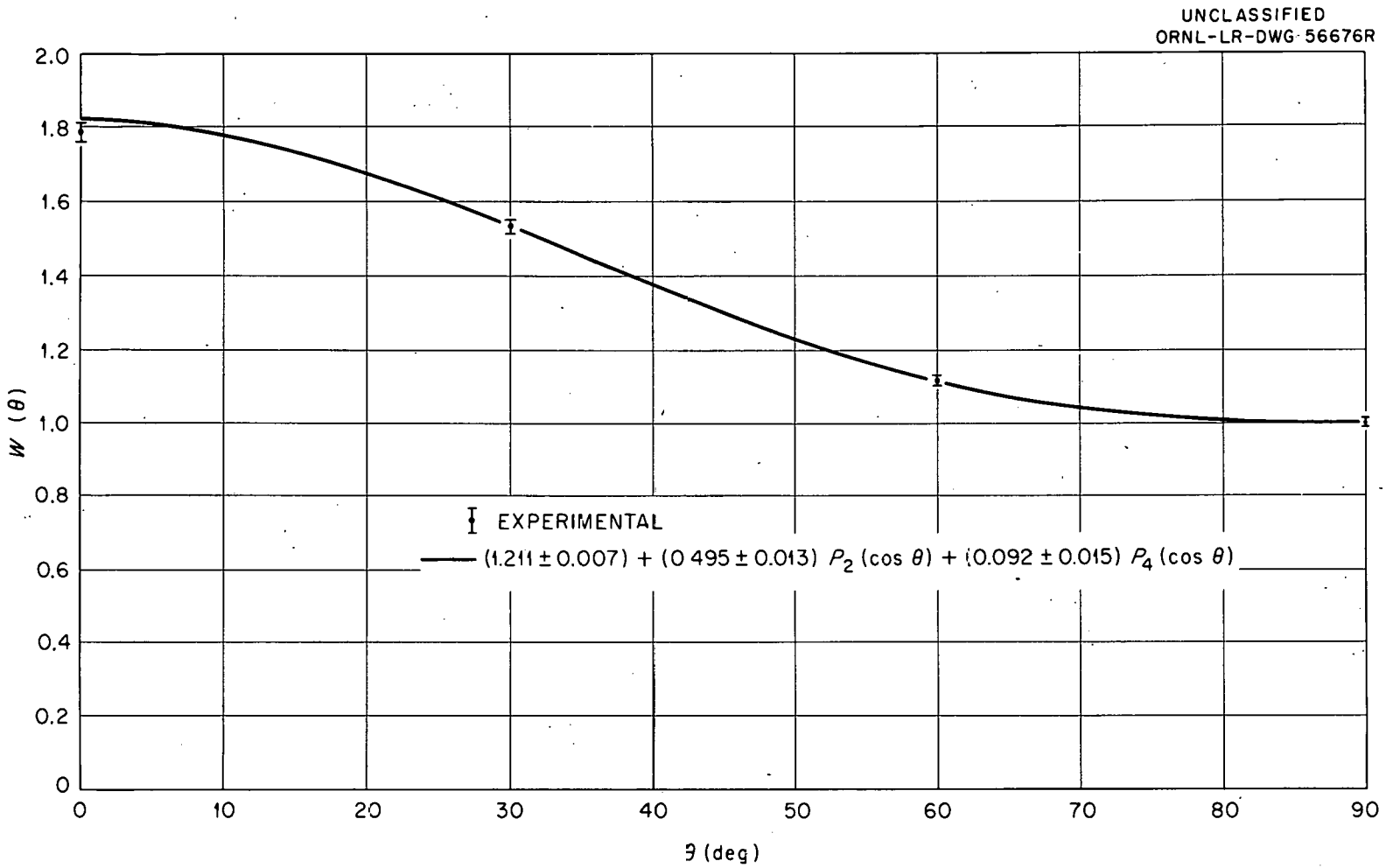


Fig. 15. Fission Fragment Angular Distribution for $U^{234}$ Excited by 843 kev Neutrons. Curve Obtained by Least Squares Fit to the Four Data Points.

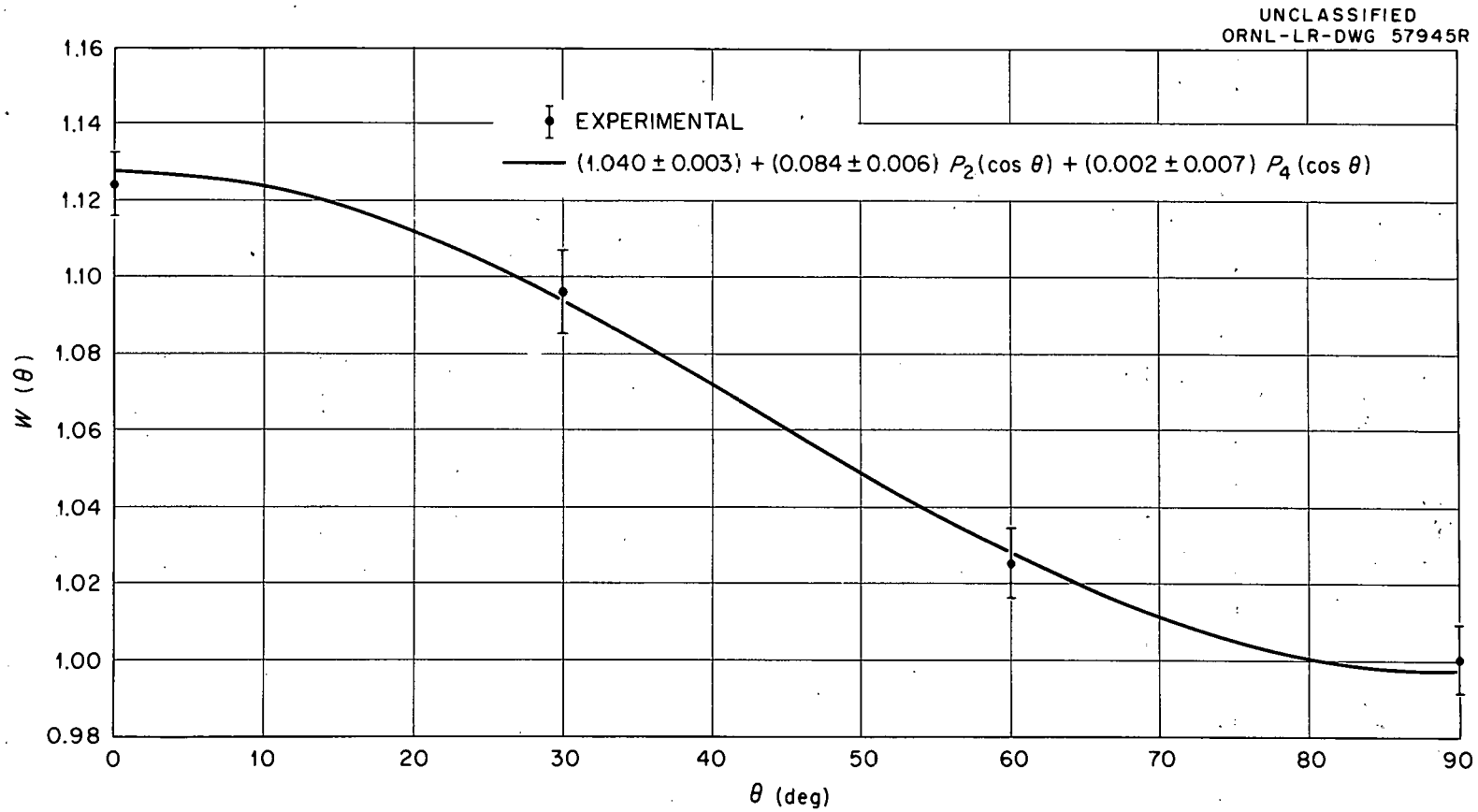


Fig. 16. Fission Fragment Angular Distribution for $U^{234}$ Excited by 1051 kev Neutrons. Curve Obtained by Least Squares Fit to the Four Data Points.

TABLE XVI

NEUTRON TRANSMISSION FACTORS FOR U-234

The $T_\ell$ from Em58 are listed for comparison with the $\tau_\ell$ from the PB potential.

| $E_n$ = | 500 | 850 | 1050 |
|---|---|---|---|
| $T_o$ | .361 | .431 | .460 |
| $T_2^-$ | .077 | .171 | .221 |
| $T_2^+$ | .069 | .158 | .207 |
| $T_1^-$ | .702 | .871 | .916 |
| $T_1^+$ | .810 | .947 | .977 |
| $T_3^-$ | .018 | .101 | .189 |
| $T_3^+$ | .032 | .158 | .269 |
| $\tau_o$ | .361 | .431 | .460 |
| $\tau_1$ | .774 | .922 | .957 |
| $\tau_2$ | .072 | .163 | .213 |
| $\tau_3$ | .026 | .134 | .235 |
| $\tau_4$ | ---- | .002 | .004 |
| $\tau_5$ | ---- | ---- | .001 |
| $T_o$ | .292 | .350 | .380 |
| $T_1$ | .780 | .940 | .970 |
| $T_2$ | .055 | .127 | .167 |
| $T_3$ | .033 | .164 | .290 |

$$\sigma(\theta)_{1/2+} = .210\left[\ .361W(\tfrac{1}{2}\ \tfrac{1}{2})+\ .154W(\tfrac{1}{2}\ \tfrac{3}{2})+\ .207W(\tfrac{1}{2}\ \tfrac{5}{2})\qquad\qquad\right],$$

$$\sigma(\theta)_{1/2-} = .210\left[\ .702W(\tfrac{1}{2}\ \tfrac{1}{2})+1.620W(\tfrac{1}{2}\ \tfrac{3}{2})+\ .054W(\tfrac{1}{2}\ \tfrac{5}{2})+\ .128W(\tfrac{1}{2}\ \tfrac{7}{2})\right],$$

$$\sigma(\theta)_{3/2+} = .210\left[\qquad\qquad .154W(\tfrac{3}{2}\ \tfrac{3}{2})+\ .207W(\tfrac{3}{2}\ \tfrac{5}{2})\qquad\qquad\right], \tag{25}$$

$$\sigma(\theta)_{3/2-} = .210\left[\qquad\qquad 1.620W(\tfrac{3}{2}\ \tfrac{3}{2})+\ .054W(\tfrac{3}{2}\ \tfrac{5}{2})+\ .128W(\tfrac{3}{2}\ \tfrac{7}{2})\right].$$

The sidewise peaking makes it clear that a K = 3/2 band is dominant, bands with higher K having too small formation cross sections. $\sigma_{3/2+}$ = .48 barn and with $(\overline{\Gamma_f/\Gamma_t})$ = .117 is clearly ruled out. $\sigma_{3/2-}$ = 2.38 barns so clearly the 3/2- band is the major contributor. Since there is some fragment intensity at zero degrees, either one must say that the K axis is wobbling (K a poor quantum number) or a 1/2 band is also contributing. The trend away from sidewise peaking below 500 kev favors the latter hypothesis, and one is obliged to select the 1/2+ band because if it were the 1/2- it would override the 3/2- and lead to forward peaking. Therefore, for U-235 near saddlepoint the lowest band is a 1/2+ and the next one is a 3/2- and the spacing is probably of the order of a few hundred kilovolts.

Individual level weights within the bands can be estimated only roughly. Neglect the two higher members of the 3/2- band, and modify the 1/2+ band by dividing each term by the appropriate P(Iπ) and reduce the two upper terms a bit more by factors of .93 and .82 respectively to take into account the loss in available energy for deformation due to the higher rotation (assuming a decoupling constant of zero and $\hbar^2/2\mathcal{J}$ = 5 kev

at saddlepoint). This last correction is very crude as in reality the decoupling constant would be expected to be either $\pm$ 1 but there is no way to predict which. Then one can write:

$$\sigma(\theta) = aW(\tfrac{1}{2}\,\tfrac{1}{2})+bW(\tfrac{1}{2}\,\tfrac{3}{2})+cW(\tfrac{3}{2}\,\tfrac{3}{2})+dW(\tfrac{1}{2}\,\tfrac{5}{2}), \tag{26}$$

$$b = \frac{.154}{.361}\left(\frac{.39}{.46}\right)(.93)a = .336a\ , \tag{27}$$

$$d = \frac{.207}{.361}\left(\frac{.39}{.49}\right)(.82)a = .374a\ , \tag{28}$$

$$a + b + c + d = \sigma_f/2\pi = .0796. \tag{29}$$

$$\sigma_f\left(\frac{0}{90}\right)^{\circ} = \frac{1}{2} = \frac{.5a + b + 0c + 1.5d}{.5a + .25b + .75c + .375d}\ . \tag{30}$$

These four simultaneous equations yield:

$$\sigma_f(\theta, 500\text{kev}) = .210\left[.234W(\tfrac{3}{2}\,\tfrac{3}{2}) + .085W(\tfrac{1}{2}\,\tfrac{1}{2}) + .029W(\tfrac{1}{2}\,\tfrac{3}{2}) + .032W(\tfrac{1}{2}\,\tfrac{5}{2})\right]. \tag{31}$$

For those individual levels which fission this gives $\gamma(I\pi) \equiv (\Gamma_f/\Gamma_t)(I\pi)$ of:

$$\begin{aligned}
\gamma(1/2+) &= .085 \div .361 = .24,\\
\gamma(3/2+) &= .029 \div .154 = .19,\\
\gamma(5/2+) &= .032 \div .207 = .15,\\
\gamma(3/2-) &= .234 \div 1.620 = .14,\\
\overline{(\Gamma_f/\Gamma_t)} &= .50 \div 4.27 = .12 \text{ for all fission.}
\end{aligned} \tag{32}$$

These results look reasonable, bearing in mind that other compound levels decay only by neutron emission. Alternatively one could neglect

the possible presence of the last two levels and make a two-parameter fit to the data wholly from experiment, but this involves an assumption at greater variance with theory than the one chosen in arriving at equations (27) and (28).

Analysis at 850 kev. From experiment the actual fission fragment angular distribution normalized to $\sigma_f = 1.26$ barns and corrected for finite angular resolution (Ro53) and using the least squares fit (Fig. 15) is:

$$\sigma_f(\theta) = .100 \left[ (1 \pm .0054)P_0 + (.419 \pm .011)P_2 + (.083 \pm .017)P_4 \right] \text{ barns/ster.}$$

From force fit through all four points:

$$\sigma_f(\theta) = .100 \left[ P_0 + .426\ P_2 + .079\ P_4 - .018\ P_6 \right] .$$

The drastic change to strong forward and backward peaking points unambiguously to the appearance of a K = 1/2- band. Plugging transmission factors obtained from the PB potential into equation (22) gives, for the three bands contributing to fission at this energy:

$$\sigma(\theta)_{1/2+} = .125 \left[ .431W(\tfrac{1}{2}\ \tfrac{1}{2}) + .342W(\tfrac{1}{2}\ \tfrac{3}{2}) + .474W(\tfrac{1}{2}\ \tfrac{5}{2}) \right] .$$

$$\sigma(\theta)_{1/2-} = .125 \left[ .871W(\tfrac{1}{2}\ \tfrac{1}{2}) + 1.894W(\tfrac{1}{2}\ \tfrac{3}{2}) + .303W(\tfrac{1}{2}\ \tfrac{5}{2}) + .632W(\tfrac{1}{2}\ \tfrac{7}{2}) \right] . \quad (33)$$

$$\sigma(\theta)_{3/2-} = .125 \left[ \qquad 1.894W(\tfrac{3}{2}\ \tfrac{3}{2}) + .303W(\tfrac{3}{2}\ \tfrac{5}{2}) + .632W(\tfrac{3}{2}\ \tfrac{7}{2}) \right] .$$

Write:

$$\sigma_f(\theta) = aW(\tfrac{1}{2}\ \tfrac{1}{2}) + bW(\tfrac{1}{2}\ \tfrac{3}{2}) + cW(\tfrac{3}{2}\ \tfrac{3}{2}) + dW(\tfrac{1}{2}\ \tfrac{5}{2}) + eW(\tfrac{3}{2}\ \tfrac{5}{2}) + fW(\tfrac{1}{2}\ \tfrac{7}{2}) + gW(\tfrac{3}{2}\ \tfrac{7}{2}) \quad . \quad (34)$$

The barrier heights for the 1/2+ and 3/2- bands are probably well

under 850 kev, but the 1/2- band is estimated to be only about 70% open based on a very rough comparison of data from the HF analysis and the curve of $\sigma_f$ versus $E_n$.

For a first-order estimate of the level strengths contributing to fission, neglect the effects of neutron competition in obtaining the following equations (35) and (36):

$$c/e/g = 1.894/.303/.632 \ , \tag{35}$$

$$\frac{f + g}{d + e} = \frac{4T_3^+}{3(T_2^+ + T_3^-)} = .813 \ . \tag{36}$$

From these relations and the four obtainable from matching P coefficients with the measured angular distribution, one finds:

$$\sigma_f(\Theta) = .10 \Big[ .70W(\tfrac{1}{2}\,\tfrac{1}{2}) + .72W(\tfrac{1}{2}\,\tfrac{3}{2}) + .22W(\tfrac{3}{2}\,\tfrac{3}{2}) + .16W(\tfrac{1}{2}\,\tfrac{5}{2}) + .04W(\tfrac{3}{2}\,\tfrac{5}{2}) + .09W(\tfrac{1}{2}\,\tfrac{7}{2}) + .07W(\tfrac{3}{2}\,\tfrac{7}{2}) \Big] \text{ barns/ster.} \tag{37}$$

To account very approximately for the effects of neutron competition on the distribution, define:

$\sigma_c(I\pi) \equiv$ formation cross section for compound state $(I\pi)$.

$$\overline{P} = \frac{\sum \sigma_c(I\pi)\ P(I\pi)}{\sum \sigma_c(I\pi)} \ , \tag{38}$$

$$\gamma(I\pi) \equiv \Gamma_f/\Gamma_t = \Gamma_f/(\Gamma_f + \Gamma_n) \quad \text{for state } (I\pi) \ , \tag{39}$$

$n(I\pi) \equiv$ number of fission channels open for state $(I\pi)$.

$\beta(KI\pi) \equiv$ reduction factor applied to terms in a given $(K\pi)$ band due to

spin effects. Taken as unity for ground state level in each band.

$$\text{Set } \Gamma_f(I\pi) \propto \sum (n\beta)_{I\pi} \ . \tag{40}$$

Then

$$\overline{\Gamma}_f \propto \frac{\sum (n\beta) \text{ over all states}}{\text{number of states}} \equiv \overline{\sum (n\beta)} \ , \tag{40a}$$

$$\overline{\Gamma}_f = \frac{1}{7}\left[1 + 1 + 1 + .7+(1+.7x.98)+(1+.7x.95)+(1+.7x.90)\right] = \frac{1}{.806} . \tag{40b}$$

The quantities in the square brackets are $\sum n\beta$ for the 1/2+, 3/2+, 5/2+, 1/2-, 3/2-, 5/2-, and 7/2- states, respectively. Now:

$$\gamma(I\pi) = \frac{\Gamma_f/\overline{\Gamma}_f}{\Gamma_f/\overline{\Gamma}_f + \Gamma_n/\overline{\Gamma}_f} = \frac{.806\,\Gamma_f(I\pi)}{.806\,\Gamma_f(I\pi) + \Gamma_n(I\pi)/\overline{\Gamma}_f} \ . \tag{39a}$$

But

$$\Gamma_n(I\pi)/\overline{\Gamma}_n = P(I\pi)/\overline{P}. \tag{41}$$

So

$$\Gamma_n(I\pi)/\overline{\Gamma}_f = \frac{\overline{\Gamma}_n}{\overline{\Gamma}_f}\frac{P(I\pi)}{\overline{P}} = 2.1\ \frac{P(I\pi)}{2.67} = .787P(I\pi). \tag{41a}$$

Therefore

$$\gamma(I\pi) = \frac{\sum (n\beta)_{I\pi}}{\sum (n\beta)_{I\pi} + .975P(I\pi)} \ . \tag{39b}$$

$$\gamma(5/2+) = .492, \qquad \gamma(5/2-) = .331, \qquad \gamma(7/2-) = .325,$$

$$\frac{f+g}{d+e} = \frac{\alpha(7/2-)\gamma(7/2-)}{\alpha(5/2+)\gamma(5/2+)+\alpha(5/2-)\gamma(5/2-)} = \frac{.632(.325)}{.474(.492)+.303(.331)} = 0.616 \ . \tag{42}$$

Using this relation in place of equation (36), together with equation (35) (since neutron emission proceeds with equal facility from all the K = 3/2- levels) and the same four equations from matching P coefficients, one obtains for the fission fragment angular distribution in terms of level strengths:

$$\sigma_f(\theta) = .10\left[.78W(\tfrac{1}{2}\,\tfrac{1}{2}) + .71W(\tfrac{1}{2}\,\tfrac{3}{2}) + .19W(\tfrac{3}{2}\,\tfrac{3}{2}) + .17W(\tfrac{1}{2}\,\tfrac{5}{2}) + .03W(\tfrac{3}{2}\,\tfrac{5}{2}) + .06W(\tfrac{1}{2}\,\tfrac{7}{2}) + .06W(\tfrac{3}{2}\,\tfrac{7}{2})\right]. \qquad (43)$$

Comparison of equations (43) and (37) shows that at this energy neutron emission produces only small effects on the relative level strengths for fission. From equation (43) one finds the following values for $\gamma(I\pi)$:

$$\gamma(1/2) = .48 \text{ (average for both parities)},$$
$$\gamma(3/2) = .32 \text{ (average for both parities)},$$
$$\gamma(5/2) = .21 \text{ (average for both parities)},$$
$$\gamma(7/2-) = .15\,. \qquad (44)$$

All of the above are reasonable in view of a value of .33 (from Table 5) for $\bar{\gamma}$.

Analysis at 1050 kev. The partial cross-section formulae obtained by use of transmission factors derived from the PB potential are:

$$\sigma(\theta)_{1/2+} = .100\left[.460W(\tfrac{1}{2}\,\tfrac{1}{2}) + .442W(\tfrac{1}{2}\,\tfrac{3}{2}) + .621W(\tfrac{1}{2}\,\tfrac{5}{2})\right],$$
$$\sigma(\theta)_{1/2-} = .100\left[.916W(\tfrac{1}{2}\,\tfrac{1}{2}) + 1.954W(\tfrac{1}{2}\,\tfrac{3}{2}) + .567W(\tfrac{1}{2}\,\tfrac{5}{2}) + 1.076W(\tfrac{1}{2}\,\tfrac{7}{2})\right],$$
$$\sigma(\theta)_{3/2+} = .100\left[.442W(\tfrac{3}{2}\,\tfrac{3}{2}) + .621W(\tfrac{3}{2}\,\tfrac{5}{2})\right], \qquad (45)$$
$$\sigma(\theta)_{3/2-} = .100\left[1.954W(\tfrac{3}{2}\,\tfrac{3}{2}) + .567W(\tfrac{3}{2}\,\tfrac{5}{2}) + 1.076W(\tfrac{3}{2}\,\tfrac{7}{2})\right].$$

From experiment, the actual fission fragment angular distribution normalized to $\sigma_f$ = 1.10 barns and corrected for finite angular resolution (Ro53) and using the least squares fit (Fig. 16) is:

$$\sigma_f(\theta) = .100\left[(.874\pm.003)P_0+(.0724\pm.0271)P_2+(.0018\pm.0061)P_4\right] \text{ barns/ster.} \tag{46}$$

From force fit through all four points:

$$\sigma_f(\theta) = .100\left[.877P_0+.0754P_2+.004P_4-.006P_6\right] \text{ barns/ster.} \tag{46a}$$

The almost complete disappearance of the two higher harmonics indicates that either very special relations exist between the W(KI) for I > 3/2 or else that these levels make negligible contributions to fission. An investigation of the special relations necessary for the existence of significant contributions to $\sigma_f$ from these higher spin levels shows that the relative proportions required would be at complete variance with theory and would also force constraints on the terms of lower spin as to lead to most improbable assignments for their weights also. Consequently, it appears most likely that the higher terms really are negligible and that one can write with good accuracy:

$$\sigma_f(\theta) = .100\left[.877P_0+.075P_2\right] = aW\left(\tfrac{1}{2}\ \tfrac{1}{2}\right)+bW\left(\tfrac{1}{2}\ \tfrac{3}{2}\right)+cW\left(\tfrac{3}{2}\ \tfrac{3}{2}\right) . \tag{47}$$

Since there are only two P coefficients to match, and three unknowns, it is necessary to introduce an assumption based on theory to supply the third equation. Now theory does not predict the sharp break in the anisotropy between 850 and 1050 kev. The drop in fission cross section between these two energies can be understood in the light of data in Tables XII and XIV which show the hefty increase in competition from

neutron emission to the newly available vibrational levels in U-234. Since the extrema in the angular distribution coincide exactly energy-wise with those in the cross section, one suspects that they arise from the same cause, namely, neutron emission to the new levels. A glance at the results of the HF analysis given in Table XIV, however, would lead one to predict no drastic change in the angular distribution. This is indeed borne out. Calculations similar to those in the preceding section still lead to strong forward peaking although not quite so strong as at 850 kev. Consequently, it appears that either the HF analysis does not properly represent the nature of scattering to beta and octupole levels, or that the K quantum number in this energy region at least, has lost most of its stability.

Since the high-spin terms are at greatest variance with theory, it is perhaps safest to introduce as the third criterion some function of the lowest spin term. At 1050 kev the 1/2- band should be completely open, so let:

$$\gamma(1/2,1050\text{ kev}) = (2/1.7)\gamma(1/2,850\text{ kev}) = (2/1.7)(.48) = .57. \qquad (48)$$

This leads to:

$$\sigma_f(\theta) = .100\left[\,.79W(\tfrac{1}{2}\,\tfrac{1}{2})+.56W(\tfrac{1}{2}\,\tfrac{3}{2})+.40W(\tfrac{3}{2}\,\tfrac{3}{2})\,\right]. \qquad (49)$$

and a value of 0.40 for $\gamma(3/2)$. From Table XV, $\bar{\gamma} = .29$ so these values of $\gamma(1/2)$ and $\gamma(3/2)$ are reasonable since the other levels decay almost entirely by neutron emission.

Equation (49) accounts adequately for the experimentally observed quantities, but the disappearance of the higher spin levels from fission

is not at all explained. The substantial increase in the contribution from the W(3/2,3/2) level over that at 850 kev could be due in part to the appearance of a 3/2+ band, although from the relative formation cross sections a much more modest increase would be expected.

## IV. U-235

Figure 11 shows the experimentally determined fission fragment intensity at zero degrees divided by that at ninety degrees based on the measured points shown with their standard errors on the figure. These measurements were carried out for two reasons. The first was to serve as a correction to the U-234 measurements due to the U-235 contained on the foils as an impurity. Secondly, an attempt was made to discover any sudden change in the angular anisotropy around 900 kev neutron energy, at which point a sharp rise of approximately seven percent was found to occur in the fission cross section (Di57a,b). If the angular distribution is affected by the advent of the new fission channel which presumably accounts for the rise in the cross section, the effect is below the limits of accuracy of the measurements.

The threshold for U-235 fission lies several hundred kev below zero bombarding energy. Fragment angular anisotropy for unaligned particles requires the directional effects brought in by orbital angular momenta ($\ell > 0$), so that the distribution is isotropic near zero bombarding energy. The p-wave interaction soon makes itself felt (see Fig. 13) however, leading to the observed anisotropy which also depends on the particular combination of channels contributing to fission. Since the

results around 900 kev were negative no attempt was made to pursue the matter further.

# CHAPTER VI

## SUMMARY AND CONCLUSIONS

The angular distribution of fission fragments from neutron-induced fission of U-234 near threshold suggests the presence in U-235* near the saddle point deformation of a $K\pi = 1/2+$ band with a 3/2- band lying a few hundred kilovolts above it, and above that a 1/2- band separated again by a few hundred kilovolts from the one beneath it. Above these three bands the picture becomes obscured by the onset of neutron emission to vibrational levels in U-234. However, the way in which the angular anisotropy changes with increasing energy of the incident neutron suggests that these bands could be followed by another 3/2 or possibly a 5/2 K band and then almost certainly by one or more additional K = 1/2 bands. In any event, above about 600 kev fission occurs predominantly through K = 1/2 bands, as those with $K > 1/2$ all lead to sidewise peaking of the fragment distribution.

Rough estimates of the various band strengths and still more approximate estimates of the level strenghts within each band have been made.

At 500 kev:

$$\sigma_f(\theta, 500\text{kev}) = .210 \left[ .234W\left(\tfrac{3}{2}\ \tfrac{3}{2}\right) + .085W\left(\tfrac{1}{2}\ \tfrac{1}{2}\right) + \right.$$

$$\left. + .029W\left(\tfrac{1}{2}\ \tfrac{3}{2}\right) + .032W\left(\tfrac{1}{2}\ \tfrac{5}{2}\right) \right] \text{ barns/ster.}$$

from which one finds 62 percent of all fission proceeding via the K = 3/2- band and 38 percent via the K = 1/2+ band.

At 850 kev:

$$\sigma_f(\theta,850\text{kev}) = 0.10\left[.78W(\tfrac{1}{2}\,\tfrac{1}{2})+ .71W(\tfrac{1}{2}\,\tfrac{3}{2})+ .17W(\tfrac{1}{2}\,\tfrac{5}{2})+ .06W(\tfrac{1}{2}\,\tfrac{7}{2})+\right.$$

$$\left.+ .19W(\tfrac{3}{2}\,\tfrac{3}{2})+ .03W(\tfrac{3}{2}\,\tfrac{5}{2})+ .06W(\tfrac{3}{2}\,\tfrac{7}{2})\right] \text{ barns/ster.}$$

from which one finds 86 percent of all fission taking place via the K = 1/2+ plus the K = 1/2- bands and 14 percent via the K = 3/2- band. It is not possible to separate the contributions from the two K = 1/2 bands but it is safe to say that the 1/2- will account for more than the 1/2+ due to the strong p-wave interaction.

At 1050 kev:

$$\sigma_f(\theta,1050\text{kev}) = 0.10\left[.79W(\tfrac{1}{2}\,\tfrac{1}{2})+ .56W(\tfrac{1}{2}\,\tfrac{3}{2})+ .40W(\tfrac{3}{2}\,\tfrac{3}{2})\right] \text{ barns/ster.}$$

showing a contribution of 77 percent from the 1/2 bands and 23 percent from the 3/2 band or bands.

At the two lower energies the level strengths within the bands are in reasonable agreement with predicted values, but this is not true at 1050 kev. This points up a lack of understanding of some of the finer details either of the mechanism of fission over the barrier or of inelastic neutron scattering to vibrational levels. The calculated K-band cross sections predict substantial contributions from the 5/2 and the 7/2 spin states, whereas in actuality these contributions are virtually nonexistent. The contribution from the K = 3/2 band is larger than would be expected on the basis of the results at 850 kev, but this could arise from the incidence of an additional 3/2 band above 850 kev. The contribution from such a band would also make the angular distribution more nearly isotropic thus making it appear in part as if the higher

spin contributions were absent. However, the observed effects seem quite too strong to be explained by this alone.

The extrema in the total fission cross section occur at 850 and 1050 kev, coincident with those in the plot of angular anisotropy versus energy. The drop in the total fission cross section between these two energies is due to competition from neutron emission to the vibrational levels in U-234 which becomes quite effective in this region of energy. Therefore it is logical to connect the change in the anisotropy with this effect also. Although the Hauser-Feshbach analysis does not predict such a change, it is quite possible that decay probabilities to these levels are not accurately accounted for by the application of the same rules that are used to calculate decay probabilities to levels of the ground state rotational band. Possibly decay from the higher spin states to these vibrational states is favored. If K remains a good quantum number remote from the saddle point there is also the possibility that a sort of K selection rule exists which slows down transitions for which $\Delta K > 1/2$. This might help to account for the somewhat larger than expected contribution from the K = 3/2- band without need for introducing an additional 3/2 band. The smoothness of the change in anisotropy suggests that only a single process is at work here. As a consequence of these arguments it is suggested that neutron emission to the vibrational levels accounts for the change in angular distribution, and that laws governing the relative probabilities of neutron emission to collective vibrational levels do not follow the simple Hauser-Feshbach picture.

An alternate possibility is that K loses stability over a narrow energy region, regaining some or all of it at higher energies. A wobbling of the K axis would certainly smear out the higher order harmonics much more drastically than the second order. Possibly the top of the barrier for the dominant fissioning band is a region of K instability.

Below 500 kev the angular anisotropy departs rapidly from sidewise peaking. It has been assumed that this is due to a K = 1/2+ band, but it could be due instead to a certain wobbling of the K axis, that is, to K not being a very good quantum number. If the curve could be established to much lower energies this point might be clarified since if the K = 1/2 band does exist the distribution should exhibit forward peaking at sufficiently low energies to preclude any sizeable contribution from the 3/2- band. In this regard it is interesting to compare results of measurements on other even-even target nuclei.

Th-232 shows a maximum sidewise peaking at 1.6 Mev (He56). At higher energies the anisotropy shifts and remains forward peaked. Below 1.6 Mev it trends rapidly towards isotropy but the measurements were not carried far enough in this direction to determine whether or not it ever becomes forward peaked. Analyses by Wilets and Chase (Wi56) and by Hittmair (Hi60) of the angular distribution at 1.6 Mev indicate that fission occurs here primarily via the K = 3/2- band. A similar analysis made by the author using transmission factors from the PB potential (not included herein) confirms this.

Th-230 has been investigated (Si60, Go59) and is found to behave much like Th-232 but in this case the curve was established to lower

energies (Go59) and sure enough, the anisotropy was found to shift to forward peaking at the lowest energies. This is strong evidence for the goodness of K near threshold and supports the level assignments made herein for U-234 at 500 kev as consisting in part of K = 1/2+ terms rather than introducing the concept of a wobbling K axis.

U-236 exhibits strong sidewise peaking near threshold, followed by forward peaking at higher energies (Si60). U-238 shows only forward peaking but is trending strongly towards isotropy at the lowest energy measured (Si60). Summarizing these results, let f stand for forward, and s for sidewise peaking. Then the sequence for the various isotopes as energy is increased is:

| | |
|---|---|
| Th-230 | f,s,f. |
| Th-232 | ?,s,f. |
| U-234 | ?,s,f. |
| U-236 | ?,s,f. |
| U-238 | ?,?,f. |

In every case at the lowest energies where measurements were made the trend is strongly in the direction to reproduce the pattern found for Th-230. Clearly further measurements are indicated. There is nothing in Bohr's theory dictating that the K band sequence near the saddle point must be 1/2, 3/2, 1/2. This would have to come from a continuation of the work of Nilsson and others into the region of deformation characterized by $\beta$ of the order of unity. A K band spectrum of this sort is not unreasonable, however, and these nuclei being of similar structure might be expected to show similarities in their K band sequences.

In conclusion, the results of this work do lend credence to Bohr's theory of fission. Near threshold it is possible to recognize to some

extent at least, the individual levels through which fission proceeds over the barrier as long as some sort of partial orientation of the angular momenta is present during the reaction. The preponderance of forward peaking over most of the energy range indicates the importance to fission of the $K = 1/2$ bands since all others produce sidewise peaking.

Further work with the even-even isotopes at still lower energies is clearly called for in order to determine whether or not the pattern established for Th-230 is indeed followed in all cases. With careful attention to background it may be possible to secure enough counts to at least determine the directions of the anisotropies. Such work is planned for the near future. It would then be of interest to explore the level structure from a theoretical point of view after the fashion of Mottelson and Nilsson (Mo59) to find out what sort of K band sequence would be predicted for the extreme deformations extent at the saddle point.

# BIBLIOGRAPHY


Ba59 A. P. Baerg, R. M. Bartholomew, F. Brown, L. Katz, and S. B. Kowalski. "The Angular Distribution of Photofission Fragments." Appendix by P. M. Dyson, J. M. Kennedy, and E. Vogt. "Calculation of Angular Resolution Corrections." Can. J. Phys. 37, 1418-1437 (Dec. 1959).

An excellent paper containing much valuable data on odd- and even-mass targets, for photofission in the energy range of 6 to 20 Mev.

Bl52 J. M. Blatt and V. F. Weisskopf. Theoretical Nuclear Physics. Wiley, New York, 1952.

Bø40 J. K. Bøggild, K. J. Brostrøm, and T. Lauritsen. "Cloud Chamber Studies of Fission Fragment Tracks," Kgl. Danske Videnskab, Selskab, Mat.-fys. Medd. 18, No. 4, 32 pages (Nov. 1940).

Bo52 A. Bohr. "The Coupling of Nuclear Surface Oscillations to the Motion of Individual Nucleons," Kgl. Danske Videnskab, Selskab, Mat.-fys. Medd. 26, No. 14, 40 pages (1952).

One of the first of many excellent articles on collective motion by A. Bohr.

Bo53 A. Bohr and B. R. Mottelson. "Collective and Individual-Particle Aspects of Nuclear Structure," Kgl. Danske Videnskab, Selskab, Mat.-fys. Medd. 27, No. 16 (Sept. 1953).

A comprehensive treatment of the collective model.

Bo54 A. Bohr. "The Collective Model of the Nucleus." Unpublished lecture notes for the fall term, 1954, at Princeton Univ., Princeton, N. J.

Similar to (Bo53) but also contains a treatment of anisotropy in fission.

Bo55 A. Bohr. "On the Theory of Nuclear Fission," Proc. Internat. Conf. Peaceful Uses Atomic Energy, Geneva, 1955. Paper P/911.

The classic paper on fission fragment anisotropy. The ideas set forth herein are still current.

Bo57 A. Bohr and B. R. Mottelson. "Electric Dipole Moment Associated with Octupole Vibrations of a Spheroidal Nucleus," Nuclear Phys. 4, 529-31 (Oct. 1957).

Low lying, odd parity states in heavy nuclei are described. Pertinent to fission channel analyses.

Bo39 N. Bohr and J. A. Wheeler. "The Mechanism of Nuclear Fission," Phys. Rev. 56, 426-50 (1 Sept. 1939).

The classic paper on nuclear fission. Based on liquid drop concepts.

Br54 J. E. Brolley, Jr. and W. C. Dickinson. "Angular Distribution of Fragments from Neutron-Induced Fission," Phys. Rev. 94, 640-2 (1 May 1954).

Br55 J. E. Brolley, Jr., W. C. Dickinson, and R. L. Henkel. "Angular Dependence of the Neutron-Induced Fission Process, II," Phys. Rev. 99, 159-65 (1 July 1955).

Bu62 B. Buck and G. R. Satchler. To be published.

Co58 C. T. Coffin and I. Halpern. "Angular Distributions in Fission Induced by Alpha Particles, Deuterons, and Protons," Phys. Rev. 112, 536-43 (15 Oct. 1958).
Projectiles were 11 Mev Protons, 22 Mcv deuterons, and 43 Mev alphas. Targets were Bi-209, Ra-226, Th-232, U-238, U-235, Np-237, and Pu-239. All gave fore-and-aft peaking.

Co54 B. L. Cohen, W. H. Jones, G. H. McCormick, and B. L. Ferrell. "Angular Distributions of Fission Fragments from 22 Mev Proton-Induced Thorium Fission," Phys. Rev. 94, 625-9 (1 May 1954).
They found a correlation between angular and mass asymmetry.

Co55 B. L. Cohen, B. L. Ferrell-Bryan, D. J. Coombe, and M. K. Hullings. "Angular Distribution of Fission Fragments from 22 Mev Proton-Induced Fission of U-238, U-235, U-233, Th-232, and Th-230." Phys. Rev. 98, 685-7 (1 May 1955).
An extension of the work reported in (Co54).

Cr58 L. Cranberg and J. S. Levin. "Inelastic Neutron Scattering by U-238," Phys. Rev. 109, 2063-70 (15 March 1958).
Inelastic scattering levels found to correlate fairly well, but not exactly, with plateaus in the low-energy tail of the fission cross section.

Da60 J. W. T. Dabbs, F. J. Walter, L. D. Roberts, G. W. Parker, and J. O. Thomson. "Fission Fragments from Aligned U-233 and U-235 Nuclei," Oak Ridge National Laboratory Report, ORNL-2910, 60-2, (10 Feb. 1960). Unpublished.
The results depend on the nature of a chemical bond which has yet to be firmly established, because an anomolous type of bonding seems to be indicated.

Di53 W. C. Dickinson and J. E. Brolley, Jr. "Angular Distribution of Fragments from Neutron-Induced Fission," Phys. Rev. 90, 388 (15 April 1953).

Di57a B. C. Diven. "Fission Cross Section of U-235 for Fast Neutrons," Phys. Rev. 105, 1350-3 (15 Feb., 1957).

Di57b B. C. Diven. Private communication.

Dr60 V. A. Druin, Yu. V. Lobanov, and S. M. Polikanov. "Angular Distribution of Fission Fragments in Fission Induced by Heavy Ions," J. Exptl. Theoret. Phys. (U.S.S.R.) 37, 38-40 (July 1959). Trans: Soviet Phys. -- JETP 10, 26-8 (Jan. 1960).

Em58 W. S. Emmerich. Cross Section Calculations for Fast Neutron Scattering. Part V, Optical Model Transmission Coefficients. Westinghouse Research Laboratory Report 6-94511-R19, Pittsburgh, Pa., (29 April 1958). Unpublished.

Ev55a R. D. Evans. The Atomic Nucleus. McGraw-Hill, New York, 1955.
Relations developed in Appendix B facilitate coulomb scattering calculations.

Ev55b E. Everhart, G. Stone, and R. J. Carbone. "Classical Calculation of Differential Cross Section for Scattering from a Coulomb Potential with Exponential Screening," Phys. Rev. 99, 1287-90 (15 Aug. 1955).
A rather extensive evaluation of the effects of electron screening on coulomb scattering.

Fa54 A. W. Fairhall, I. Halpern, and E. J. Winhold. "Angular Anisotropy of Specific Thorium Photofission Fragments," Phys. Rev. 94, 733-4 (1 May 1954).
Photon source was 16 Mev bremsstrahlung from a thick target. A correlation was found between angular- and mass-asymmetry.

Fa58 H. Faissner and F. Gonnenwein. "Angular Distribution in the Photofission of Thorium," Z. Physik 153, 257-68 (5 Dec. 1958).
The quadrupole term was not statistically significant at their bremsstrahlung energy of 15.8 Mev.

Ga59 C. J. Gallagher, Jr. and T. D. Thomas. "Vibrational States in U-234 Excited by Np-234 Decay, and Evidence for an E-0 Transition Between States with $I \neq 0$," Nuclear Phys. 14, 1-20 (Dec. 1959).
Many collective energy levels are given for U-234. These are of significance in evaluating the possible effects of inelastic neutron scattering on the angular distribution of fission fragments from an excited U-235 compound nucleus.

Ge10 H. Geiger. "The Scattering of Alpha Particles by Matter," Proc. Roy. Soc. (London) A83, 492-504 (17 Feb. 1910).
One of the best of the early experiments on coulomb scattering.

Gl53 F. M. Glass. Private Communication.

Gl55 S. Glasstone. Principles of Nuclear Reactor Engineering. D. Van Nostrand Co., Inc., New York, 1955.

Go59 B. M. Gokhberg, G. A. Otroshchenko, and V. A. Shigin. "Effective Cross Section and Anisotropy of the Fission of Np-237 and Th-230," Doklady Akad. Nauk S.S.S.R. 128, 1157-9 (21 Oct. 1959). Trans: Soviet Phys. -- Doklady 4, 1074-6 (March-April 1960).
Contains very good data in the low energy region (up to 1500 kev). However, the fission cross section of Th-230 is only relative, since mass of material on fission foil was not known.

Gr59 J. J. Griffin. "Energy Dependence of Fission Fragment Anisotropy," Phys. Rev. 116, 107-118 (1 Oct. 1959).
An excellent treatment of the ideas of A. Bohr as presented in (Bo55). More detail has been added, and also statistical considerations which are useful at energies well above the barrier.

Ha58 I. Halpern and V. M. Strutinski. "Angular Distribution in Particle-Induced Fission at Medium Energies," Proc. Second United Nations Internat. Conf. Peaceful Uses Atomic Energy 15, 408-17, Paper P/1513, Sept. 1958. A United Nations Pub..

Ha59a I. Halpern. "Nuclear Fission," Ann. Rev. Nuclear Sci. 9, 271-342 (1959).
An excellent article.

Ha59b I. Halpern. "A Suggested Explanation for the Anomolous Anisotropies in High Energy Fission," Nuclear Phys. 11, 522-30 (1 June 1959).
Contains an interesting suggestion of a mechanism to account for the reversal of the sign of the anisotropy at high energy. In qualitative agreement with several aspects of high energy angular distributions.

Ha60 S. H. Hanauer. The Angular Distribution of Alpha Particles Emitted by Oriented Np-237 Nuclei. Ph.D. dissertation, University of Tenn., Knoxville, Tenn., 1960. Unpublished.
Of interest, since alpha emission is indirectly connected with fission via collective properties of the parent nucleus.

Ha56 G. C. Hanna, J. C. D. Milton, W. T. Sharp, N. M. Stevens, and E. A. Taylor. Proc. Symp. Phys. of Fission held at Chalk River, Ont., May 14-18, 1956. Report CRP-642-A, of the Atomic Energy of Canada Ltd., Chalk River, Ont.. Also issued as AECL 329, by U. S. Atomic Energy Commission.
Somewhat out dated, but is an excellent account of the status of fission physics generally as of 1956.

Ha52 Walter Hauser and Herman Feshbach. "The Inelastic Scattering of Neutrons," Phys. Rev. 87, 366-73 (15 July 52).
The classic paper on the subject.

He56 R. L. Henkel and J. E. Brolley, Jr.. "Angular Distribution of Fragments from Neutron-Induced Fission of U-238 and Th-232," Phys. Rev. 103, 1292-5 (1 Sept. 1956).
More complete data are available now. However, the results for Th-232 were subjected to a channel analysis by Wilets, in (Wi56).

He50 G. Herzberg. Molecular Spectra and Molecular Structure; I. Spectra of Diatomic Molecules. D. Van Nostrand Co., Inc., New York. Second ed. 1950.
Contains a fine treatise on rotational and vibrational levels which is directly applicable to channel analysis of fission.

Hi53 D. L. Hill and J. A. Wheeler. "Nuclear Constitution and the Interpretation of Fission Phenomena," Phys. Rev. 89, 1102-45 (1 March 1953).
The classic paper on the collective model for fission. Liquid drop concepts are retained, but collective features are added, making the model much more attractive.

Hi60 O. Hittmair. "Winkelverteilungen von Kernspaltungen in Resonanzbereich," Nuclear Phys. 18, 346-52 (Aug.(2), 1960).

Ho59 R. J. Howerton. "Tabulated Neutron Cross Sections," UCRL 5226, 1959.

Hu54 R. Huby. "Phase of Matrix Elements in Nuclear Reactions and Radioactive Decay," Proc. Phys. Soc. (London) 67A, 1103-5, 1954.
Points out error in phase of Z function.

Hu58 D. J. Hughes and R. B. Schwartz. "Neutron Cross Sections," Brookhaven National Laboratory Report, BNL 325, Second ed. (1958).

In58 D. R. Inglis. "Fission Asymmetry," Ann. Phys. 5, No. 2, 106-140 (Oct. 1958).
Mainly concerned with mass asymmetry. Detailed discussion of possible shapes near saddle point.

Ke59 P. M. Endt and M. Demeur. Nuclear Reactions, Vol. I. North Holland Pub. Co., Amsterdam 1959.
Contains a contribution by Kerman on the rotational model which is excellent.

La55 R. W. Lamphere and R. E. Greene. "Neutron-Induced Fission Cross Sections of U-234 and U-236," Phys. Rev. 100, 763-70 (1 Nov. 1955).
Describes methods and equipment partly pertinent to this work.

La49 N. O. Lassen. "On the Energy Loss by Fission Fragments along Their Range," Kgl. Danske Videnskab. Selskab, Mat.-fys. Medd. 25, No. 11, 42 pages, (Dec. 1949).
Pertinent to scattering of fission fragments.

Lo56 O. V. Lozhkin, N. A. Perfilov, and V. P. Shamov. "The Angular Distribution of Fragments from Fission of Uranium at High Excitation Energies," J. Exptl. Theoret. Phys. (U.S.S.R.) 29, 292-5 (Sept. 1955). Trans: Soviet Physics -- JETP 2, 116-8 (Jan. 1956).

Ma60 J. B. Marion and J. L. Fowler. Fast Neutron Physics. Interscience Publishers, New York, 1960.
An excellent book on experimental methods and equipment. The section on fission detectors is particularly applicable.

Me58 J. W. Meadows. "Angular Distribution of Fragments from Fission of U-238 and Th-232 by 45, 80, and 155 Mev Protons," Phys. Rev. 110, 1109-13 (1 June 1958).
Describes change of anisotropy with energy, showing change in sign near 150 Mev. Curve extended to 600 Mev from other data.

Mo57 S. A. Moszkowski. "Models of Nuclear Structure," Encyclopedia of Physics 39, 411-550. Springer-Verlag, Berlin, 1957.
Some of the material is appropriate to fission angular distributions. This portion is similar to (He50).

Mo59 B. R. Mottelson and S. G. Nilsson. "The Intrinsic States of Odd-A Nuclei Having Ellipsoidal Equilibrium Shape," Kgl. Danske Videnskab. Selskab, Mat.-fys. Medd. 1, No. 8, 105 pages (1959).
A very comprehensive work. The distortions considered are, however, much below those extant at saddle point.

Ni55 S. G. Nilsson. "Binding States of Individual Nucleons in strongly Deformed Nuclei," Kgl. Danske Videnskab. Selskab, Mat.-fys. Medd. 29, no. 16 (69 pages, 1955).

Pe62 F. Perey and B. Buck. To be published in Nuclear Physics.

Pe60 N. A. Perfilov and Z. I. Solov'Eva. "Angular Distribution of Long-Range Alphas Connected with Fission," J. Exptl. Theoret. Phys. (U.S.S.R.) 37, 1157-9 (Oct. 1959). Trans: Soviet Physics JETP 10, 824-5 (April 1960).
Results may be interpreted as evidence for the existence of alpha particle clusters in the excited compound nucleus.

Pi59 G. A. Pik-Pichak. "Anisotropic Fission of Rotating Nuclei," J. Exptl. Theoret. Phys. (U.S.S.R.) 36, 961-2 (March 1959). Trans: Soviet Physics -- JETP 9, 679-80 (Sept. 1959).
Contains arguments purporting to connect tendency towards isotropy for increasing $Z^2/A$ with xn'f events and the increase in fissionability with $Z^2/A$. Quite a logical explanation.

Pr58 A. N. Protopopov and V. P. Eismont. "On the Angular Anisotropy in the Emission of Fragments upon Fission of Pu-239 by 14 Mev Neutrons," J. Exptl. Theoret. Phys. (U.S.S.R.) 34, 250-1 (Jan. (1958). Trans: Soviet Physics -- JETP 7, 173-4 (July 1958).
They find an anisotropy of $1.15 \pm 0.05$, whereas U-233 shows anisotropy of $1.28 \pm 0.07$. Contrary to theoretical prediction.

Pr59 A. N. Protopopov and V. P. Eismont. "Dependence of the Angular Anisotropy of Fission on the Nuclear Structure," J. Exptl. Theoret. Phys. (U.S.S.R.) 36, 1573-4 (May 1959). Trans: Soviet Physics -- JETP 9, 1116-7 (Nov. 1959).

The authors attempt to explain results such as they quote in (Pr58) on basis of increase of fissionability with $Z^2/A$ causing a difference in activation energy parallel to, and perpendicular to, the beam. Note the difference between this explanation, which does not depend on n'f events, with that given in (Pi59). However, this one lacks the conviction of the former.

Ro57 M. E. Rose. Elementary Theory of Angular Momentum. Wiley, New York, 1957.

Ro53 M. E. Rose. "The Analysis of Angular Correlation and Angular Distribution Data," Phys. Rev. 91, 610-15 (1 Aug. 1953).

Si60 J. E. Simmons and R. L. Henkel. "Angular Distribution of Fragments in Fission Induced by Mev Neutrons," Phys. Rev. 120, 198-210 (1 Oct. 1960).

A very valuable piece of work. It covers the energy range from 0.5 to 9 Mev, and from 14 to 23 Mev neutron energy, for targets of Th-230, U-233, U-234, U-235, U-236, U-238, Np-237, and Pu-239, with measurements taken at angles of 0, 22.5, 45, 67.5, and 90 degrees. Instrumental uncertainties and energy spread were rather large, so some fine structure may have been missed.

St60a N. R. Steenberg and R. C. Sharma. "Alpha Decay and Fission of Aligned Nuclei," Can. J. Phys. 38, 290-314 (Feb. 1960).

A theoretical analysis. Although dealing primarily with aligned nuclei, the concepts are more generally applicable.

St59 R. H. Stokes, J. A. Northrop, and K. Boyer. "Measurement of the Fission Thresholds of Pu-239, U-233, U-235, and U-238, using the (d,p) Reaction," Phys. Rev. 115, 1277-86 (1 Sept. 1959).

An excellent experimental approach to the study of threshold regions of fissionable nuclei. Holds promise of supplying further valuable data.

St57b V. M. Strutinski. "Statistical Theory for the Angular Distribution of Fission Fragments," Atomic Energy 2, No. 6, 621-7 (1957). (A translation of the Soviet Jl. Atomic Energy.)

A statistical application of the ideas of A. Bohr to regions where a large number of fission channels are open.

St57c W. E. Stein. "Velocities of Fragment Pairs from U-233, U-235, and Pu-239 Fission," Phys. Rev. 108, 94 (1 Oct. 1957).

St60b V. M. Strutinski. "Angular Anisotropy of Gamma Quanta that Accompany Fission," J. Exptl. Theoret. Phys. (U.S.S.R.) 37, 861-3 (Sept. 1959). Trans: Soviet Physics -- JETP 10, 613-15 (March 1960).

Shows how fragments may be emitted with high spins, and how this in turn might be detected by an angular anisotropy in the gamma quanta emitted from the decaying fragments. This effect is not large, and background problems would make it difficult to evaluate with accuracy experimentally.

Sw60 W. J. Swiatecki. Private communication, July, 1960.

Tu40 L. A. Turner. "Nuclear Fission," Revs. Mod. Phys. 12, 1-29 (Jan. 1940).

Va60 U. L. Vallinder and H. Tyren. "Angular Distribution of Fragments from Fission of Uranium Induced by 185-Mev Protons," Nuclear Phys. 15, 152-4 (1 Feb. 1960).

Wh56 J. A. Wheeler. "Fission," Physica 22, 1103-14 (1956).

An excellent theoretical description of the fission process in general, including a discussion of angular and mass asymmetry.

Wh61 J. A. Wheeler. "Physics of Fission," Encyclopedia of Physics XLI/2 (to be published), Springer-Verlag, Berlin, 1959.

Wi59 E. P. Wigner. Group Theory. Academic Press, New York, 1959.

Contains an excellent discussion of rotation functions. However, this book is a translation of an earlier edition wherein a left handed system of coordinates was used. The 1959 edition employs the right handed system except that occasionally the change was not carried out. For example, the expression for $d^{I}_{MK}(\beta)$ corresponds to that for $d^{I}_{MK}(-\beta)$ in a right-handed system. Compare with Ro57.

Wi56 L. Wilets and D. M. Chase. "Angular Distribution of Fission Fragments at Threshold According to the Bohr Model," Phys. Rev. 103, 1296-7 (1 Sept. 1956).

An analysis similar to that undertaken in this report. Experimental data of rather high accuracy is important for this type of analysis, however, as otherwise definite channel assignments are impossible. The channel assignments made here cannot be considered definite, but represent a logical possibility.

Wi40 E. J. Williams. "Multiple Scattering of Fast Electrons and Alpha Particles, and "Curvature" of Cloud Tracks Due to Scattering," Phys. Rev. 58, 292-306 (15 Aug. 1940).

The paper should be read by anyone doing coulomb scattering calculations.

Wi52 E. J. Winhold, P. T. Demos, and I. Halpern. "The Angular Distribution of Fission Fragments in the Photofission of Thorium," Phys. Rev. 87, 1139-40 (15 Sept. 1952).

Although better results have become available, this article contains the first reported observations of anisotropy in angular distributions of fragments from fission, which came as a surprise to the authors since the liquid drop theory of the time predicted only isotropy. Extremely important work, therefore, since it stimulated experimentalists and theorists alike and has led to a better understanding of fission.

Wi53 E. J. Winhold. Photofission of Thorium and Uranium. Ph.D. dissertation, Mass. Inst. of Tech., Cambridge, Mass., Sept. 1953.

An extension of the work begun in (Wi52).

Wo60 G. T. Wood. "Evidence for $0^+$ and $1^-$ Levels in U-234 Populated in the One-Minute Beta Decay of Pa-234," Phys. Rev. 119, 2004-9 (15 Sept. 1960).

A level found at 795 kev is interpreted as K=0, I=1, and of negative parity, in good agreement with (Ga59).

# APPENDIX A

## GEOMETRICAL RESOLUTION OF THE COLLIMATOR

Let $\theta$ be the angle between the axis of collimation and the path of a fission fragment through the collimator, and $\bar{\theta}$ be the average deviation for all fragments which traverse the collimator without colliding with the walls. To calculate $\bar{\theta}$ approximately, let $\theta_1$ and $\theta_3$ be the two extreme values of $\theta$ in the plane of collimation, and $\theta_2$ be the extreme value (which can occur in two ways) in a plane normal to that of collimation. See Fig. 17. Then $\theta_1 = 11.2^\circ$, $\theta_2 = 13.2^\circ$, and $\theta_3 = 8.2^\circ$.

$\bar{\theta}_0 = 1/2 \times 1/4 \, (\theta_1 + 2\theta_2 + \theta_3) = 5.7^\circ$ (for neutron beam parallel to the collimator axis).

$\bar{\theta}_{90} = 1/2 \times 1/2 \, (\theta_1 + \theta_3) = 4.9^\circ$ (for neutron beam normal to the collimator axis).

For a measurement of the (0/90) degree fragment ratio:

$$\bar{\theta} = 1/2 \, (\theta_0 + \theta_{90}) = 5.3^\circ,$$

and this will clearly be very nearly right for the measurements of the (30/60) degree ratios.

In order to determine the extent of error introduced by the sort of approximation used to obtain $\bar{\theta}_0$, the problem was set up for the electronic computer. Fragments were assumed to be emitted isotropically from an element, $dA_1$, of the foil at the bottom of a collimator hole, and to make their exit through an element of area, $dA_2$, at the top of the hole. Let $r_{12}$ denote the distance between $dA_1$ and $dA_2$, and $\theta$ be the angle between $r_{12}$ and the collimator axis as before. Then:

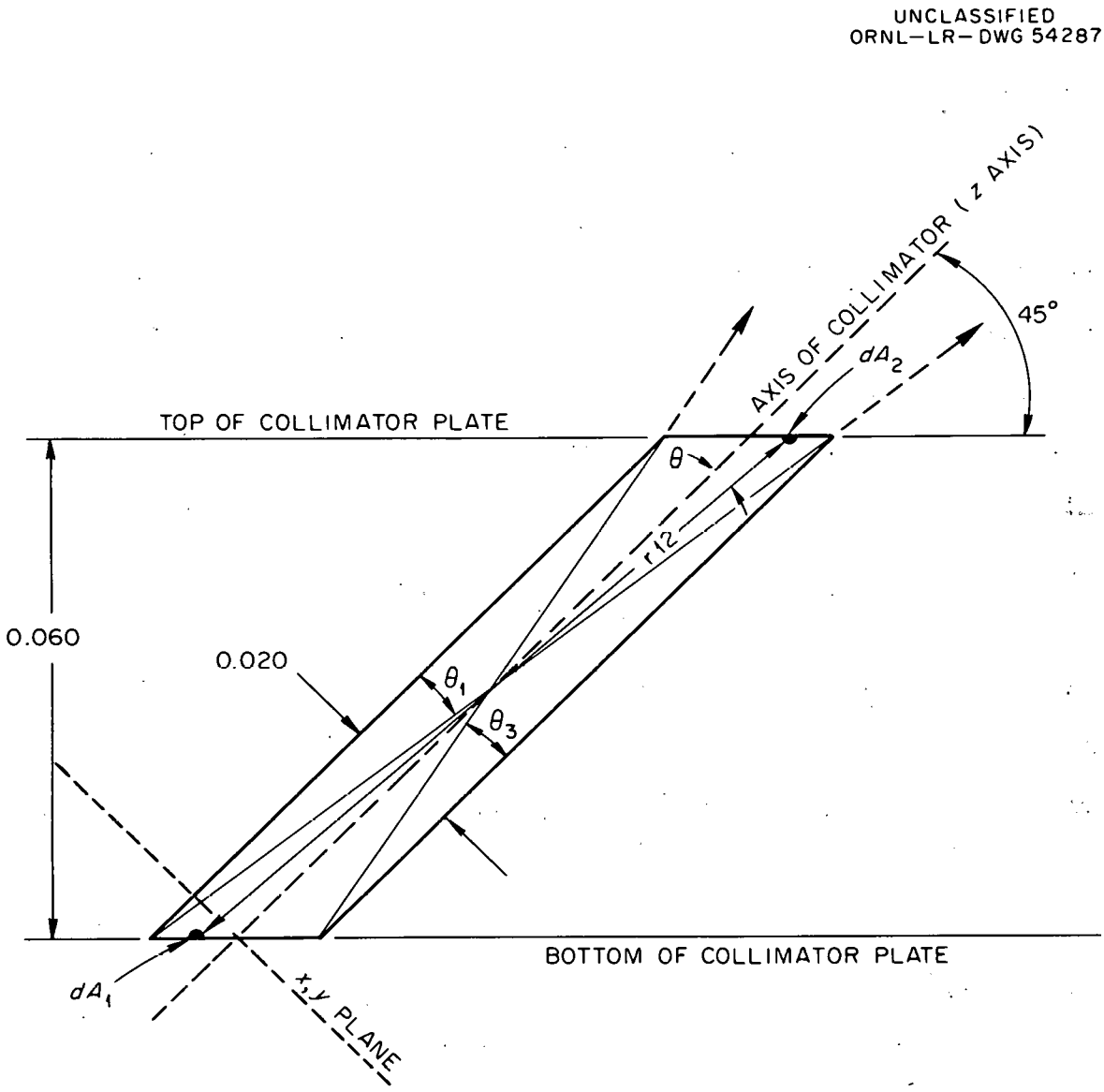


Fig. 17. Cross Section Through a Collimator Hole in a 0.060-in. Thick Aluminum Collimator Plate.

$$\bar{\theta} = \frac{\int \theta dA_1 n \cdot dA_2 / r_{12}^2}{\int dA_1 n \cdot dA_2 / r_{12}^2} \quad . \tag{50}$$

Take the coordinate system origin at the center of the bottom hole (on the axis of the collimator), and x and y axes in the usual sense in a plane normal to the axis of collimation. Let the subscripts, 1 and 2, refer to coordinates of $dA_1$ and $dA_2$, respectively. Make the small angle approximation, $\theta = \sin \theta$, and replace the integrals by finite summations where one unit equal 0.001". Then the equation for machine calculation is:

$$\bar{\theta}_0 = \frac{1}{2} \frac{\sum_{x_1, x_2, y_1, y_2} \sqrt{2(x_2 - x_1)^2 + (y_2 - y_1)^2 (1/r_{12}^4)}}{\sum_{x_1, x_2, y_1, y_2} (1/r_{12}^3)} \quad , \tag{51}$$

where

$$r_{12}^2 = (x_2 - x_1)^2 + (y_2 + y_1)^2 + (85 + x_2 + x_1)^2 \, ,$$

and the limits are

$x_1$ taken from -10 to +10 ,

$x_2$ taken from -10 to +10 ,

$y_1$ taken from $-\sqrt{100 - x_1^2}$ to $+\sqrt{100 - x_1^2}$,

$y_2$ taken from $-\sqrt{100 - x_2^2}$ to $+\sqrt{100 - x_2^2}$ .

Evaluating in increments of 2 units ($x_i$ or $y_i$ equals 2) gave $\bar{\theta}_0 = 5.62^\circ$. Evaluating in increments of 1 unit gave $\bar{\theta}_0 = 5.54^\circ$.

This more accurate result is 2.8% less than that obtained by use of the approximate method. Applying this factor, 0.972, to the value of $\bar{\theta}$ obtained after consideration of the effect of neutron beam direction, remembering that what is really wanted is not just the average angular deviation from the collimator axis, but the deviation with respect to a given angle from the neutron beam, an overall figure of

$$\delta\theta_c = 5.3 \times 0.972 = 5.2^\circ$$

is obtained for the average angular spread introduced by the collimator into the measurements of angular distribution of fission fragments relative to a neutron beam.

The fact that the neutron beam itself was not a plane parallel beam, but instead emerged from a line source 3 cm in length, and struck foils of one inch diameter introduced a further spread in angle. These foils were located with their centers on the beam axis and 8.6 cm from the near end of the neutron source. They were inclined at an angle of either 45 or 15 degrees to the beam. Considering the fact that the neutrons were emitted from a line source, and following an approximate method similar to that first used to evaluate the collimator resolution, the average angular spread due to the beam is found to be $4.2^\circ$ for the (0/90) degree ratio measurements and $4.8^\circ$ for the (30/60), to within an estimated limit of 5%. An average of $4.5^\circ$ is appropriate for those points where both ratios were measured. This, compounded with the $5.2^\circ$ from the collimator and an estimated $2^\circ$ average error in alignment of foils and target gives an overall average angular spread of $7.1^\circ$.

# APPENDIX B

## COULOMB SCATTERING OF FISSION FRAGMENTS

A precise evaluation of coulomb scattering of fragments from the walls of the collimator and by the gas in the passages, while possible in principle, would be a formidable undertaking purely on geometrical grounds. Fortunately it is not necessary here, as a few general considerations of a semiquantitative nature suffice to show that this scattering, while not zero, was of such small magnitude as to exert a completely negligible effect on the angular distribution measurements. Additional arguments point out that such scattering as did take place from the collimator walls was not detrimental to the angular resolution, but on the contrary lay in the direction of improvement.

Fission fragments lose energy principally by collisions with electrons, and such collisions do not measurably affect their directions. Only towards the end of the range do nuclear (non-ionizing) collisions become of importance. (These cause the fragment to lose energy through momentum transfer alone, and give rise to the term, "ionization defect," which refers to the lack of equality between fragment energy and energy lost by ionization. It has been observed especially for heavy charged particles such as fission fragments, and to a much lesser extent for alpha particles.) Measurements of the bending of fragment tracks in a cloud chamber have yielded data from which the probability of deflection as a function of angle has been worked out for 5 mm increments of path length along the range (Bø40). These results combined with the range-

energy relations of Lassen (La49) show that nuclear collisions are discernible only in the energy range below 30 Mev. In the energy interval from 30 to 15 Mev the fragments lose about 2.5% of their energy by nuclear collisions, while the average angle of deflection between the beginning and end of this interval amounts to only $3^{\circ}$ and in no case exceeds $6^{\circ}$.

Measured along the axis of collimation (at $45^{\circ}$ to the foil surface) the average thickness of the uranium deposit amounted to 10 Mev, and the distance from surface of foil to exit from the collimator was equivalent to another 10 Mev as an average figure. Therefore particles emitted with more than 50 Mev did not contribute to scattering. The amplifier bias was equivalent to about 13-Mev ionization energy, or to fragment energies of about 20 Mev, taking mass defect into account. Therefore only fragments with initial energies between 30 and 50 Mev needed to be considered; and it has been found (St57c) that all fragments have an initial energy of 40 Mev or greater, and that less than 1% have energies below 50 Mev.

It follows that coulomb scattering could not occur ahead of the collimator, and that within it only those rare particles within the 20 to 30 Mev bracket could contribute. For these, the average angle of deflection was less than $3^{\circ}$ and the maximum less than $6^{\circ}$. Most of the particles which struck the walls were lost, since the strong preference for forward scattering, together with geometrical and momentum transfer effects made it impossible for a fragment to strike the aluminum walls, undergo Rutherford scattering, and emerge again unless it struck the walls at a grazing angle of only 2 or 3 degrees. Therefore only

particles which had an initial direction within 2 or 3 degrees of the axis of collimation were capable of being scattered and still escape with sufficient energy to be counted in the ion chamber. Geometrical considerations together with the narrowness of the effective energy interval make it clear that even this process was extremely unlikely.

# APPENDIX C

## BACKGROUND FROM SCATTERED NEUTRONS

Besides the primary beam of neutrons from a gas target there always exists a background of scattered neutrons somewhat degraded in energy and usually quite random in direction. These produce a background counting rate which should be taken into account. In this experiment the fission fragments due to these neutrons are believed to have been emitted isotropically. In what follows it will become clear that multiply-scattered neutrons need not be considered, and that objects outside the counter itself did not significantly contribute to the scattering. The simplifying assumption is made that the angle of orientation of the counter relative to the beam axis did not materially alter the ratio of scattered to primary neutron flux, and the calculations have been carried through for the counter axis of symmetry aligned with the beam direction.

An experimental evaluation of the effect of scattering presents formidable difficulties since ordinary shadow cone techniques are not applicable. Were it not for the low count rates caused by collimating, some success might follow from use of methods similar to those employed with this counter but without collimators to evaluate the effect of inelastically scattered neutrons on the measured fission cross-section ratio of normal uranium to that of U-235 (La55). In that experiment the effect was calculated by methods similar to those used herein except for use of the inelastic cross section and energy spectrum, neglect of elastically scattered neutrons, omission of collimators, and closer

spacing between foils and gas target source. The experimental evaluation consisted of increasing the sizes of counter components in proper proportion, calculating the increased scattering and comparing it with the measured effect on the cross-section ratio. The calculation was made at 2.8 Mev and gave an expected change in the measured cross-section ratio of 2.9%, whereas measurements yielded 2.8% plus or minus 0.3%. This sort of agreement inspires confidence that the rather geometrically similar calculations herein may be reasonably accurate. However, an overall uncertainty of 20% has been assigned to the calculated ratio, s, of scattered to primary flux. s is of the order of 15%, which would indicate a 3% uncertainty in the final result except that this is further reduced by the existence of some degree of isotropy in the true distribution. The uncertainty which carries over to the measured fragment intensity ratios lies in the neighborhood of 1 to 2% (1.2% at 843 kev), about as large as the counting statistical errors. Its extreme value occurs at the minimum in the distribution curve, at 503 kev, where it amounts to 2.0%. Since the effect of the scattered neutron flux was to introduce an additional isotropic component into the fragment angular distributions, it is clear that the corrections must always result in enhancing the measured departures from isotropy, and that there is no correction or added uncertainty where the measured distribution is isotropic.

It has been found by experiments that the scattering of neutrons with energies less than a few Mev is predominantly isotropic in the center-of-mass system (GL55, p. 150). The average value of the cosine of the

scattering angle is therefore zero, but in laboratory coordinates will be 2/3A for a scatterer of mass number, A, and this gives a convenient measure of the degree of forward scattering. For aluminum, the dominant scattering medium in the chamber, this amounts to less than 2 degrees out of 90, so that the assumption of isotropy for the elastically scattered neutrons is reasonable. A small amount of inelastic scattering was present in some instances, and where the emitted neutrons had energies above the U-234 fission threshold, say above about 550 kev, they should be taken into account. These neutrons can also be considered to be primarily isotropic due to the discrimination of the centrifugal barrier potential against emission of neutrons of angular momenta other than zero. The effective cross section for scattering must then be the elastic, plus a portion of the inelastic judiciously chosen to represent that fraction of the inelastically scattered neutrons whose energies lie in the range to effect fission in the U-234. The cross sections used in the calculations have been taken from the extensive compilation by Howerton (Ho59).

The bulk of the scattering was elastic. If E' is the energy of a scattered neutron, E the energy of the incident one, and $\theta$ the scattering angle, then

$$E'/E = 1/2 \left[ (1 + \alpha) + (1 - \alpha) \cos \theta \right] , \qquad (52)$$

where $\alpha = (A - 1)^2/(A + 1)^2$. The maximum decrease in energy occurs for $180^\circ$ collisions, and for aluminum amounts to 14%, with an average of only 7%. Therefore, for most cases the scattered neutrons were about as effective in causing fissions as the unscattered ones. However, where the

fission cross section changes rapidly with energy, as near threshold, this degradation in energy should be considered when evaluating the magnitude of the correction. This has been taken into account where necessary in the calculations.

Scattering from the following parts of the chamber have been calculated:

1. The brass (67% Cu, 33% Zn) backing plate. This includes allowance for fixtures attached to it.
2. The aluminum cover. The front face and cylindrical wall are evaluated separately.
3. The aluminum collector plates.
4. The aluminum collimators and foil mounting plates as a unit.
5. Scattering from the 0.002" thick nickel foil backings is found to be negligible.
6. Teflon spacers and fluorothene mounting posts.
7. External objects and room scattering have been estimated and found to be negligible.

Consider item 5 first. Neutrons scattered from that portion of the nickel foil backings immediately behind the deposits must traverse one or the other of these deposits, but not both. Introduce the following notation:

M = Molecular, or atomic, weight of scatterer.

d = Density in grams/cc.

$N_1$ = Molecules, or atoms, per cc.

t = Thickness in cm.

$\phi$ = Primary flux density incident on foils.

$\phi'$ = Scattered flux density incident on foils.

$s = \phi'/\phi$.

$\sigma$ = Effective scattering cross section.

For the nickel foils:

$d = 8.9$

$M = 58.7$

$\sigma$ = Approximately 3 barns.

$s = (1/2)N_1 t\sigma$

$= 0.5 \times 6.02 \times 10^{23} \times (d/M)t\sigma$

$= 0.0465\sigma\%$ ($\sigma$ in barns)

$= 0.0465 \times 3$

$= 0.14\%$, which is deemed negligible.

That portion of each collimator lying immediately opposite the uranium deposits may be treated likewise after subtracting out the material removed by drilling, with the result:

$s = 0.55\sigma\%$ ($\sigma$ in barns) for both collimators.

A more general method must be applied to other sources of scattering. The product of solid angle subtended by the uranium foils from any scattering element, multiplied by the path length in the uranium deposit of a neutron emanating from this element, is independent of the angle between the normal to the foil surface and line to the scattering element, and is simply equal to the solid angle subtended by the uranium deposit from an equal distance on the normal. With this in mind and referring to Fig. 18, which shows the dimensions and parameters pertinent to the scat-

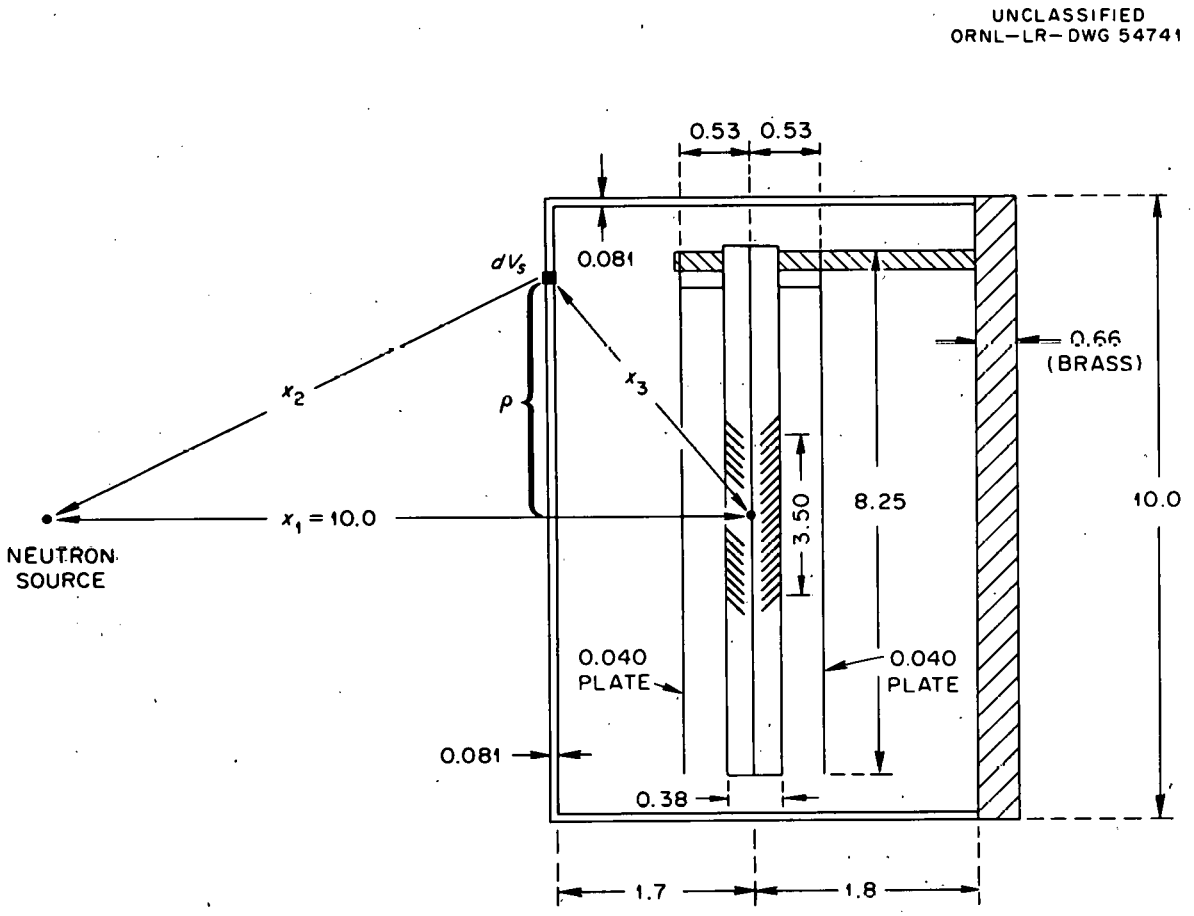


TEFLON ( $CF_2$ , DENSITY = 2.2 g/cc) SPACERS (6)

$t$ = 0.318 WIDTH = 0.65 MEAN LENGTH = 2.13

$\bar{x}_3$ = 3.8

FLUOROTHENE ( $C_2F_3Cl$ , DENSITY = 2.12 g/cc) POST (3)

DIAMETER = 0.63 LENGTH = 3.2

VERTICAL DISTANCE TO FOIL CENTER = 3.8

Fig. 18. Fission Chamber Details.

tering calculations, the following expression can be written for s:

$$s = N_1 \sigma \mathcal{f} (x_1^2/4\pi) \int dV_s/(x_2^2 x_3^2) , \qquad (53)$$

where

$\mathcal{f}$ = a factor of the order of 0.90 which takes into account the variation in intensity with angle of neutrons emitted from the tritium target (Ma60, p. 87). It is the relative intensity in the average direction of scatterer divided by the intensity at $5^\circ$ (the average direction of foil area). It is somewhat energy dependent, but over the energies and angles of interest will not vary by over 5%, but will, of course, be somewhat different for the various sources of scattering.

$x_1$ = Distance between foils and a point source equivalent to the line source of neutrons from the gas target. Equal to 10.0 cm for all cases.

$dV_s$ = A volume element of the scatterer.

$x_2$ = Distance from neutron source to $dV_s$.

$x_3$ = Distance from $dV_s$ to center of foils.

The scattering contributed by the aluminum face of the counter is evaluated as follows:

$$dV_s = 2t\pi\rho d\rho,$$
$$\mathcal{f} = I(22^\circ)/I(5^\circ) = 0.85,$$
$$x_2^2 = \rho^2 + 8.3^2,$$
$$x_3^2 = \rho^2 + 1.7^2.$$

$$s = N_1 \sigma t \oint x_1^2 (1/4\pi) \int_0^5 \frac{2\pi\rho d\rho}{x_2^2 x_3^2}$$

$$= \frac{1}{4} N_1 \sigma t \oint x_1^2 \int_0^{25} \frac{dy}{(y + 68.9)(y + 2.89)}$$

$$= 0.0602\sigma \times 0.081 \times 0.85 \times 100 \times 0.25(1/66) \left[ \ln \frac{y + 68.9}{y + 2.89} \right]_{25}^{0}$$

$$= 0.308\sigma\% \text{ } (\sigma \text{ in barns}). \qquad (54)$$

This method, with suitable modifications, has been applied to all other parts of the counter with the following results:

| Component | s in % |
|---|---|
| Brass back | $1.47\ \sigma_{brass} = 0.98\ \sigma_{Cu} + 0.49\ \sigma_{Zn}$. |
| Teflon spacers | $0.0294\ \sigma_{tef.} = 0.0294(\sigma_C + 2\sigma_F)$. |
| Fluorothene posts | $0.0120\ \sigma_{flu.} = 0.0120(2\sigma_C + 3\sigma_F + \sigma_{Cl})$. |
| Face of cover | $0.308\ \sigma_{Al}$. |
| Wall of cover | $0.125\ \sigma_{Al}$. |
| Collector plates | $0.450\ \sigma_{Al}$. |
| Collimator-foil asy. | $1.53\ \sigma_{Al}$. |

Neglecting the tiny contribution from the chlorine and combining the rest gives:

$$s = 0.053\ \sigma_C + 0.095\ \sigma_F + 2.40\ \sigma_{Al} + 0.98\ \sigma_{Cu} + 0.49\ \sigma_{Zn}.$$

At 843 kev this amounts to:

$$s = 0.053(2.8) + 0.095(4.0) + 2.40(4.0) + 0.98(3.4) + 0.49(3.5)$$

$$= 0.148 + 0.380 + 9.60 + 3.34 + 1.72$$

$$= 15.2\%.$$

The effect of this scattered flux on the measured ratio of fragment intensity at any two angles is found as follows:

$\phi_t$ = total flux density at foil center

$= \phi + \phi'$

$= \phi(1 + s)$.

Let:

$R_t$ = the observed count ratio corrected for unequal foil masses (from normalization in thermal flux) and for counts from the U-235 impurity.

$R$ = true count ratio which would be due solely to primary flux of unit intensity.

$R' = 1/1$

= count ratio due to scattered flux of unit intensity.

Then:

$$R_t = (R + sR')/(1 + s)$$

$$= (R + s)/(1 + s) .$$

$$R = R_t(1 + s) - s.$$

At 843 kev, $R_t$ = 1.68 and 1.33 for angle ratios of $(0/90)^\circ$ and $(30/60)^\circ$, respectively. The true count ratios in the absence of scattering would then be:

$R(0/90)^\circ = 1.68 \times 1.15 - 0.15$

$= 1.78$ (a 6% increase).

$R(30/60)^\circ = 1.33 \times 1.15 - 0.15$

$= 1.38$ (a 3.8% increase).

The uncertainties introduced by the limited accuracy of evaluation of s

are then:

$$6 \times 0.2 = 1.2\% \text{ and}$$

$$3.8 \times 0.2 = 0.8\%.$$

Scattering from nearby objects was negligible. By far the most potent object was the iron turntable, which may be represented by a disc 5 cm thick and 20 cm in diameter situated immediately beneath the foils at a distance of 38 cm, and 39 cm from the neutron source. Then $x_1 = 10.0$, $x_2 = 39$, $x_3 = 38$, $N_1 = 8.4 \times 10^{22}$, $d = 7.89$ g/cc, and $\sigma$ will not exceed 3 barns. The half value layer, $\tau$, is then

$$(\ell n\ 2)/(0.084 \times 3) = 2.75 \text{ cm},$$

so multiple scattering was appreciable, and there was also a small amount of absorption and inelastic scattering. So the extreme assumption that all the neutrons incident on the table were scattered gives a value of s somewhat higher than actually existed. Thus:

$$s = (10/39)^2(1/38)^2(100\ \pi/4\pi) = 1/27\%.$$

Room scattering can be neglected on the grounds of intensity, and also extent of energy degradation. The flux of scattered neutrons has been considered by Langsdorf (Ma60, p. 768), who has found that air and room scattering for an average laboratory setup may be expected to be of the same order of magnitude. Lumped together he finds for scattering from air and remote objects:

$$s = (x_1/L)^2(4p/(1 - p)),$$

where

L = equivalent radius of room space (200 to 500 cm).

p = fraction of neutrons reflected from walls of assumed

spherical shell of radius, L (approximately 0.2).

For this experiment, $x_1$ = 10. Taking L = 200 gives s = 1/4%. These neutrons will have been scattered several times, and so degraded in energy as to be ineffective in causing fission in U-234.

These results have been substantiated by previous work (La55) wherein this counter was used in $2\pi$ geometry with one foil of U-235 and one of U-238 back-to-back. In that case the room-scattered neutrons were effective in producing fission in U-235 but not in U-238, and so disturbed the measurements of fission cross-section ratios. The magnitude of the effect was evaluated simply by taking one measurement with the counter close to the neutron source, and another with the counter remote, say, twice as far, from the source. The primary flux was thereby reduced without materially affecting the room-scattered flux. In this way the magnitude of the correction to the cross-section ratio was found to be about 0.3%, indicating an s of this order also. The energy spectrum of such multiply-scattered neutrons lies so low that a completely negligible fraction of them exceed the U-234 fission threshold.

In summary then, only the materials of the counter itself need be taken into account, and a calculation of s to 20% accuracy will suffice to limit the average uncertainty from this source in the measured ratios to something of the order of 1 to 1.5%.

# APPENDIX D

## MATHEMATICS AND NOTATION

### I. D FUNCTIONS

There is as yet no standard form for expressing the generalized three-dimensional rotation functions, the so-called "D functions". For this reason seeming inconsistencies are frequently encountered in scientific writings where they are used. A few which bear most directly on the subject of this report will be noted at the end of this section. The D function used herein is defined below and some of its properties are briefly discussed.

Perhaps the simplest possible wave function is that for the rigid rotator with angular momentum J along the z axis. Here $J^2 = J_z^2$, $J_z = m$, rotation takes place in the xy plane, and solution of the Schrodinger wave equation yields:

$$\psi_m^j(\phi) = (1/\sqrt{2\pi})e^{im\phi} , \qquad (55)$$

where $\phi$ may be taken as the orientation of the major symmetry axis of the rotator with respect to a fixed line, say Ox, in the xy plane.

Now let the coordinate axes be rotated through an angle $\alpha$ about z so that Ox goes to Ox' (this is exactly the first Euler rotation in the general case to follow). Then by inspection one sees that in terms of the new coordinates, $\psi \rightarrow \psi'$:

$$\psi'^j_m(\phi) = R\psi_m^j(\phi) = (1/\sqrt{2\pi})e^{im\phi'} = (1/\sqrt{2\pi})\, e^{im(\phi-\alpha)} = e^{-im\alpha}\psi_m^j(\phi). \qquad (56)$$

UNCLASSIFIED
ORNL-LR-DWG 67305

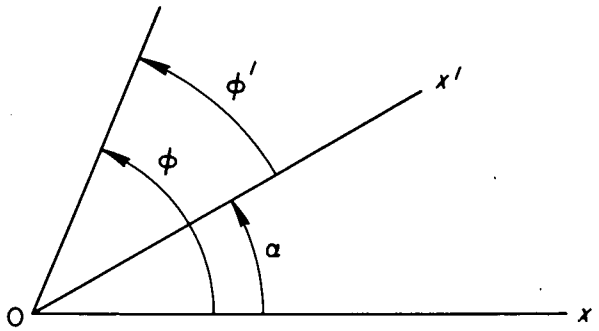


Fig. 19. Coordinate Rotation in xy Plane.

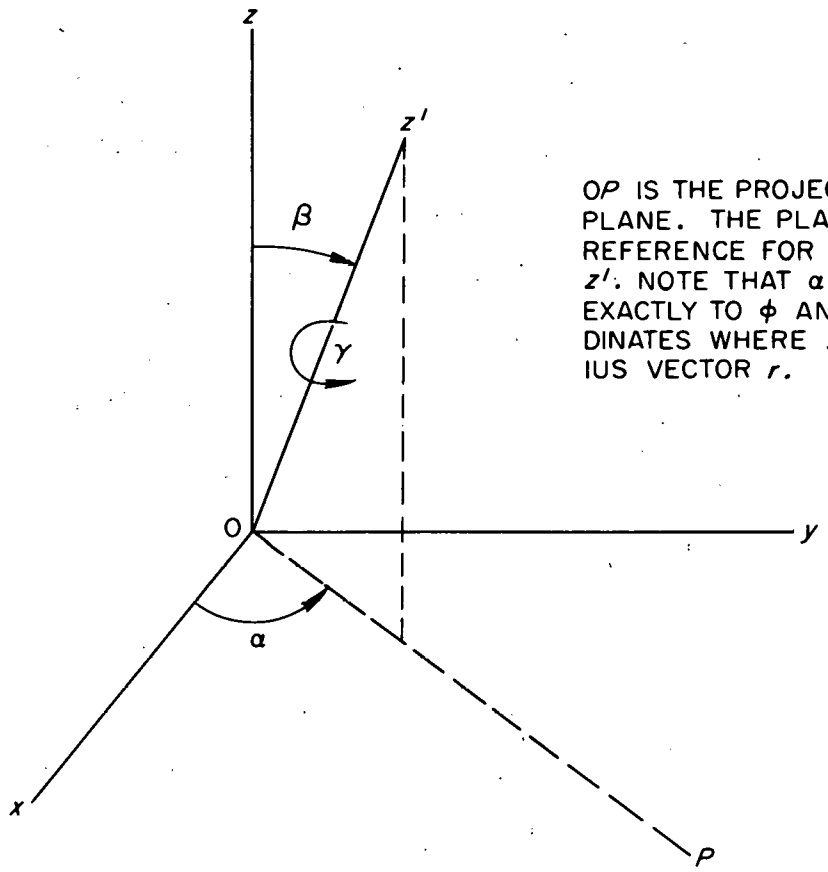


$OP$ IS THE PROJECTION OF $z'$ ON THE $xy$ PLANE. THE PLANE $POz'$ IS THE ZERO REFERENCE FOR THE ROTATION $\gamma$ ABOUT $z'$. NOTE THAT $\alpha$ AND $\beta$ CORRESPOND EXACTLY TO $\phi$ AND $\theta$ IN POLAR COORDINATES WHERE $z'$ WOULD BE THE RADIUS VECTOR $r$.

Fig. 20. Euler Angles.

Expressed as a D function;

$$e^{-im\alpha} = R = D^{*j}_{mm}(\alpha 0\alpha). \tag{57}$$

$$e^{im\alpha} = R^{-1} = D^{j}_{mm}(\alpha 0\alpha). \tag{58}$$

The D function is a unitary matrix in the most general case and the inverse is equal to the Hermitian conjugate. The concept embodied in the above example applies to the general case where it is necessary to define a rotation of coordinates in terms of three separate rotations of which unfortunately only two can be put in the simple exponential (diagonal) form above. The rotations chosen here are: first the one already described, secondly a rotation in a right-handed sense through an angle $\beta$ about the new (intermediate) position of the y axis designated as $y_i$, and finally a rotation in a right-handed sense of $\gamma$ about z' the final position of the z axis. These are the same as those used by Rose, Bohr, Mottelson, and the majority of others but opposite to those used by Wigner.

Let I equal the total angular momentum, M its component along z, and K its component along z'. Then the function $D^{I}_{MK}(\alpha\beta\gamma)$ is so defined that the generalization of the simple example given above becomes:

$$\psi^{I}_{M} = \sum_{K} D^{I}_{MK}(\alpha\beta\gamma)\psi'^{I}_{K} . \tag{59}$$

$$\psi'^{I}_{M} = \sum_{K} D^{I}_{MK}(-\gamma,-\beta,-\alpha)\psi^{I}_{K} = \sum_{K} D^{*I}_{KM}(\alpha\beta\gamma)\psi^{I}_{K} . \tag{60}$$

The function which accomplishes this turns out to be:

$$D^{I}_{MK}(\alpha\beta\gamma) = e^{iM\alpha} d^{I}_{MK}(\beta) e^{iK\gamma} . \tag{61}$$

$$d^I_{MK}(\beta) = \left[(I+M)!(I-M)!(I+K)!(I-K)!\right]^{1/2} \cdot \tag{61a}$$

$$\cdot \sum_x \frac{(-1)^x (\sin \beta/2)^{K-M+2x} (\cos \beta/2)^{2I-(K-M+2x)}}{(I-K-x)!(I+M-x)!(x+K-M)!x!} ,$$

where the summation index, x = 0,1,2,3,..... terminating with the integer which first makes any one of the factorials in the denominator zero (0! = 1).

This D is the same function used by Bohr and Mottelson, and in Mo57, and the complex conjugate of that used in Ro57 where there is a good discussion of its properties.

The relation between $d^I_{MK}(\pi-\beta)$ and $d^I_{MK}(\beta)$ can be derived by replacing $\beta$ by $\pi-\beta$ in the above expression and letting $x = I+M-x'$ and summing over x', remembering that $(-1)^{x'} = (-1)^{-x'}$ since x' is integer only, and recalling that $\sin(\pi-\beta)/2 = \cos\beta/2$ and $\cos(\pi-\beta)/2 = \sin\beta/2$. This and other properties and relations are tabulated below for handy reference.

$$d^I_{MK}(\pi-\beta) = (-1)^{I+M} d^I_{M,-K}(\beta) . \tag{62}$$

$$d^I_{KM}(\pi-\beta) = (-1)^{I+K} d^I_{K,-M}(\beta) . \tag{63}$$

$$d^I_{MK}(\beta) = (-1)^{M-K} d^I_{KM}(\beta) = d^I_{-K,-M}(\beta) = (-1)^{M-K} d^I_{-M,-K}(\beta) . \tag{64}$$

$$d^I_{MK}(-\beta) = d^I_{KM}(\beta) = (-1)^{M-K} d^I_{KM}(-\beta) . \tag{65}$$

$$\left[D^I_{MK}(\alpha\beta\gamma)\right]^{-1} = D^I_{MK}(-\gamma,-\beta,-\alpha) = D^{\dagger I}_{MK}(\alpha\beta\gamma) = D^{*I}_{KM}(\alpha\beta\gamma) =$$

$$= e^{-iK\alpha} d^I_{KM}(\beta) e^{-iM\gamma} = (-1)^{K-M} D^I_{-K,-M}(\alpha\beta\gamma) . \tag{66}$$

$$D^{I_1}_{M_1K_1} D^{I_2}_{M_2K_2} = \sum_j C^{I_1I_2j}_{M_1M_2M} C^{I_1I_2j}_{K_1K_2K} D^{I}_{(M_1+M_2),(K_1+K_2)} . \tag{67}$$

$$\sum_M D^{*I}_{MK_1} D^{I}_{MK_2} = \delta_{K_1K_2}, \qquad \sum_K D^{*I}_{M_1K} D^{I}_{M_2K} = \delta_{M_1M_2} . \tag{68}$$

$$D^{*I}_{MK} D^{I}_{MK} = (-1)^{M-K} D^{I}_{-M,-K} D^{I}_{MK} = (-1)^{M-K} \sum_x C^{IIx}_{-MMO} C^{IIx}_{-KKO} P_x(\cos\theta). \tag{69}$$

$$\int D^{*I_1}_{M_1K_1}(\alpha\beta\gamma) D^{I_2}_{M_2K_2}(\alpha\beta\gamma) \, d\Omega = \frac{8\pi^2}{2I_1+1} \delta_{I_1I_2} \delta_{M_1M_2} \delta_{K_1K_2}, \tag{70}$$

where

$$\int d\Omega = \int_0^{2\pi} d\alpha \int_0^{\pi} \sin\beta d\beta \int_0^{2\pi} d\gamma . \tag{70a}$$

The Legendre polynomials and other spherical harmonics are special cases of D functions:

$$P_\ell(\cos\theta) = D^{\ell}_{00}(0\theta0) = d^{\ell}_{00}(\theta) = \sqrt{\frac{4\pi}{2\ell+1}} Y_{\ell0}(\theta,0) . \tag{71}$$

$$Y_{\ell m}(\theta\phi) = \sqrt{\frac{2\ell+1}{4\pi}} D^{\ell}_{m0}(\phi,\theta,0) . \tag{72}$$

$$P^{|m|}_\ell(\cos\theta) = (\sin^m\theta) \frac{d^m}{d(\cos\theta)^m} P_\ell(\cos\theta) =$$

$$= (-1)^m \delta(m,|m|) \sqrt{\frac{(\ell+|m|)!}{(\ell-|m|)!}} D^{\ell}_{m0}(\phi\,\theta\,0) . \tag{73}$$

The $d^I_{MK}(\alpha\beta\gamma)$ defined above is the same as equation (4.13) on page 52 of Ro57 after applying the appropriate transformation. It corresponds

to the $\mathcal{O}_{\ell mm'}(\beta) = \mathcal{O}_{IMK}(\beta)$ on page 543 of Mo57. The complete D function is identical to that of Mo57 and to the one found in the writings of Bohr and of Mottelson. The small d is a real function whereas D is complex. The D of Ro57 is the complex conjugate of the one used here. Some authors, for example Joos in his book on "Theoretical Physics" (1940 ed.), use a slightly different representation in that the second ($\beta$) rotation is taken around $x_i$ instead of about $y_i$.

The second edition of Wigner's book on Group Theory (Wi59) is a translation with some changes in notation of his first edition which was written in German and employed a left-handed coordinate system. The translation work uses a right-handed system with Euler angles taken in a positive direction and identical to those of Rose (Ro57). The D function differs from that of Rose by a phase factor and in being the complex conjugate. The relationship between the two is important since these two representations are encountered quite frequently. It is

$$ {}_R D^I_{KM}(\alpha\beta\gamma) = (-1)^{K-M} {}_W D^{*I}_{KM}(\alpha\beta\gamma) = {}_W D^I_{KM}(-\alpha,-\beta,-\gamma) , \qquad (74) $$

where the leading subscript, R or W, designates the author. The relationship is curiously reminiscent of the left-handed coordinate system used in the original German edition of Wigner's book.

The rotations and D function are very clearly defined in Ro57, but to be consistent with the convention so established, the equation in the middle of page 55 describing a symmetric top should read

$$ \psi_{LKM}(\alpha\beta\gamma) = \sqrt{(2L+1)/8\pi^2}\, D^{\dagger L}_{KM} = \sqrt{(2L+1)/8\pi^2}\, D^{*L}_{MK}(\alpha\beta\gamma) \ . \qquad (75) $$

An oft-quoted derivation of certain symmetry properties (see

Chapter II) of spheroidal nuclei first appeared in Bo52. The end result is correct but there is an ambiguity regarding phase in the derivation which is difficult to resolve because the D function is not specifically defined in Bo52. On page 19 a rotation referred to as $R_1$ about the 1 axis, reversing the 2 and 3 axes, is said to transform

$$D^I_{MK}(\alpha\beta\gamma) \longrightarrow e^{i\pi(I+K)} D^I_{M,-K}(\alpha\beta\gamma). \tag{76}$$

In terms of the D function specified by eq. (61) herein, the rotation would have to be taken about the 2 (y') axis to effect this transformation. In Mo57 this argument is reproduced from Bo52 but with the added complication of an error in the sign of $\gamma$ which clearly arose from a misinterpretation of the notation used in Bo52.

A rotation of $\pi$ about <u>any</u> axis in the x'y' plane causes $\alpha \longrightarrow (\alpha \pm \pi)$ and $\beta \longrightarrow (\pi - \beta)$. This can be seen by inspection since such a rotation reverses z' whose polar angles in the xyz frame are $\alpha$ and $\beta$. The change in $\gamma$ due to such a rotation will depend on the particular choice of axis in the x'y' plane.

## II. VECTOR ADDITION COEFFICIENTS

The notation adopted for the Clebsch-Gordan coefficients is $C^{abc}_{\alpha\beta\gamma}$ where abc = $\Delta$ and $\alpha+\beta = \gamma$ are necessary for C to be non-zero. The abc are two angular momenta and their resultant in any order, and $\alpha\beta\gamma$ are their respective z components. Although redundant, all three of the components are carried for purposes of clarity and to avoid confusion.

The notation for the Racah coefficients, W(abcd;ef), is well

standardized. The following relation is employed in Chapter V:

$$\sum_m (-1)^m C^{j\ell I}_{mOm} C^{j\ell' I}_{mOm} C^{IIx}_{-mmO} = (-1)^{x-j}(2I+1) C^{\ell\ell' x}_{000} W(\ell\ell' II; xj) . \tag{77}$$

The proof follows: Now

$$W(abcd;ef) C^{afc}_{\alpha,\gamma-\alpha,\gamma} = \left[(2e+1)(2f+1)\right]^{-1/2} \cdot$$

$$\cdot \sum_\beta C^{abe}_{\alpha,\beta,\alpha+\beta} C^{edc}_{\alpha+\beta,\gamma-\alpha-\beta,\gamma} C^{bdf}_{\beta,\gamma-\alpha-\beta,\gamma-\alpha} , \tag{78}$$

and

$$W(abcd;ef) = (-1)^{e+f-b-c} W(afed;cb) , \tag{79}$$

so

$$W(\ell\ell' II; xj) = (-1)^{x+j-\ell'-I} W(\ell jxI; I\ell') , \tag{80}$$

$$W(\ell\ell' II; xj) C^{\ell\ell' x}_{000} = (-1)^{x+j-\ell'-I} W(\ell jxI; I\ell') C^{\ell\ell' x}_{000} = \left[(2I+1)(2\ell'+1)\right]^{-1/2} \cdot$$

$$\cdot \sum_m (-1)^{x+j-\ell'-I} C^{\ell jI}_{Omm} C^{IIx}_{m,-m,O} C^{jI\ell'}_{m,-m,O} . \tag{81}$$

But

$$C^{\ell jI}_{Omm} C^{IIx}_{m,-m,O} C^{jI\ell'}_{m,-m,O} = (-1)^{\ell+j-I} C^{j\ell I}_{mOm} (-1)^{2I-x} C^{IIx}_{-m,mO} (-1)^{j-m} \sqrt{\frac{2\ell'+1}{2I+1}} C^{j\ell' I}_{mOm} =$$

$$= C^{j\ell I}_{mOm} C^{j\ell' I}_{mOm} C^{IIx}_{-mmO} \sqrt{\frac{2\ell'+1}{2I+1}} (-1)^{I+2j+\ell-m-x} . \tag{82}$$

So

$$W(\ell\ell' II; xj) C^{\ell\ell' x}_{000} = \frac{(-1)^{3j+\ell-\ell'}}{2I+1} \sum_m (-1)^{-m} C^{j\ell I}_{mOm} C^{j\ell' I}_{mOm} C^{IIx}_{-mmO} . \tag{83}$$

Now j = integer or half-integer. In either case $(-1)^{3j} = (-1)^{-j}$. The sum over m is over equal positive and negative values of m.

$$(-1)^{x-j}(2I+1)W(\ell\ell' II;xj)C_{000}^{\ell\ell' x} = (-1)^{x-2j+\ell-\ell'} \sum_{-m} (-1)^m C_{-m,0,-m}^{j\ell I} \cdot$$

$$\cdot\ C_{-m,0,-m}^{j\ell' I}\ C_{m,-m,0}^{IIx} \cdot \tag{84}$$

Now $C_{-\alpha,-\beta,-\gamma}^{abc} = (-1)^{a+b-c} C_{\alpha\beta\gamma}^{abc}$ so the expression on the right becomes:

$$(-1)^{x-2j+\ell-\ell'} \sum_{-m} (-1)^m\ C_{mOm}^{j\ell I}\ C_{mOm}^{j\ell' I}\ C_{-mmO}^{IIx}\ (-1)^{2j+2I+\ell-\ell'-2I-x} =$$

$$= (-1)^{2\ell} \sum_{-m} (-1)^m\ C_{mOm}^{j\ell I}\ C_{mOm}^{j\ell' I}\ C_{-mmO}^{IIx} =$$

$$= \sum_{m} (-1)^m\ C_{mOm}^{j\ell I}\ C_{mOm}^{j\ell' I}\ C_{-mmO}^{IIx}, \tag{85}$$

which concludes the proof.

Although the Z coefficients as originally introduced suffered from a phase error as pointed out by Huby (Hu54), they have been used, with the addition of a factor to correct the phase, to express results because tables for them are available. $|Z| = |\bar{Z}|$ but in some cases the sign is different. They are defined as follows:

$$Z(\ell_1 j_1 \ell_2 j_2; sL) \equiv i^{L-\ell_1+\ell_2} \sqrt{(2\ell_1+1)(2\ell_2+1)(2j_1+1)(2j_2+1)} \cdot$$

$$\cdot\ C_{000}^{\ell_1 \ell_2 L}\ W(\ell_1 j_1 \ell_2 j_2; sL) \cdot \tag{86}$$

$$\bar{Z}(\ell_1 j_1 \ell_2 j_2; sL) = \sqrt{(2\ell_1+1)(2\ell_2+1)(2j_1+1)(2j_2+1)} \cdot$$

$$\cdot\ C_{000}^{\ell_1 \ell_2 L}\ W(\ell_1 j_1 \ell_2 j_2; sL) . \tag{87}$$

# APPENDIX E

## SUMMARY OF LEAST SQUARES FITS

During the course of this work six 4-point angular distributions were obtained and fit by the method of least squares. Of these only two have been used in the channel analyses reported herein. The least squares fits for all six are recorded here, however. They include the correction for finite angular resolution of the measuring apparatus made according to the method reported by M. E. Rose (Ro53). The correction amounts to an increase of 2.6 percent and 8.8 percent in the coefficients of the $P_2$ and $P_4$ terms respectively, where $P_x$ is the usual Legendre polynomial, $P_x(\cos\theta)$. $\chi^2$ and $P(\chi^2)$ have the usual statistical meanings and afford rough estimates of the reliabilities of the fits. For one degree of freedom such as is the case here (four points and three parameters), a $P(\chi^2)$ from 5 to 95 percent is deemed reasonable. Thus with the exception of U-235 at 3690 kev the three-parameter Legendre polynomial expansions yield acceptable fits to the data. $\chi^2 = \sum r_i^2/\partial_i^2$ where $r_i$ is the residual at point i, that is, the difference between the y coordinate of the point and the curve at $x_i$. $\partial_i$ is the standard deviation in the measured y parameter at $x_i$. Then $P(\chi^2)$, obtained from charts, is the probability that another set of measurements would give a value of $\chi^2$ greater than that obtained in the test under consideration.

The results are expressed in Table XVII as follows:

$$W(\theta) = a_0+a_2\cos^2\theta+a_4\cos^4\theta = A_0+A_2P_2(\cos\theta)+A_4P_4(\cos\theta).$$

The reason for the large $\chi^2$ value for U-235 at 3690 kev is not known.

TABLE XVII

LEAST SQUARES FITS TO FOUR-POINT ANGULAR DISTRIBUTIONS

| Isotope | $E_n$ | $a_0$ | $a_2$ | $a_4$ | $\chi^2$ | $P(\chi^2)\%$ |
|---|---|---|---|---|---|---|
| U-234 | 843 | .9952±.0083 | .3848±.0603 | .4388±.0740 | .9558 | 33 |
| U-234 | 1051 | .9973±.0053 | .1213±.0315 | .0091±.0320 | .3776 | 54 |
| U-234 | 3735 | .9993±.0039 | .2259±.0243 | .0151±.0258 | .2906 | 59 |
| U-235 | 844 | .9986±.0027 | .2316±.0201 | .1286±.0216 | .0576 | 81 |
| U-235 | 1052 | .9981±.0029 | .1177±.0173 | .0303±.0183 | .0264 | 87 |
| U-235 | 3690 | 1.0069±.0268 | .1933±.1625 | -.0614±.1727 | 4.8559 | 3 |
| | | $A_0$ | $A_2$ | $A_4$ | | |
| U-234 | 843 | 1.2112±.0065 | .5072±.0619 | .1003±.0169 | | |
| U-234 | 1051 | 1.0395±.0033 | .0861±.0323 | .0021±.0073 | | |
| U-234 | 3735 | 1.0720±.0025 | .1429±.0249 | -.0035±.0059 | | |
| U-235 | 844 | 1.0543±.0023 | .0892±.0206 | -.0029±.0049 | | |
| U-235 | 1052 | 1.0434±.0018 | .0958±.0178 | .0070±.0041 | | |
| U-235 | 3690 | 1.0610±.0170 | .0977±.1667 | -.0140±.0395 | | |

These coefficients contain the corrections for finite angular resolution.
The expressions have not been normalized to the total fission cross sections.

It may indicate the presence of higher order harmonics in the measured distribution, making it impossible to secure a proper fit with terms only up to $P_4$. In any case the results should not be used in any sort of analysis without further checking. The fits in the other five cases are seen to be reasonable according to this $\chi^2$ test.

The least squares fits were carried out on the ORNL "ORACLE" computer through the courtesy of Harvey Carter of the Mathematics Group.

THIS PAGE

WAS INTENTIONALLY

LEFT BLANK

ORNL-3306
UC-34 — Physics
TID-4500 (17th ed., Rev.)

INTERNAL DISTRIBUTION

1. Biology Library
2-3. Central Research Library
4. Laboratory Shift Supervisor
5. Reactor Division Library
6. ORNL — Y-12 Technical Library Document Reference Section
7-56. Laboratory Records Department
57. Laboratory Records, ORNL R.C.
58. A. Chetham-Strode
59. J. W. T. Dabbs
60. R. L. Ferguson
61-62. J. L. Fowler
63. R. G. Jordan (Y-12)
64-73. R. W. Lamphere
74. C. E. Larson
75. F. K. McGowan
76. J. P. Murray (K-25)
77. A. M. Perry
78. G. R. Satchler
79. H. W. Schmitt
80. M. J. Skinner
81. A. H. Snell
82. J. A. Swartout
83. F. J. Walters
84. A. M. Weinberg
85. H. Feshback (consultant)
86. W. A. Fowler (consultant)
87. M. Goldhaber (consultant)
88. M. S. Livingston (consultant)
89. J. R. Richardson (consultant)
90. J. H. Van Vleck (consultant)
91. J. A. Wheeler (consultant)

EXTERNAL DISTRIBUTION

92. Division of Research and Development, AEC, ORO
93-651. Given distribution as shown in TID-4500 (17th ed., Rev.) under Physics category